EPIGENETICS TRAITS IN MAMMALIAN TISSUES. FROM NEW TECHNOLOGY TO NEW HYPOTHESES

EDITED BY: Michael E. Symonds and Rafael Franco
PUBLISHED IN: Frontiers in Genetics and Frontiers in Cell and Developmental Biology

frontiers Research Topics

ISSN 1664-8714
ISBN 978-2-88963-037-0
DOI 10.3389/978-2-88963-037-0

About Frontiers

Frontiers is more than just an open-access publisher of scholarly articles: it is a pioneering approach to the world of academia, radically improving the way scholarly research is managed. The grand vision of Frontiers is a world where all people have an equal opportunity to seek, share and generate knowledge. Frontiers provides immediate and permanent online open access to all its publications, but this alone is not enough to realize our grand goals.

Frontiers Journal Series

The Frontiers Journal Series is a multi-tier and interdisciplinary set of open-access, online journals, promising a paradigm shift from the current review, selection and dissemination processes in academic publishing. All Frontiers journals are driven by researchers for researchers; therefore, they constitute a service to the scholarly community. At the same time, the Frontiers Journal Series operates on a revolutionary invention, the tiered publishing system, initially addressing specific communities of scholars, and gradually climbing up to broader public understanding, thus serving the interests of the lay society, too.

Dedication to Quality

Each Frontiers article is a landmark of the highest quality, thanks to genuinely collaborative interactions between authors and review editors, who include some of the world's best academicians. Research must be certified by peers before entering a stream of knowledge that may eventually reach the public - and shape society; therefore, Frontiers only applies the most rigorous and unbiased reviews.
Frontiers revolutionizes research publishing by freely delivering the most outstanding research, evaluated with no bias from both the academic and social point of view. By applying the most advanced information technologies, Frontiers is catapulting scholarly publishing into a new generation.

What are Frontiers Research Topics?

Frontiers Research Topics are very popular trademarks of the Frontiers Journals Series: they are collections of at least ten articles, all centered on a particular subject. With their unique mix of varied contributions from Original Research to Review Articles, Frontiers Research Topics unify the most influential researchers, the latest key findings and historical advances in a hot research area! Find out more on how to host your own Frontiers Research Topic or contribute to one as an author by contacting the Frontiers Editorial Office: researchtopics@frontiersin.org

EPIGENETICS TRAITS IN MAMMALIAN TISSUES. FROM NEW TECHNOLOGY TO NEW HYPOTHESES

Topic Editors:
Michael E. Symonds, University of Nottingham, United Kingdom
Rafael Franco, Universitat de Barcelona & CiberNed, Spain

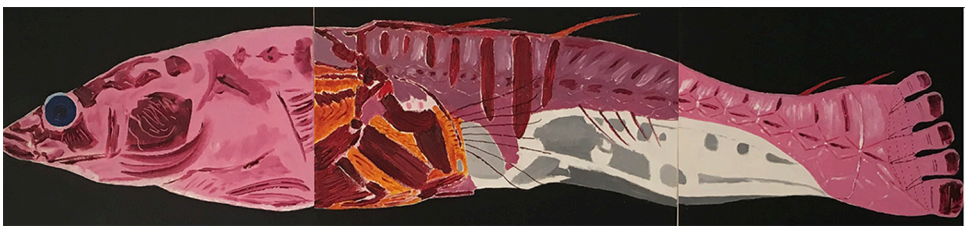

Image: "Fish with nails" by Rafael Franco. Oil painting on canvas.

How with the same genome a neuron is so different from a muscle cell?

In Eva Jablonka and Lamb's words, "epigenetics is one of the four dimensions of evolution".

Actually, epigenetics should anything which occur in living cells that cannot be only explained by the genes/genome.

After decades thinking and acting as if the genome determined the absolute fate of any life form in Earth, the relevance of epigenetics for mammalian life, disease and death is now recognized. In fact, assuming similar genomes, lifespan, lifestyle, and risk of diseases, etc. results from a balance between genes and epigenetic traits. The Research Topic aimed to show the differences of epigenetic traits between tissues, their physiological relevance and potential to target epigenetic mechanisms in human diseases.

Citation: Symonds, M. E., Franco, R., eds. (2019). Epigenetics Traits in Mammalian Tissues. From New Technology to New Hypotheses. Lausanne: Frontiers Media.
doi: 10.3389/978-2-88963-037-0

Table of Contents

frontiers in Genetics

EDITORIAL
published: 05 July 2019
doi: 10.3389/fgene.2019.00635

Editorial: Epigenetics in Mammalian Tissues

Rafael Franco[1,2*] *and Michael E. Symonds*[3]

[1] Department Bioquimica i Biomedicina Molecular, Universitat de Barcelona, Barcelona, Spain, [2] CIBERNED, Centro de Investigación en Red, Enfermedades Neurodegenerativas, Instituto de Salud Carlos III, Madrid, Spain, [3] Early Life Research Unit, Division of Child Health, Obstetrics and Gynaecology, and Nottingham Digestive Disease Centre and Biomedical Research Centre, School of Medicine, University of Nottingham, Nottingham, United Kingdom

Keywords: cytocrin, Turner syndrome (TS), X chromosome, epigenetic abnormalities, DNA methylation

Editorial on the Research Topic

Epigenetics in Mammalian Tissues

The challenge of understanding epigenetics and reaching a consensus for its role(s) in development is substantial. This is illustrated in the wide range of topics covered by the research topic "Epigenetics in Mammalian Tissues." The discovery of new concepts in epigenetics during pregnancy and early development is on-going, together with their potential impact on susceptibility to later disease. A diverse range of examples are included within this issue that cover methodological approaches together with responses of individual tissues and organs ranging from the placenta to the eye.

The paper focused on the eye shows evidence of epigenetic factors in diseases affecting organs involved in sense perception. This could be important because in contrast to genetic inheritance of disease, epigenetic factors may be acquired by a variety of circumstances. In the case of the eye, adverse exposure to sunlight can trigger a range of responses that can contribute to the onset of cataracts to glaucoma (Alkozi et al.).

It is fascinating that cells with the same DNA content may give rise to such diverse tissues, and epigenetic factors are important in this regard. Undoubtedly, development and function of the central nervous system (CNS) is under epigenetic modification, as it is composed of a myriad of phenotypically different cells. For example, whereas the liver is primarily composed of hepatocytes and fibroblasts, the CNS contains neurons and glia with hundreds of diverse neurons. One paper in the special issue focuses on the epigenetic processes taking place in the CNS and how this impacts on the nuclear architecture during development, function, and disease onset (Ito and Takizawa).

Another paper describes a study (He et al.) using a transgenic mouse to model Turner disease, which is a chromosomal disease characterized "by complete or partial X monosomy in some or all cells" (Saenger et al., 2001). It compares mice with one single paternally or maternally inherited X chromosome, of which embryos with paternal inheritance have greater risk of miscarriage (Hall and Gilchrist, 1990; Robinson, 1990). This is probably due to epigenetic factors such as paternally imprinted genes in the placenta or genome-wide differences in chromatin condensation. Differences in the outer zone of the placenta occupied by glycogen cells together with a substantial adaptation of glycogen/glucose storage and metabolism are described. They conclude that changes in glucose metabolism are not directly caused by changes in X-linked genes but are more likely to be a consequence of an altered cellular composition mediated by placental adaptation in early development.

The study of the impact of the X chromosome on health and disease is fascinating. One aspect relates to *in vitro* fertilization, and (Min et al.) suggest that epigenetic factors could be involved in the differential expression of X-linked genes in male compared with female *in vitro* fertilization-derived

OPEN ACCESS

Edited by:
Emmanouil Dermitzakis, University of Geneva, Switzerland

***Correspondence:**
Rafael Franco
rfranco123@gmail.com

Specialty section:
This article was submitted to Epigenomics and Epigenetics, a section of the journal Frontiers in Genetics

Received: *25 January 2019*
Accepted: *17 June 2019*
Published: *05 July 2019*

Citation:
Franco R and Symonds EM (2019) Editorial: Epigenetics in Mammalian Tissues. Front. Genet. 10:635. doi: 10.3389/fgene.2019.00635

blastocysts. They also demonstrate epigenetic regulation of X chromosome reactivation with somatic-cell nuclear transfer. Under these conditions, clonal reprogramming of X-chromosome appears incomplete and may differently occur in cells within a single blastocyst.

There are a wide range of methods available for examining epigenetics including the assessment of patterns of DNS methylation, histone acetylation, etc. The paper by Jeon et al. is technical in nature and describes how it is possible to run parallel assessments of methylation status in hundreds of CpG sites. Their approach is based on bisulfite polymerase chain reaction sequencing (TBPseq). The field has also advanced by exploring how to enhance or depress methylation/acetylation as a therapeutic approach. For example, inhibition of histone acetylation leads to an increase in the expression of genes that enhance cognition and could have potential in treating Alzheimer's disease (Cuadrado-Tejedor et al., 2013; Cuadrado-Tejedor et al., 2015).

It should also be noted the term epigenetic is not used by all scientists in the same way. One article revisits the concept that epigenetics defines everything that is not genetic, i.e., existing in the DNA sequence, that affects phenotype. On doing so, hormonal regulation, that ultimately impacts on gene expression, could be considered epigenetic. This reasoning makes it necessary to choose a word to define events occurring inside the cell, i.e., those participating after a hormone interacts with a cell surface receptor until a transcription factor is activated or inactivated and gene expression is enhanced or repressed. The word used by Navarro et al. has the prefix "cyto" and the suffix "crin," as there are interacting intracellular cascades with actions at the nuclear level. Specific cytocrin pathways may explain the differential effect of any hormone on mammalian tissues or cells thereby linking epigenetic factors and epigenetic mediators to epigenetic traits. This type of concept could explain the impact of modulating maternal nutrition for which supplementation of the maternal diet with fructose, in rats, modulates the maternal microbiome (Astbury et al.) and it was accompanied with reduced gene expression of markers of gut barrier function that could adversely affect its function in later life.

In conclusion, our understanding of epigenetic regulation of mammalian tissues is only beginning to become established. Furthermore, as illustrated by the diverse nature of papers included in this edition, the topic has substantial scope for transforming our understanding of development and disease onset.

REFERENCES

Cuadrado-Tejedor, M., Garcia-Barroso, C., Sanzhez-Arias, J., Mederos, S., Rabal, O., Ugarte, A., et al. (2015). Concomitant histone deacetylase and phosphodiesterase 5 inhibition synergistically prevents the disruption in synaptic plasticity and it reverses cognitive impairment in a mouse model of Alzheimer's disease. *Clin. Epigenetics* 7:108. doi: 10.1186/s13148-015-0142-9

Cuadrado-Tejedor, M. L., Ricobaraza, A., Torrijo, R., Franco, R., Garcia-Osta, A. (2013). Phenylbutyrate is a multifaceted drug that exerts neuroprotective effects and reverses the Alzheimer's disease-like phenotype of a commonly used mouse model. *Curr. Pharm. Des.* 19 (28), 5076–5084. doi: 10.2174/1381612811319280006

Hall, J. G., and Gilchrist, D. M. (1990). Turner syndrome and its variants. *Pediatr. Clin. North Am.* 37, 1421–1436. doi: 10.1016/S0031-3955(16)37018-3

Robinson, A. (1990). "Demography and prevalence of Turner syndrome," in *Turner syndrome*. Eds. R. G. Rosenfeld and M. M. Grumbach (New York: Marcell Dekker), 93–100.

Saenger, P., Wikland, K. A., Conway, G. S., Davenport, M., Gravholt, C. H., Hintz, R., et al. (2001). Recommendations for the diagnosis and management of Turner syndrome. *J. Clin. Endocrinol. Metab.* 86 (7), 3061–3069. doi: 10.1210/jcem.86.7.7683

Conflict of Interest Statement: The authors declare that the research was conducted in the absence of any commercial or financial relationships that could be construed as a potential conflict of interest.

frontiers in Genetics

ORIGINAL RESEARCH
published: 13 July 2017
doi: 10.3389/fgene.2017.00097

Simultaneous Methylation-Level Assessment of Hundreds of CpG Sites by Targeted Bisulfite PCR Sequencing (TBPseq)

*Kyuheum Jeon[1,2], Byungkuk Min[1], Jung S. Park[1] and Yong-Kook Kang[1,2]**

[1] Development and Differentiation Research Center, Korea Research Institute of Bioscience & Biotechnology, Daejeon, South Korea, [2] Department of Functional Genomics, Korea University of Science and Technology, Daejeon, South Korea

Methylated-DNA sequencing technologies are producing vast amounts of methylome data from cancer samples, from which cancer-associated differentially methylated CpG sites (cDMCs) are continuously identified and filed. The inclusion of as many cDMCs as possible helps improve the accuracy of cancer diagnosis and sometimes identify cancer subtypes. However, the lack of an established method for the analysis of 100s of cDMCs practically impedes their robust use in clinical medicine. Here, we tested the availability of targeted bisulfite-PCR-sequencing (TBPseq) technology for the assessment of methylation levels of a myriad of CpGs scattered over the genome. In randomly selected 46 cancer cell lines, multiplexed PCR yielded a variety of amplicons harboring 246 CpGs residing at promoters of 97 cancer-associated genes, all of which were sequenced in the same flow cell. Clustering analysis of the TBPseq-assessed methylation levels of target CpGs showed that the lung and liver cancer cell lines correlated relatively strongly with each other while they weakly correlated with colon cancer cells. CpGs at the *LIFR* gene promoter, which are known to be hypermethylated in colon cancers, indeed were heavily methylated in the tested colon cancer cells. Moreover, the *LIFR* promoter hypermethylation was found in colon cancer cells only, but not in biliary tract, liver, lung, and stomach cancers cell lines. A meta-analysis with public cancer methylome data verified the colon cancer specificity of *LIFR* promoter methylation. These results demonstrate that our TBPseq-based methylation assessment could be considered an effective, accurate, and competitive method to simultaneously examine a large number of target cDMCs and patient samples.

Keywords: DNA methylation, cancer, LIFR, targeted NGS, sequencing, diagnosis

OPEN ACCESS

Edited by:
Rafael Franco,
University of Barcelona, Spain

Reviewed by:
Qi Xie,
Cleveland Clinic, United States
Eva Martínez-Pinilla,
Universidad de Oviedo Mieres, Spain
Shicheng Guo,
University of California, San Diego, United States

***Correspondence:**
Yong-Kook Kang
ykkang@kribb.re.kr

Specialty section:
This article was submitted to Epigenomics and Epigenetics, a section of the journal Frontiers in Genetics

Received: *24 March 2017*
Accepted: *28 June 2017*
Published: *13 July 2017*

Citation:
Jeon K, Min B, Park JS and Kang Y-K (2017) Simultaneous Methylation-Level Assessment of Hundreds of CpG Sites by Targeted Bisulfite PCR Sequencing (TBPseq). Front. Genet. 8:97. doi: 10.3389/fgene.2017.00097

INTRODUCTION

The potential role of epigenetic processes in human diseases is exemplified by aberrant DNA methylation in cancer (Heyn and Esteller, 2012). Hence, a key challenge in this field is an ability to detect these alterations genome-wide in high-resolution within a large number of samples to identify cancer associations. Several effective technologies have been widely used to characterize genome-scale patterns of DNA methylation: (1) whole-genome bisulfite sequencing (WGBS), which treats DNA with bisulfite and is followed by next-generation sequencing (NGS) technology,

providing a complete overview of CpG methylation at base-pair resolution and an unbiased assessment of the profile of DNA methylomes (Lister et al., 2008, 2009; Laurent et al., 2010); (2) Infinium HumanMethylation 450 BeadChip, a DNA methylation array technology, which assays approximately 450,000 individual CpG sites that cover 99% of all RefSeq genes, allowing the high-resolution DNA methylation profiling of human samples (Bibikova et al., 2011; Sandoval et al., 2011); (3) reduced representation bisulfite sequencing (RRBS), which reduces the representation libraries by DNA digestion using a methylation-insensitive restriction enzyme such as *Msp*I, is suitable for obtaining information from most CpG islands (Meissner et al., 2005) and has been used to identify changes during cell differentiation (Bock et al., 2011); and (4) methylated DNA binding domain sequencing (MBD-seq) and methylation DNA immunoprecipitation sequencing (MeDIP-seq), which combine the advantages of NGS and enrichment of methylated DNA regions by immunoprecipitation (Down et al., 2008; Serre et al., 2010), are suitable for covering large parts of the genome in a quantitative manner and have been successfully used to identify aberrantly methylated disease-related CpGs (Feber et al., 2011).

These methylated-DNA sequencing technologies have been used to produce vast amounts of methylome data from 1000s of cancer samples worldwide, from which innumerable cancer-associated differentially methylated CpGs (cDMCs) have been identified. Although the cDMCs identified this way are continuously being filed and validated as cancer biomarkers (Model et al., 2007; Li et al., 2009, 2012; Hinoue et al., 2012; Khamas et al., 2012; Nikolaidis et al., 2012; Simmer et al., 2012; Naumov et al., 2013; Mitchell et al., 2014), the practical application of the cDMCs to clinical diagnosis has been rare, and the use of them in a pack of 10s or 100s in a single assay is even rarer. The inclusion of as many cDMCs as possible can help increase the diagnostic capability, and identify and classify cancer subtypes from an epigenetic perspective. Once a pack of cDMCs are set as cancer biomarkers through scrupulous validation processes, they are ready for use in probing into methylation states of cancer samples. Compared with the whole genome-scale sequencing and the analysis of the correspondingly large amount of data, this target-based approach would be much cost effective, less time-consuming, less labor-intensive, and thus far more competitive. Owing to all these benefits, the targeted methylation analysis method could undoubtedly be considered a better choice for cancer diagnosis. Unfortunately, however, there has been no established technology until date to analyze 10s or 100s of CpGs at a time, which serves as a major barrier to the practicality and high diagnostic capabilities of large-scale cDMC use in clinical medicine.

In this study, we tested the applicability of a targeted bisulfite PCR sequencing (TBPseq) technology, a promising approach for the methylation analysis of a large-size pack of CpGs. Our study was designed with an aim to show that some CpGs previously known as biomarkers for certain cancers could indeed be exposed as being differentially methylated in the same type of cancer cells among different cell lines examined. To confirm this possibility, we assessed the methylation frequencies of 100s of CpGs, which have been known to be cancer-related, in 46 cell lines representing five different cancer types (biliary tract, colon, liver, lung, and stomach cancers). We have succeeded in providing evidence that our TBPseq method is accurate and effective for the methylation analysis of a large number of samples and target CpGs at a time.

MATERIALS AND METHODS

Ethics Statement and Cell Culture

This study was carried out in strict accordance with the recommendations in the Guide for the Care and Use of Laboratory Animals of the National Livestock Research Institute of Korea. The protocol was approved by the Committee on the Ethics of Animal Experiments of the Korea Research Institute of Bioscience and Biotechnology.

Colon cancer cells were cultured in RPMI-1640 media (Gibco) containing 10% heat-inactivated fetal bovine serum (RMBIO, United States), 0.5% non-essential amino acids, 100 U/ml penicillin, and 0.1 mg/ml streptomycin at 37°C and 5% CO_2. CCD-18co cell was cultured in DMEM media (Gibco) containing 10% heat-inactivated fetal bovine serum (RMBIO, United States), 0.5% non-essential amino acids, 100 U/ml penicillin, and 0.1 mg/ml streptomycin at 37°C and 5% CO_2.

Reverse Transcription-Polymerase Chain Reaction (RT-PCR)

For reverse transcription-polymerase chain reaction (RT-PCR), total RNAs were obtained from cultured cells using RNeasy mini kit (Qiagen) and were used to synthesize cDNAs using reverse transcriptase (Superscript III, Invitrogen) as described elsewhere (Cho et al., 2015). PCR was performed with h-taq DNA polymerase (SolGent) in the following conditions: 15 min of enzyme activation at 95°C followed by 40 cycles of 95°C for 20 s, 55°C for 30 s, and 65°C for 1 min. The list of PCR primers is as follows: 5′-CAGGGGATGGCAAGATAG-3′ and 5′-TCTTTTATTGTCCACCATCC-3′ for *LIFR*; 5′-AACAGTGC CTTGAGGAGAG-3′ and 5′-GGGCTGTTTAGGTAATTCG-3′ for *LIFR-AS1*; 5′-AATCCCATCACCATCTTCCA-3′ and 5′-TG GACTCCACGACGTACTCA-3′ for *GAPDH*.

Combined Bisulfite Restriction Analysis (COBRA)

Genomic DNAs extracted from culture cell lines were treated with bisulfite using EpiTect kit (Qiagen), as described elsewhere (Cho et al., 2014). The bisulfite converted gDNAs were used as templates in PCR to amplify the region of interest harboring either *Taq*I (5′-TCGA-3′) or *Bst*UI (5′-CGCG-3′) sequence. The list of PCR primers is as follows: 5′-TTTTTAGAAGGTTATGGAAG-3′ and 5′-CTC TCCAACTAATTTCATTT-3′ for *LIFR*; 5′-TTAAGTGAAGA AATTTTGAA-3′ and 5′-TTATCTCCAAATATCACAAA-3′ for *MLH1* (1); 5′-GTTTTTATTGGTTGGATATT-3′ and 5′-AA ATACCAATCAAATTTCTC-3′ for *MLH1* (2); 5′-AGTTA TTTTAGGGGAAGTAA-3′ and 5′-AAAACCCTACAATTA AACAC-3′ for *HOXA11*. The resulting PCR products were

digested with either *Taq*I or *Bst*UI and resolved on 2% agarose gel.

Bisulfite Treatment and Multiplex PCR

Genomic DNAs (gDNA) were extracted from cancer cell lines and were treated with bisulfite using EpiTect Bisulfite Kit (Qiagen) according to the manufacturer's instruction. Multiplexed PCR was prepared with 113 pairs of primers in total. To design the multiplex PCR primers, promoter sequences between 1 kb upstream and 500 bp downstream from transcription start sites (TSSs) of multiple target genes were extracted using the 'bedtools getfasta' (Quinlan, 2002), and then the C→T and G→A converted target DNA sequences were generated from the extracted sequences by 'bismark_genome_preparation' (Krueger and Andrews, 2011). With these sequences as input templates, we ran a web-based 'Batchprimer3' engine (You et al., 2008) to obtain primers in batches which were then split into six subsets after experimental verifications of their proper operations by gel electrophoreses of multiplex PCR products from various combinations of primer sets. The list of primer pairs and their amplicon sequences is presented in the Supplementary File 1. Multiplex PCR was performed with each primer group using h-Taq DNA polymerase (SolGent) in the following conditions: 15 min of enzyme activation at 95°C followed by 50 cycles of 95°C for 20 s, 46°C for 1 min, and 65°C for 2 min (Oh et al., 2015; Park et al., 2017).

Library Construction for Illumina Sequencing

Entire amplicons obtained from eight rounds of multiplex PCR were pooled together in equal volumes. For sequencing library construction, we performed a series of enzymatic reactions such as 5′-end phosphorylation, adaptor ligation, and additional cycles of PCR to attach barcode and other modules. 5′-end phosphorylation was performed with 1 μg of pooled amplicons using T4 polynucleotide kinase (NEB) at 37°C for 30 min. 5′-end phosphorylated amplicons then were ligated with 15 μM of home-made Illumina adaptors by incubating them at RT for 1 h. Finally, adaptor ligated amplicons were amplified using index and universal primers by DNA polymerase (SolGent) for indexing in the following conditions: 15 min of enzyme activation at 98°C followed by 25 cycles of 98°C for 10 s, 65°C for 30 s, and 72°C for 30 s (Min et al., 2016). Every intermittent purification was conducted using Expin^{TM} PCR SV purification kit (GeneAll). The equal amount of barcoded libraries were pooled, and they were applied to a parallel deep sequencing in a single flow cell using Illumina Hi-seq 2500.

Detection of Cancer-Related Differentially Methylated CpG (cDMC) and Statistical Analysis

Raw read sequences were pre-processed to remove Illumina adapter sequences and low quality bases using "trim_galore," and the trimmed reads were mapped on the C→T and G→A converted target sequences were generated using "bismark genome preparation." Target CpG methylation levels were measured by "Bismark methylation extractor," and CpGs with the low read coverage (<100) including amplification failed targets were filtered out. Following data analyses were conducted in R statistical environment[1] unless stated otherwise. A dataset containing normalized DNA methylation levels of target CpGs was generated using "DESeq." To compare overall methylation pattern among cancer types, principal component analysis (PCA) was conducted using "prcomp" function and the results were illustrated by "plotPCA" function. Pearson correlation coefficients (r) between individual cancer samples and cancer groups were calculated by "cor" function and a scatter matrix was produced using "heatscatter" function in "LSD" package. For the detection of cDMCs, relative methylation levels between cancer types were calculated, and CpGs showed statistically significant differences (FDR < 0.0001 and fold-change > 2) were determined by "DESeq." For a meta-analysis, cancer type-specific DNA methylome data generated by Infinium 450k array (Illumina) for colon, lung, liver, and stomach cancer samples were downloaded from GDC[2]. Methylation levels (beta-values) of target CpGs were extracted from the methylome data and compared them between different cancer types. Statistical significance was calculated using Wilcoxon rank sum test. All plots were generated using R and MS Excel.

RESULTS

Evaluation of the Targeted Bisulfite PCR Sequencing Method

To assess the methylation levels of a large number of CpG sites *en bloc,* we designed a method for TBPseq, a multiplex PCR-combined targeted sequencing strategy, as illustrated in **Figure 1A**. From the literature and public cancer DNA methylation databases, we randomly selected 246 CpG sites at the promoters of 97 genes that are known to be frequently associated with various types of cancers. Cytosine-to-thymine converted versions of sequence stretches as bisulfite-treated template DNAs were fed to the BatchPrimer3 (You et al., 2008) to design primer pairs for multiplex PCR (Supplementary File 1). The resulting PCR products were processed for deep sequencing. Supplementary Figure S1 shows representative results of multiplex PCR and mapping of the sequenced amplicon reads harboring individual target CpGs.

We first evaluated whether TBPseq could output the amplicon data accurately and unbiasedly and was sufficient to reflect the methylation states of input DNA. As outlined in **Figure 1B**, whole genomic DNA of a 293T cell was repeatedly copied using the ϕ29 DNA polymerase. The resultant demethylated DNA was re-methylated using a CpG-specific *Sss*I methylase, treated with bisulfite, and then used in the multiplex PCR as a template. The results from amplicon sequencing showed that the mean methylation level was 60.4 ± 9.9% when the *Sss*I-remethylated DNA template was used, whereas the levels were 1.6 ± 2.5% and 29.8 ± 8.2%

[1]https://www.r-project.org/

[2]https://portal.gdc.cancer.gov

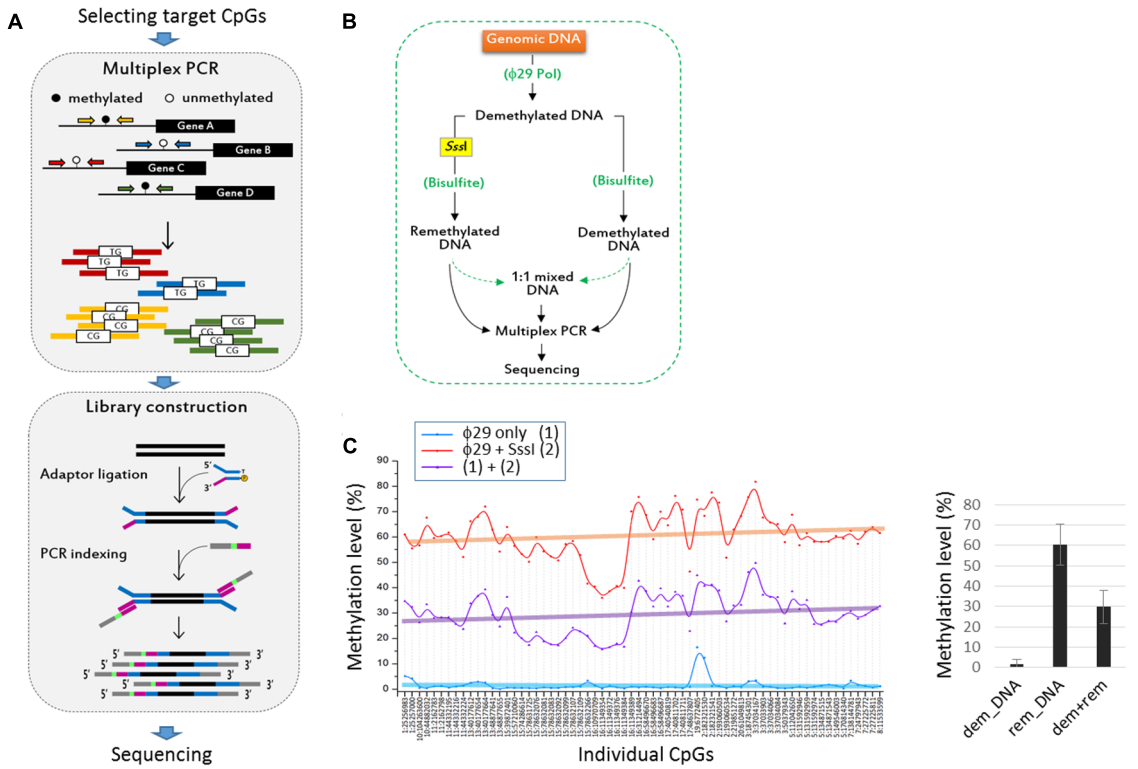

FIGURE 1 | Evaluation of the targeted bisulfite PCR sequencing (TBPseq) method. **(A)** Illustration of TBPseq method. Colored horizontal arrows denote primers for target amplification. Amplicons have methylated (5′-CG-3′) or unmethylated (5′-TG-3′) sequences for target CpGs, the ratio of which is used for calculating methylation frequencies of the target CpGs. A total of 113 primer pairs were split into six groups of about 20 pairs for separate multiplexed PCR. **(B)** Strategy for evaluating the TBPseq method. The whole genomic DNA of 293T cells was amplified using ϕ29 DNA polymerase. A half of the resulting newly synthesized and unmodified (demethylated) DNA was re-methylated *in vitro* using CpG dinucleotide-specific *Sss*I methylase. The remethylated and demethylated DNA fractions were equally treated with bisulfite and used as template in multiplex PCR with 20–25 primer pairs per reaction. Multiplex PCR was additionally performed with an equal mixture (1:1 mixed DNA) of the remethylated and demethylated DNA templates. The three different groups of amplicons were modified and differentially barcoded for Illumina sequencing. **(C)** Methylation levels of target CpG sites. Each CpG site has three different methylation levels that were obtained from demethylated DNA (ϕ29 only, blue), remethylated DNA (ϕ29 + SssI, red), and an equal mixture of them (purple). In the right panel, the mean methylation levels of target CPGs in the three DNA groups are shown (error bars, standard deviation). Individual CpG sites are indicated by their genomic position as "chromosome (chr) number:coordinate" using GRCh37/hg19 as reference genome.

when the demethylated DNA template only or an equal mixture of remethylated and demethylated DNA, respectively, was used (**Figure 1C**). The 60% methylation level obtained from the use of the remethylated DNA indicated an incomplete methylation, possibly by insufficient *Sss*I enzyme activity or *Sss*I-catalyzed cytosine-to-uracil conversion in SAM deficient condition (Bandaru et al., 1995; Zingg et al., 1996; Stier and Kiss, 2013). Nevertheless, the 30% methylation level acquired from the 1:1 mixed DNA template implied that the methylation frequencies of target CpGs at genomic regions were well-preserved even after the multiplex PCR and library preparation processes during TBPseq.

Correlation Analysis of Targeted Bisulfite PCR Sequencing Data

The target CpGs were examined in 46 cancer cell lines—3 biliary tract, 12 colon, 13 liver, 5 lung, and 13 stomach cancer cell lines (**Figure 2A**). We randomly chose these five groups of cancer cell lines and selected cancer-related CpGs, unaware of their associations with certain cancer types. With these choices, we hoped that some of the previously established cancer-cDMC matches would be exposed by our TBPseq analysis. For each cell line, duplicated sequencing libraries was produced and all libraries, containing 92 barcodes in total, were all pooled for sequencing in a single flow cell. As a result, 1.6×10^8 reads (1.6×10^6 reads on an average per sample) in sum were obtained, with the average mapping efficiency of 79.7 ± 7.7%. Of the target amplicons, 78.8% had >100 read counts while 57.6% had >1,000. Overall, the mean coverage count was 9,256 (**Figure 2B**). Target amplicons with <100 read counts were removed from the methylation analysis because they were less reproducible between the replicates. Thus, methylation data analysis was performed for 165 CpGs from 67 gene promoters.

The mean methylation levels of the 165 target CpGs varied among the cell lines, ranging from 32 to 62% (**Figure 2C**). The group methylation levels are shown in **Figure 2D**; the colon

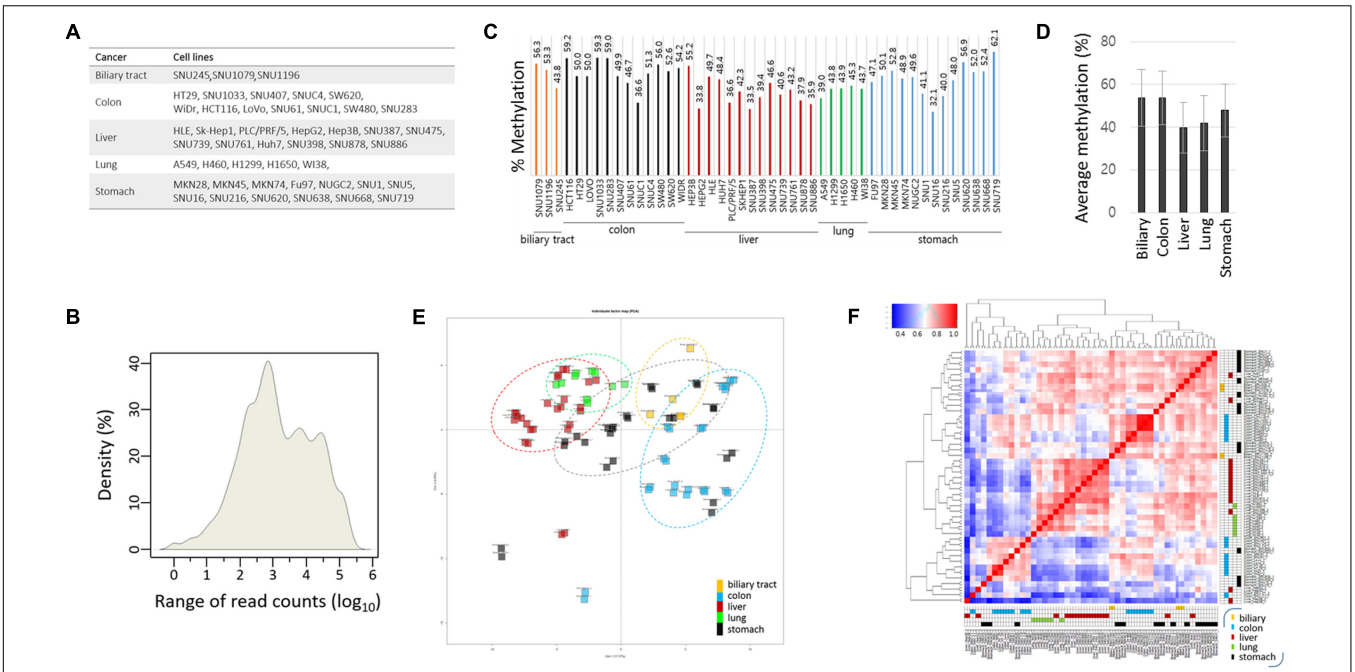

FIGURE 2 | Targeted bisulfite PCR sequencing statistics and correlation analysis. **(A)** List of cancer cell lines used in TBPseq. **(B)** Kernel density plot of read counts from the whole cancer samples. Individual target sequences have various read counts ranging from several 10s to 100s of 1000s. The mean methylation levels of target sequences in individual cancer cell lines **(C)** and in groups **(D)**. Error bars, standard deviations. **(E)** Principal compartment analysis (PCA). Different cancer cell groups are circled in different colors. The intimate proximity of sample replicates on the PCA plot demonstrates the reproducibility and reliability of TBPseq method. **(F)** Unsupervised hierarchical clustering of Pearson correlation for target CpG methylation levels among cancer cell lines. Each cancer cell line is distinctively colored by the cancer type: yellow, biliary tract cancer; blue, colon cancer; red, liver cancer; green, lung cancer; black, stomach cancer.

cancer cell group showed the highest level (52.0 ± 6.7%) whereas the liver cancer cell group (40.7 ± 7.0%) showed the lowest level of methylation. Using the methylation levels of target CpGs, we assessed the degree of correlation among the cancer cell lines. Principal component analysis (**Figure 2E**) and unsupervised hierarchical clustering analysis (**Figure 2F**) showed that both the lung and liver cancer cell lines were gathered together and strongly correlated to each other, whereas the stomach cell lines were the most dispersed showing an intra-tumor heterogeneity. Correlations between the replicates were very high, as shown by their proximity on the PCA plot, which demonstrates the reproducibility and reliability of the TBPseq method. Pearson correlation values and scatter plots between the cancer cell line groups are shown in Supplementary Figure S2. The results showed that colon cancer cells were weakly correlated with liver and lung cancer cell lines ($r < 0.77$) while stomach cell lines were, interestingly, strongly correlated to all other cancer cell lines ($r > 0.86$), regardless of the highly heterogeneous feature among the within-group cell lines.

Identification of Cancer-Specific Methylated CpG Sites

A heat map of the methylation levels revealed differentially methylated CpGs among the cancer cell lines (**Figure 3A**). Using DESeq in *R*, we identified cDMCs between the cancer cell groups, and we designated individual CpG sites by their genome position (GRCh37/hg19 as reference genome). In the comparison of the colon vs. the other cancer groups, chr5:38557143 ($FDR = 9.25 \times 10^{-13}$) and chr3:37034084 ($FDR = 2.32 \times 10^{-11}$) at the *LIFR* and *MLH1* gene promoters, respectively, were found to be differentially methylated; both CpGs were consistently hypermethylated in the colon cancer cell lines while hypomethylated in the other cell lines (**Figure 3B**). The *LIFR* CpGs were previously reported to be specifically methylated in colon cancer samples (Cho et al., 2011). The *MLH1* promoter was also shown to be heavily methylated in colon cancer samples (Kane et al., 1997; Cunningham et al., 1998; Herman et al., 1998). The colon cancer-specific methylation at *LIFR* and *MLH1* promoters was verified by combined bisulfite restriction analysis (COBRA), a method used to determine DNA methylation levels at a specific genomic locus using restriction endonucleases (Xiong and Laird, 1997; Kang et al., 2001, 2002). COBRA using *Taq*I (5′-TCGA-3′) showed that the *LIFR* promoter was methylated specifically in the colon cancer cell lines but not in the liver and lung cancer cell lines (**Figure 3C**). The distal region of the *MLH1* promoter, which corresponds to the 5′ shore of the CpG island and is adjacent to the identified *MLH1* cDMC (chr3:37034084), was shown methylated in a colon cancer-specific manner, whereas the proximal region residing within the CpG island was equally unmethylated in all cell lines examined.

Chr7:27225772 at the *HOXA11* promoter and chr17:63554340 at the *AXIN2* promoter were also detected as colon

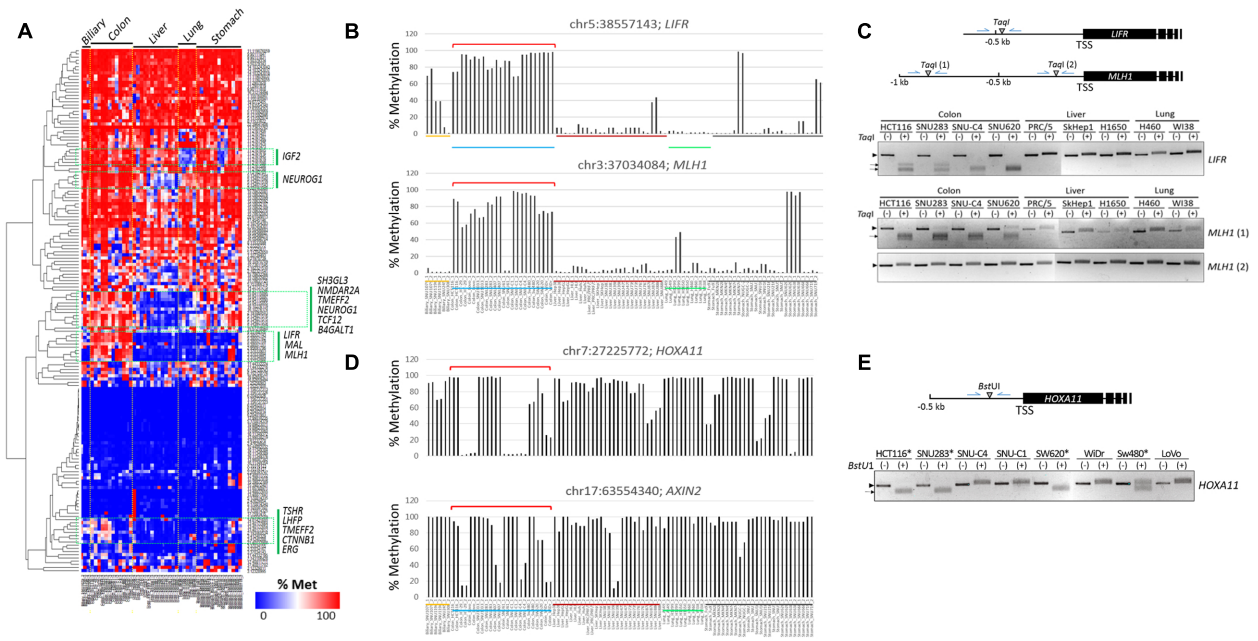

FIGURE 3 | Identification of CpG sites specifically methylated in colon cancer cell lines. **(A)** Heat map of the methylation levels of target CpGs. Target CpGs that are differentially methylated among the cell lines are indicated by green boxes with the associated gene symbols. Methylation levels of the *LIFR* and *MLH1* **(B)** and *HOXA11* and *AXIN2* **(D)** CpG sites in colon cancer cell lines. Chromosomal locations of target CpG sites are represented as the chromosome (chr) number and coordinate of the position of cytosine. Cell lines of different cancer groups are indicated in different colors below: biliary tract, colon, liver, lung, and stomach cancer cell lines are yellow, blue, dark red, green, and black, respectively. Brackets (red) denote colon cancer cell lines showing differential methylation patterns. **(C,E)** Combined bisulfite restriction analysis (COBRA). Schematics show the relative positions of the transcription start sites (TSSs) of target genes and the restriction enzyme (*Taq*I or *Bst*UI) site. Genomic DNA was treated with bisulfite to convert unmethylated cytosines to uracils, which are then amplified as thymines, and then used as a template in PCR. The PCR products were digested with the indicated restriction enzyme. If the region of interest were methylated, the PCR product would be digested. In **(E)**, only colon cancer cell lines were included, and *HOXA11* promoter-methylated cell lines are indicated by asterisks. Arrow heads and arrows indicate the band positions of intact and enzyme-digested PCR products, respectively.

cancer-specific cDMCs. However, their methylation levels were not uniform, showing extremely polarized methylation states in the colon cancer cell lines (**Figure 3D**). For example, the *HOXA11* cDMC was either unmethylated (HT-29, Lovo, SNU61, SNU-C1, and SNU-C4) or heavily methylated (HCT116, SNU1033, SNU188, SNU407, and SW620) in the colon cancer cell lines. A similar polarization of methylation states among the colon cancer cell lines was observed at the *AXIN2* cDMC. COBRA experimental results confirmed a different methylation state at the *HOXA11* promoter among the colon cancer cell lines (**Figure 3E**).

In the comparison between the liver cancer and the other cancer groups, cDMCs (*FDR* < 0.0001) were detected at the promoters of the *SPARC, NEUROG1, SH3GL3,* and *ITGA4* genes (**Figure 4A**). These cDMCs were frequently hypomethylated in the liver cancer cell lines. Lung cancer-specific cDMCs were found at the promoters of *SH3GL3, IGF2,* and *TMEFF2* (**Figure 4B**). No CpG site was identified to be specific for stomach cancer cells at *FDR* < 0.0001, which conformed to the heterogeneous character of stomach cancer cell lines (**Figures 2E,F**) and the higher correlation of the stomach cell lines with the other cancer cell lines (Supplementary Figure S2). **Table 1** lists the cancer-specific cDMCs and their associated genes.

Meta-analysis of cDMCs and Functional Validation

We performed a meta-analysis of publicly available DNA methylome data from colon ($n = 313$ for cancer samples and $n = 38$ for normal samples), liver (377 and 50), lung (843 and 74), and stomach (395 and 2) cancer patient samples in Genomic Data Commons portal (Supplementary File 2). In line with our TBPseq results, the cg03723506 and cg11291081 CpGs, which represent the Infinium (Illumina) CpG identification numbers[3] and are the same CpGs with the *LIFR* and *MLH1* cDMCs, respectively (see the **Figure 5** legend), showed a heavier methylation in a colon cancer-specific manner (**Figure 5A**). In the case of *LIFR* cg03723506, the difference in methylation level between the colon cancer and normal samples was remarkable ($p < 2.2 \times 10^{-16}$; Wilcoxon rank sum test). However, no significant differential methylation patterns at *MLH1* cg11291081 was observed between the normal controls (55.5%) and the colon cancer samples (48.9%; $p = 0.75$). We also found the expression of *MLH1* mRNA in the most colon cell lines whose cg11291081 were methylated (data not shown). Thus, the result indicates that the hypermethylation at *MLH1* cg11291081 in the colon cancer

[3]https://support.illumina.com

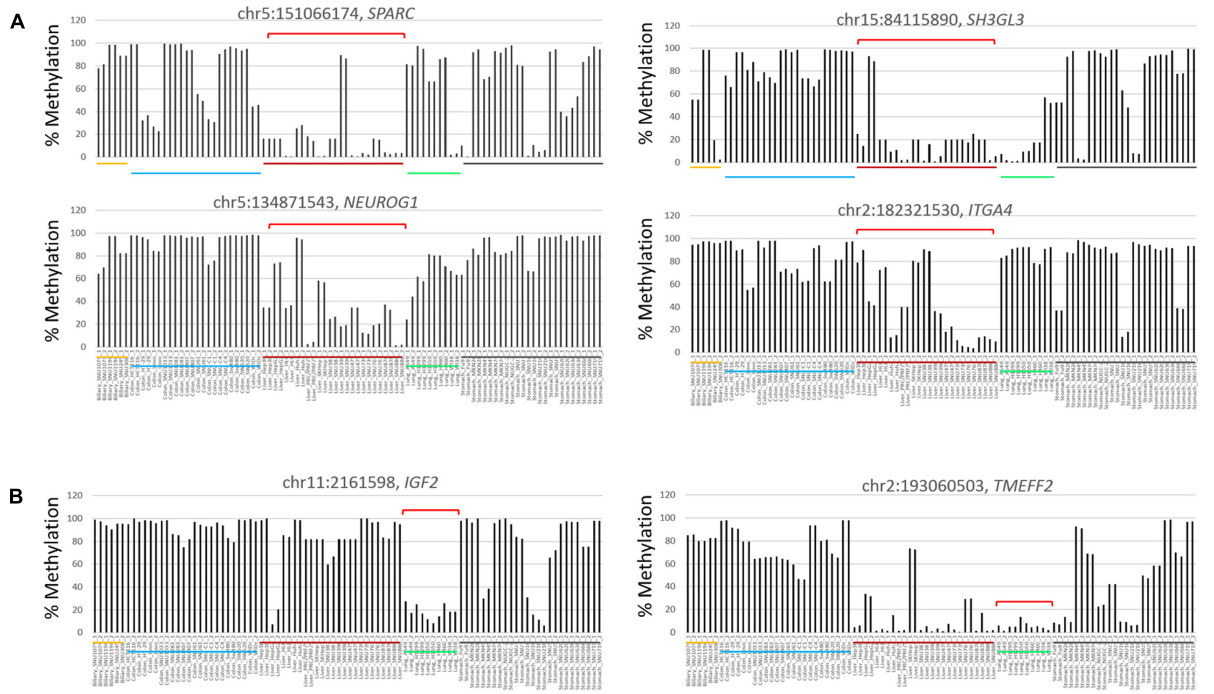

FIGURE 4 | Differentially methylated CpG sites in liver and lung cancer cell lines. Target CpGs at the *SPARC, SH3GL3, NEUROG1*, and *ITGA4* gene promoters are frequently undermethylated in liver cancer cell lines **(A)** and so are those at the *IGF2* and *TMEFF2* gene promoters in lung cancer cell lines **(B)**. Brackets (red) denote those of cell lines showing group-specific methylation patterns for indicated CpGs. Chromosomal locations of target CpG sites are represented as the chromosome (chr) number and coordinate of the position of cytosine. Each cancer cell line group is underlined below the bars (yellow, biliary tract; blue, colon; red, liver; lung, green; black, stomach cells).

cell lines occurs in a tissue-specific fashion, rather than in a cancer-specific fashion.

We next examined if the *LIFR* cg03723506 methylation was linked to the expression of the associated genes. We analyzed the colon cancer cell lines (**Figure 2A**) along with a normal colon cell line (CCD-18co) for *LIFR* promoter methylation and mRNA expression. The *LIFR* cDMC is located at the promoter region shared by the *LIFR* and *LIFR*-AS genes (**Figure 5B**). The COBRA result showed that the *LIFR* cDMC was unmethylated in the CCD-18co control cells whereas it was heavily methylated in most colon cancer cell lines (**Figure 5C**). RT-PCR result showed that both the *LIFR* and *LIFR-AS* transcripts were detected in the normal CCD-18co cells only but not in the other colon cancer cell lines (**Figure 5D**). Other non-colon cancer cell lines such as SNU449 liver cells which were not methylated at the *LIFR* cg03723506 cDMC also expressed the *LIFR* and *LIFR-AS* genes (Supplementary Figure S3). This result suggests an intimate negative correlation between the *LIFR* cg03723506 hypermethylation and the expression of its associated genes.

DISCUSSION

We developed a PCR-based targeted sequencing approach that is optimized for DNA methylation analysis. We targeted 246 CpG sites in this study, but the size and scale could be expanded, if necessary. The panel composition is highly flexible and can accommodate a variety of experimental designs, a big advantage over other methylation analysis platforms such as the array-based Infinium BeadChip. The WGBS method is, in general, conducted with a limited number of samples with coverage usually ranging from 5 to 15 times per CpG, which limits the statistical significance of the findings. Compared to this WGBS, our TBPseq method can accommodate large numbers (several 10s or more) of samples in the same flow cell and produce 10s of 1000s of read counts on an average per target CpG. In addition, TBPseq uses only selected targets for analysis, instead of the whole genome as a target, which saves time during the data analysis. As a TBPseq-like targeted methylation analysis approach, a bisulfite padlock probes sequencing (BSPP-seq) method is featured by targeted capture of bisulfite-converted DNAs, the flexibility in selecting targets, and its library-free sequencing protocol (Diep et al., 2012). However, the engine for designing padlock probes and the matching bioinformatics pipeline are unfamiliar, and the requirement of a large amount (>200 ng) of sample DNA in single BSPP-seq may limit its application to certain clinical diagnosis. Taken together, our TBPseq represents a cost-effective, high-throughput, and time-saving method capable of single-base resolution analysis. With these benefits, the TBPseq will, we hope, facilitate the exploration and development of methylation biomarkers and conduce to the improvement of cancer detection in clinics.

TABLE 1 | CpG sites differentially methylated among cancer cell groups.

Genes associated	CpG location[a]	Mean count	% Meth (± STD)[b]	FDR
Colon cancer cell lines vs. others				
LIFR	5:38557162	25837.86	82.10 (± 0.62)	2.21×10^{-13}
	5:38557159			6.75×10^{-13}
	5:38557143			9.25×10^{-13}
MLH1	3:37033903	23971.48	69.50 (± 11.27)	3.19×10^{-11}
	3:37033894			3.19×10^{-11}
	3:37034084			2.32×10^{-11}
	3:37034066			1.24×10^{-6}
HOXA11	7:27225772	66302.95	52.07	1.61×10^{-10}
AXIN2	17:63554340	81734.54	70.93 (± 0.61)	1.10×10^{-8}
	17:63554353			1.67×10^{-7}
PPARG	3:12329011	52496.36	40.96	1.19×10^{-5}
Liver cancer cell lines vs. others				
SH3GL3	15:84115855	34259.59	29.03 (± 1.44)	1.30×10^{-13}
	15:84115890			1.87×10^{-9}
	15:84115895			1.45×10^{-5}
SPARC	5:151066174	45657.91	23.92	8.03×10^{-12}
NEUROG1	5:134871543	63209.05	34.05 (± 11.02)	2.28×10^{-10}
	5:134871539			1.08×10^{-7}
	5:134871515			1.67×10^{-7}
	5:134871510			4.10×10^{-7}
	5:134871516			1.23×10^{-6}
	5:134871509			4.44×10^{-6}
	5:134871544			2.67×10^{-5}
	5:134871540			4.68×10^{-5}
RB1	13:48877655	2194.00	11.73	2.45×10^{-6}
ITGA4	2:182321530	61811.37	39.17	6.54×10^{-6}
NPM1	5:170814340	2871.80	16.06 (± 3.79)	1.09×10^{-5}
	5:170814379			7.65×10^{-5}
RB1	13:48877641	2047.34	7.95	1.09×10^{-5}
NMDAR2A	16:10276119	28688.10	13.47	1.43×10^{-5}
CDKN2A	9:21975739	58680.32	77.24	3.93×10^{-5}
CBLB	3:105587507	2925.30	19.60	3.96×10^{-5}
KLF5	13:73632762	89833.42	81.36	5.18×10^{-5}
PAX3	2:223163989	64484.74	43.06	6.30×10^{-5}
Lung cancer cell lines vs. others				
IGF2	11:2161605	67594.01	26.45 (± 2.24)	4.66×10^{-22}
	11:2161598			2.82×10^{-20}
	11:2161586			5.51×10^{-13}
TMEFF2	2:193060503	35910.80	5.60	2.42×10^{-7}
FHIT	3:61237270	582.14	2.90	7.29×10^{-6}
LHFP	13:40177664	15799.21	0.50 (± 0.08)	1.91×10^{-5}
	13:40177654			9.83×10^{-5}

[a]*Chromosome number and location is separated by colon. It refers to GRCh37/hg19 human reference genome.* [b]*Mean % methylation ± standard deviation.*

Targeted bisulfite-PCR-sequencing produced a broad range (from several 10s to 150,000) of reads per target, which is likely to depend on the annealing strengths of primer pairs. Primer pairs with a low performance pose a problem, leading to insufficient reads; however, those with an extremely high performance could also be problematic because vigorous amplifications of target sequences by strong primers could indirectly interfere with the weak primer-mediated amplifications of other target sequences by exploiting most of the PCR resources (McPherson and Hames, 1995). This is an especially serious concern when performing multiplexed PCR (Sninsky et al., 1999). We are currently trying to devise a method to evenly produce target amplicons, for example, by optimizing combinations of primer pairs for multiplexing. Fortunately, this is feasible because our TBPseq primer panel is highly flexible and easily reconfigurable to various situations and requests.

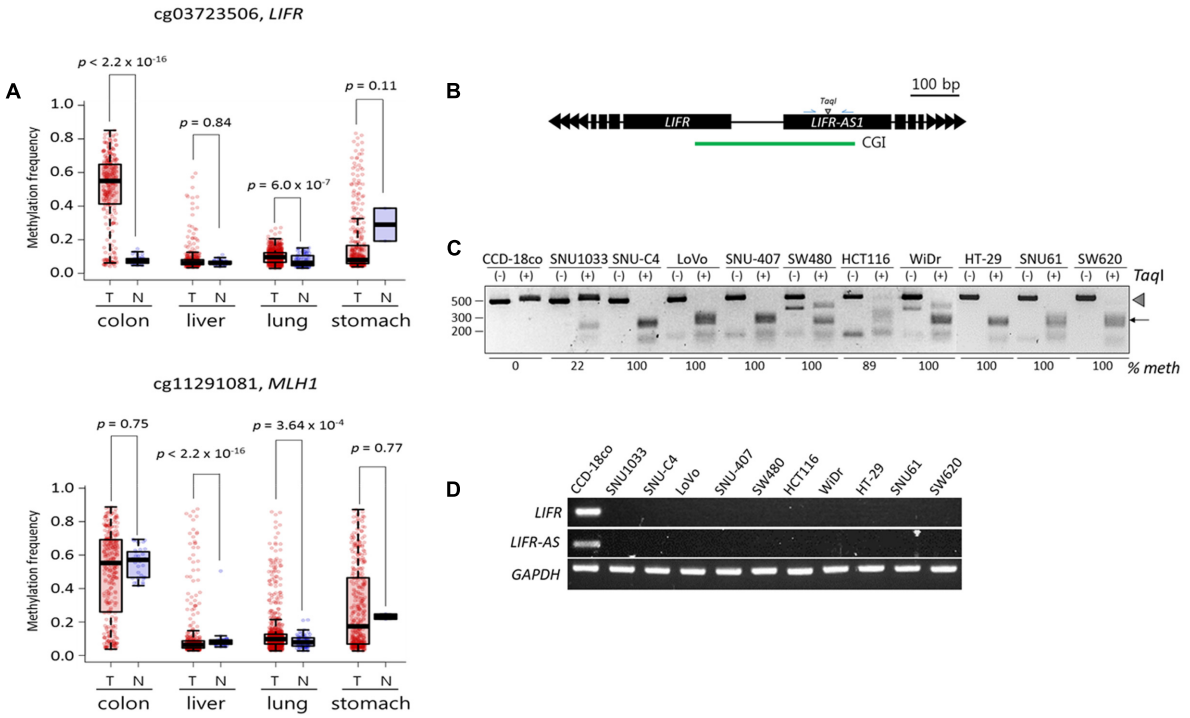

FIGURE 5 | Validation of the *LIFR* promoter methylation for cancer specificity and its relationship with the expression of associated genes. **(A)** DNA methylation levels of target CpGs in public cancer methylome data (Infinium 450K BeadChip array) of four cancer types: colorectal (n = 313 for cancer samples and n = 38 for normal samples), liver (377 and 50), lung (843 and 74), and stomach (395 and 2) cancers. Infinium CpG identification numbers (IDs) together with the associated gene names are shown; the Infinium IDs cg03723506 and cg11291081 indicate chr5:38557143 and chr3:37033894, respectively, in the **Figure 3B**. Statistical significance was calculated using Wilcoxon rank sum test. T: tumor samples, N: normal samples. **(B)** Schematic drawing of COBRA region at the *LIFR* promoter. Blue arrows, primers. CGI, CpG island (green line). **(C)** COBRA analysis. Genomic DNA was extracted from each colon cancer cell lines along with a normal control colon cell line (CCD-18co) and subjected to COBRA using the *TaqI* enzyme to examine the methylation state at the *LIFR* gene promoter. Arrowhead and arrow indicate the positions of intact and *TaqI*-digested DNA fragments, respectively. The fraction (% meth) of methylated DNA was measured by band intensity analysis and noted under each cell line. **(D)** RT-PCR. The same cancer cell lines used in COBRA **(C)** were subjected to RT-PCR to measure the transcript levels of the *LIFR* and *LIFR-AS* genes.

We designed multiplexing primers following the principle that each amplicon should be 60–100 bp in length and contain a single CpG site, if possible. This is because the presence of multiple CpG sites in a small-sized target sequence could prevent the accurate assessment of methylation frequency, as the base composition and the GC content of template DNA after bisulfite conversion would greatly differ by the methylation level. However, the requirement of minimal CpGs within the amplicon sequences for TBPseq analysis raises questions regarding which CpG should be preferred among many adjacent CpGs and how representative the selected CpG(s) would be for the region of interest. This is an important concern especially when a methylation analysis platform is used to examine a group of representative CpGs, as in TBPseq and Infinium BeadChip. There were, in fact, some infrequent cases in which two adjacent CpGs within a single amplicon were oppositely methylated (unpublished observation). A possible explanation of this is that a protein may bind to the DNA region to block methylation one of the two CpGs. Therefore, although such cases were scarce and restricted to only certain regions, based on our results, inclusion of multiple CpGs as targets are recommended for the accurate measurement of the methylation level of a certain genomic region as well as adherence to rigorous validation processes. In order to choose an appropriate CpG, the one that has an Infinium BeadChip CpG ID number would be a better choice, because the majority of public methylome data have been obtained from the Infinium BeadChip platform and are referred to by their Infinium CpG ID. By sharing the same CpGs with the Infinium platform in the methylation analysis, our data could be directly and conveniently compared with the big public data.

In this study, we separately and randomly selected five groups of cancer cell lines and 246 cancer-related CpGs, irrespective of the specific relationships of certain CpGs to certain cancer types, among them. Because of this, we could perform a blind experiment to test whether TBPseq is able to expose some known cDMC-cancer type associations that are well-established as cancer methylation markers, the results of which could demonstrate the competence of the TBPseq method. Conforming to our expectation, TBPseq succeeded in determining the colon cancer-*LIFR* CpG matches, which demonstrates high efficiency of TBPseq technology in target-based high-throughput methylation analysis.

As shown in **Figure 3**, the *LIFR* promoter methylation was detected only in the colon cancer cell lines and not in other cancer cell lines such as biliary tract, liver, lung, and stomach cancer cells. This result is supported by a previous report of colon cancer-specific methylation at the *LIFR* promoter (Cho et al., 2011), although that study was not expanded to survey other cancer samples. Our results from the analysis of cancer cell lines (**Figures 5C,D**) as well as the meta-analysis of public DNA methylome data (**Figure 5A**) unambiguously showed increased methylation levels at the *LIFR* gene promoter in colorn cancer samples compared to other types of cancers and normal colon samples. Furthermore, the promoter methylation correlated with downregulation of the *LIFR* gene expression, which leads to a speculation of the importance of *LIFR* suppression in the development of colon cancer development. Our results suggest that the *LIFR* cDMCs may not only be used as a DNA methylation biomarker for cancer identification, but by extension, for cancer typing as well.

In addition to the *LIFR* cDMC, the *MLH1* cg11291081 cDMC was found heavily methylated in the colon cancer cell lines while it was only barely methylated in the other cancer cell lines (**Figure 3C**), which misled us to consider it as a colon cancer-specific methylation marker. We finally concluded the cg11291081 was variously methylated in a tissue-specific manner after we found it was ∼50% methylated in the normal colon samples but ∼8% in the normal liver and lung samples (**Figure 5A**). Although the *MLH1* cg11291081 hypermethylation turned out to be tissue-specific, instead of cancer-specific, it did not mean that our TBPseq failed its task, because the method succeeded in pointing the cg11291081 anyway as a differential marker specific to the colon cancer cell lines against the other cancer cell lines. Meanwhile, the hypermethylation at the *MLH1* promoter has been well-known in colon cancers (Kane et al., 1997; Cunningham et al., 1998; Herman et al., 1998; Simpkins et al., 1999; Toyota et al., 1999; Nakagawa et al., 2001; Wallner et al., 2006; Weisenberger et al., 2006; Ahlquist et al., 2008; Hinoue et al., 2012; Li et al., 2013). These earlier studies primarily analyzed the body of *MLH1* promoter CGI, whereas the cg11291081 site examined in this study resides in the shore of the CGI. The different CpG positions may explain the different results between ours and those earlier studies.

In the very near future, through meta-analysis and co-methylation analysis of public cancer methylome data, packs of cDMC markers that are significantly associated with certain types of cancers could be collected. We envision targeting these groups of cDMC markers and using TBPseq to analyze patient cancer samples. Those results could serve as important reference material for determining cancer diagnosis and prognosis, and could be extended for the development of a therapeutic plan.

AUTHOR CONTRIBUTIONS

KJ and JP performed the experiments. BM and KJ carried out bioinformatic and statistical analysis. Y-KK and KJ had designed the experiments, interpreted the results and written the manuscript. All authors read and approved the final manuscript.

FUNDING

This work was supported by grants from the National Research Foundation of Korea (015R1A2A2A01003117), National Research Foundation-Science Research Center program (2011-0030049), KIOM program (K16130), and KRIBB program.

ACKNOWLEDGMENT

We thank G. Kang, Y. I. Yeom, and E. Cho for the cancer cell genomic DNAs.

SUPPLEMENTARY MATERIAL

The Supplementary Material for this article can be found online at: http://journal.frontiersin.org/article/10.3389/fgene.2017.00097/full#supplementary-material

REFERENCES

Ahlquist, T., Lind, G. E., Costa, V. L., Meling, G. I., Vatn, M., Hoff, G. S., et al. (2008). Gene methylation profiles of normal mucosa, and benign and malignant colorectal tumors identify early onset markers. *Mol. Cancer* 7:94. doi: 10.1186/1476-4598-7-94

Bandaru, B., Wyszynski, M., and Bhagwat, A. S. (1995). HpaII methyltransferase is mutagenic in *Escherichia coli*. *J. Bacteriol.* 177, 2950–2952. doi: 10.1128/jb.177.10.2950-2952.1995

Bibikova, M., Barnes, B., Tsan, C., Ho, V., Klotzle, B., Le, J. M., et al. (2011). High density DNA methylation array with single CpG site resolution. *Genomics* 98, 288–295. doi: 10.1016/j.ygeno.2011.07.007

Bock, C., Kiskinis, E., Verstappen, G., Gu, H., Boulting, G., Smith, Z. D., et al. (2011). Reference maps of human ES and iPS cell variation enable high-throughput characterization of pluripotent cell lines. *Cell* 144, 439–452. doi: 10.1016/j.cell.2010.12.032

Cho, S., Park, J. S., and Kang, Y. K. (2014). AGO2 and SETDB1 cooperate in promoter-targeted transcriptional silencing of the androgen receptor gene. *Nucleic Acids Res.* 42, 13545–13556. doi: 10.1093/nar/gku788

Cho, S. M., Park, J. S., Min, B., Kwon, S., and Kang, Y. K. (2015). Rapid generation of secondary fibroblasts through teratoma formation. *Biotechniques* 59, 34–41. doi: 10.2144/000114309

Cho, Y. G., Chang, X., Park, I. S., Yamashita, K., Shao, C., Ha, P. K., et al. (2011). Promoter methylation of leukemia inhibitory factor receptor gene in colorectal carcinoma. *Int. J. Oncol.* 39, 337–344. doi: 10.3892/ijo.2011.1050

Cunningham, J. M., Christensen, E. R., Tester, D. J., Kim, C. Y., Roche, P. C., Burgart, L. J., et al. (1998). Hypermethylation of the hMLH1 promoter in colon cancer with microsatellite instability. *Cancer Res.* 58, 3455–3460.

Diep, D., Plongthongkum, N., Gore, A., Fung, H. L., Shoemaker, R., and Zhang, K. (2012). Library-free methylation sequencing with bisulfite padlock probes. *Nat. Methods* 9, 270–272. doi: 10.1038/nmeth.1871

Down, T. A., Rakyan, V. K., Turner, D. J., Flicek, P., Li, H., Kulesha, E., et al. (2008). A Bayesian deconvolution strategy for immunoprecipitation-based DNA methylome analysis. *Nat. Biotechnol.* 26, 779–785. doi: 10.1038/nbt1414

Feber, A., Wilson, G. A., Zhang, L., Presneau, N., Idowu, B., Down, T. A., et al. (2011). Comparative methylome analysis of benign and malignant peripheral nerve sheath tumors. *Genome Res.* 21, 515–524. doi: 10.1101/gr.109678.110

Herman, J. G., Umar, A., Polyak, K., Graff, J. R., Ahuja, N., Issa, J. P., et al. (1998). Incidence and functional consequences of hMLH1 promoter hypermethylation in colorectal carcinoma. *Proc. Natl. Acad. Sci. U.S.A.* 95, 6870–6875. doi: 10.1073/pnas.95.12.6870

Heyn, H., and Esteller, M. (2012). DNA methylation profiling in the clinic: applications and challenges. *Nat. Rev. Genet.* 13, 679–692. doi: 10.1038/nrg3270

Hinoue, T., Weisenberger, D. J., Lange, C. P., Shen, H., Byun, H. M., Van Den Berg, D., et al. (2012). Genome-scale analysis of aberrant DNA methylation in colorectal cancer. *Genome Res.* 22, 271–282. doi: 10.1101/gr.117523.110

Kane, M. F., Loda, M., Gaida, G. M., Lipman, J., Mishra, R., Goldman, H., et al. (1997). Methylation of the hMLH1 promoter correlates with lack of expression of hMLH1 in sporadic colon tumors and mismatch repair-defective human tumor cell lines. *Cancer Res.* 57, 808–811.

Kang, Y. K., Koo, D. B., Park, J. S., Choi, Y. H., Chung, A. S., Lee, K. K., et al. (2001). Aberrant methylation of donor genome in cloned bovine embryos. *Nat. Genet.* 28, 173–177. doi: 10.1038/88903

Kang, Y. K., Park, J. S., Koo, D. B., Choi, Y. H., Kim, S. U., Lee, K. K., et al. (2002). Limited demethylation leaves mosaic-type methylation states in cloned bovine pre-implantation embryos. *EMBO J.* 21, 1092–1100. doi: 10.1093/emboj/21.5.1092

Khamas, A., Ishikawa, T., Mogushi, K., Iida, S., Ishiguro, M., Tanaka, H., et al. (2012). Genome-wide screening for methylation-silenced genes in colorectal cancer. *Int. J. Oncol.* 41, 490–496. doi: 10.3892/ijo.2012.1500

Krueger, F., and Andrews, S. R. (2011). Bismark: a flexible aligner and methylation caller for Bisulfite-Seq applications. *Bioinformatics* 27, 1571–1572. doi: 10.1093/bioinformatics/btr167

Laurent, L., Wong, E., Li, G., Huynh, T., Tsirigos, A., Ong, C. T., et al. (2010). Dynamic changes in the human methylome during differentiation. *Genome Res.* 20, 320–331. doi: 10.1101/gr.101907.109

Li, H., Du, Y., Zhang, D., Wang, L. N., Yang, C., Liu, B., et al. (2012). Identification of novel DNA methylation markers in colorectal cancer using MIRA-based microarrays. *Oncol. Rep.* 28, 99–104. doi: 10.3892/or.2012.1779

Li, M., Chen, W. D., Papadopoulos, N., Goodman, S. N., Bjerregaard, N. C., Laurberg, S., et al. (2009). Sensitive digital quantification of DNA methylation in clinical samples. *Nat. Biotechnol.* 27, 858–863. doi: 10.1038/nbt.1559

Li, X., Yao, X., Wang, Y., Hu, F., Wang, F., Jiang, L., et al. (2013). MLH1 promoter methylation frequency in colorectal cancer patients and related clinicopathological and molecular features. *PLoS ONE* 8:e59064. doi: 10.1371/journal.pone.0059064

Lister, R., O'malley, R. C., Tonti-Filippini, J., Gregory, B. D., Berry, C. C., Millar, A. H., et al. (2008). Highly integrated single-base resolution maps of the epigenome in *Arabidopsis*. *Cell* 133, 523–536. doi: 10.1016/j.cell.2008.03.029

Lister, R., Pelizzola, M., Dowen, R. H., Hawkins, R. D., Hon, G., Tonti-Filippini, J., et al. (2009). Human DNA methylomes at base resolution show widespread epigenomic differences. *Nature* 462, 315–322. doi: 10.1038/nature08514

McPherson, M. J., and Hames, B. D. (1995). *PCR 2: A Practical Approach*. Oxford: Oxford University Press.

Meissner, A., Gnirke, A., Bell, G. W., Ramsahoye, B., Lander, E. S., and Jaenisch, R. (2005). Reduced representation bisulfite sequencing for comparative high-resolution DNA methylation analysis. *Nucleic Acids Res.* 33, 5868–5877. doi: 10.1093/nar/gki901

Min, B., Cho, S., Park, J. S., Jeon, K., and Kang, Y. K. (2016). The HIST1 locus escapes reprogramming in cloned bovine embryos. *G3* 6, 1365–1371. doi: 10.1534/g3.115.026666

Mitchell, S. M., Ross, J. P., Drew, H. R., Ho, T., Brown, G. S., Saunders, N. F., et al. (2014). A panel of genes methylated with high frequency in colorectal cancer. *BMC Cancer* 14:54. doi: 10.1186/1471-2407-14-54

Model, F., Osborn, N., Ahlquist, D., Gruetzmann, R., Molnar, B., Sipos, F., et al. (2007). Identification and validation of colorectal neoplasia-specific methylation markers for accurate classification of disease. *Mol. Cancer Res.* 5, 153–163. doi: 10.1158/1541-7786.MCR-06-0034

Nakagawa, H., Nuovo, G. J., Zervos, E. E., Martin, E. W. Jr., Salovaara, R., Aaltonen, L. A., et al. (2001). Age-related hypermethylation of the 5' region of MLH1 in normal colonic mucosa is associated with microsatellite-unstable colorectal cancer development. *Cancer Res.* 61, 6991–6995.

Naumov, V. A., Generozov, E. V., Zaharjevskaya, N. B., Matushkina, D. S., Larin, A. K., Chernyshov, S. V., et al. (2013). Genome-scale analysis of DNA methylation in colorectal cancer using Infinium HumanMethylation450 BeadChips. *Epigenetics* 8, 921–934. doi: 10.4161/epi.25577

Nikolaidis, G., Raji, O. Y., Markopoulou, S., Gosney, J. R., Bryan, J., Warburton, C., et al. (2012). DNA methylation biomarkers offer improved diagnostic efficiency in lung cancer. *Cancer Res.* 72, 5692–5701. doi: 10.1158/0008-5472.CAN-12-2309

Oh, S. A., Yang, I., Hahn, Y., Kang, Y. K., Chung, S. K., and Jeong, S. (2015). SiNG-PCRseq: accurate inter-sequence quantification achieved by spiking-in a neighbor genome for competitive PCR amplicon sequencing. *Sci. Rep.* 5:11879. doi: 10.1038/srep11879

Park, M., Min, B., Jeon, K., Cho, S., Park, J. S., Kim, J., et al., (2017). Age-associated chromatin relaxation is enhanced in Huntington's disease mice. *Aging* 9, 803–822. doi: 10.18632/aging.101193

Quinlan, A. R. (2002). BEDTools: the swiss-army tool for genome feature analysis. *Curr. Protoc. Bioinformatics* 47, 11.12.1–34. doi: 10.1002/0471250953.bi1112s47

Sandoval, J., Heyn, H., Moran, S., Serra-Musach, J., Pujana, M. A., Bibikova, M., et al. (2011). Validation of a DNA methylation microarray for 450,000 CpG sites in the human genome. *Epigenetics* 6, 692–702. doi: 10.4161/epi.6.6.16196

Serre, D., Lee, B. H., and Ting, A. H. (2010). MBD-isolated genome sequencing provides a high-throughput and comprehensive survey of DNA methylation in the human genome. *Nucleic Acids Res.* 38, 391–399. doi: 10.1093/nar/gkp992

Simmer, F., Brinkman, A. B., Assenov, Y., Matarese, F., Kaan, A., Sabatino, L., et al. (2012). Comparative genome-wide DNA methylation analysis of colorectal tumor and matched normal tissues. *Epigenetics* 7, 1355–1367. doi: 10.4161/epi.22562

Simpkins, S. B., Bocker, T., Swisher, E. M., Mutch, D. G., Gersell, D. J., Kovatich, A. J., et al. (1999). MLH1 promoter methylation and gene silencing is the primary cause of microsatellite instability in sporadic endometrial cancers. *Hum. Mol. Genet.* 8, 661–666. doi: 10.1093/hmg/8.4.661

Sninsky, J. J., Innis, M. A., and Gelfand, D. H. (1999). *PCR Applications: Protocols for Functional Genomics*. San Diego, CA: Academic Press.

Stier, I., and Kiss, A. (2013). Cytosine-to-uracil deamination by SssI DNA methyltransferase. *PLoS ONE* 8:e79003. doi: 10.1371/journal.pone.0079003

Toyota, M., Ahuja, N., Ohe-Toyota, M., Herman, J. G., Baylin, S. B., and Issa, J. P. (1999). CpG island methylator phenotype in colorectal cancer. *Proc. Natl. Acad. Sci. U.S.A.* 96, 8681–8686. doi: 10.1073/pnas.96.15.8681

Wallner, M., Herbst, A., Behrens, A., Crispin, A., Stieber, P., Goke, B., et al. (2006). Methylation of serum DNA is an independent prognostic marker in colorectal cancer. *Clin. Cancer Res.* 12, 7347–7352. doi: 10.1158/1078-0432.CCR-06-1264

Weisenberger, D. J., Siegmund, K. D., Campan, M., Young, J., Long, T. I., Faasse, M. A., et al. (2006). CpG island methylator phenotype underlies sporadic microsatellite instability and is tightly associated with BRAF mutation in colorectal cancer. *Nat. Genet.* 38, 787–793. doi: 10.1038/ng1834

Xiong, Z., and Laird, P. W. (1997). COBRA: a sensitive and quantitative DNA methylation assay. *Nucleic Acids Res.* 25, 2532–2534. doi: 10.1093/nar/25.12.2532

You, F. M., Huo, N., Gu, Y. Q., Luo, M. C., Ma, Y., Hane, D., et al. (2008). BatchPrimer3: a high throughput web application for PCR and sequencing primer design. *BMC Bioinformatics* 9:253. doi: 10.1186/1471-2105-9-253

Zingg, J. M., Shen, J. C., Yang, A. S., Rapoport, H., and Jones, P. A. (1996). Methylation inhibitors can increase the rate of cytosine deamination by (cytosine-5)-DNA methyltransferase. *Nucleic Acids Res.* 24, 3267–3275. doi: 10.1093/nar/24.16.3267

Conflict of Interest Statement: The authors declare that the research was conducted in the absence of any commercial or financial relationships that could be construed as a potential conflict of interest.

frontiers in Genetics

PERSPECTIVE
published: 27 November 2017
doi: 10.3389/fgene.2017.00179

The Epigenetic Cytocrin Pathway to the Nucleus. Epigenetic Factors, Epigenetic Mediators, and Epigenetic Traits. A Biochemist Perspective

Gemma Navarro[1,2], *Nuria Franco*[3], *Eva Martínez-Pinilla*[4*] and *Rafael Franco*[2,5*]

[1] Department of Biochemistry and Physiology, Pharmacy School, Universitat de Barcelona, Barcelona, Spain, [2] Centro de Investigación en Red, Enfermedades Neurodegenerativas, Instituto de Salud Carlos III, Madrid, Spain, [3] Can Sunyolet, Martorell, Spain, [4] Departamento de Morfología y Biología Celular, Facultad de Medicina, Instituto de Neurociencias del Principado de Asturias, Universidad de Oviedo, Asturias, Spain, [5] Molecular Neurobiology Laboratory, Department of Biochemistry and Molecular Biomedicine, University of Barcelona, Barcelona, Spain

A single word, Epigenetics, underlies one exciting subject in today's Science, with different sides and with interactions with philosophy. The apparent trivial description includes everything in between genotype and phenotype that occurs for a given unique DNA sequence/genome. This Perspective article first presents an historical overview and the reasons for the lack of consensus in the field, which derives from different interpretations of the diverse operative definitions of Epigenetics. In an attempt to reconcile the different views, we propose a novel concept, the "cytocrin system." Secondly, the article questions the inheritability requirement and makes emphasis in the epigenetic mechanisms, known or to be discovered, that provide hope for combating human diseases. Hopes in cancer are at present in deep need of deciphering mechanisms to support *ad hoc* therapeutic approaches. Better perspectives are for diseases of the central nervous system, in particular to combat neurodegeneration and/or cognitive deficits in Alzheimer's disease. Neurons are post-mitotic cells and, therefore, epigenetic targets to prevent neurodegeneration should operate in non-dividing diseased cells. Accordingly, epigenetic-based human therapy may not need to count much on transmissible potential.

Keywords: nucleocrin, thermodynamics, state variables, inheritability, therapy, Alzheimer's disease, cancer, tumor therapy

OPEN ACCESS

Edited by:
Trygve Tollefsbol, University of Alabama at Birmingham, United States

Reviewed by:
Cinzia Allegrucci, University of Nottingham, United Kingdom
Mojgan Rastegar, University of Manitoba, Canada

***Correspondence:**
Eva Martínez-Pinilla
martinezpinillaeva@gmail.com
Rafael Franco
rfranco@ub.edu

Specialty section:
This article was submitted to Epigenomics and Epigenetics, a section of the journal Frontiers in Genetics

Received: *15 September 2017*
Accepted: *06 November 2017*
Published: *27 November 2017*

Citation:
Navarro G, Franco N, Martínez-Pinilla E and Franco R (2017) The Epigenetic Cytocrin Pathway to the Nucleus. Epigenetic Factors, Epigenetic Mediators, and Epigenetic Traits. A Biochemist Perspective. Front. Genet. 8:179. doi: 10.3389/fgene.2017.00179

ANCIENT ORIGINS

Discovery in the 1950s of the double helical structure of the DNA opened the era of everything being explained by Genetics/Molecular Biology, i.e., essentially in terms of the sequence of the genome. The lack of responses for the varied phenotypic (environmental, physiological, etc.,) aspects displayed by living beings has led to the fashionable "Epigenetics era." For many scientists, the field is recent and epigenetic mechanisms consist of modifying the structure of histones and of DNA methylation patterns. However, the field has ancient and appealing origins and it contains more faces/cornerstones than usually considered. This Perspective article attempts to give a holistic view of factors and players in Epigenetics. The relevant goal to achieve epigenetic-based therapies probably awaits discovering essential clues and looking at them under an appropriate perspective.

Epigenetics' precursor word, "epigenesis," was used to confront a current of thought (alive for many centuries), which assumed that different parts of the body of mammals were pre-formed in the spermatozoon (*preformation*). Both Aristotle and William Harvey who were born, respectively, 384 years before Christ and in 1578, share recognition for inventing "epigenesis." The first putted a name (in Greek) to define the development from, for instance, a chicken egg to a chick with beak, legs, wings, etc., The second coined the English word for describing the same concept. A recent review shows the origins and evolution from epigenesis to epigenetics in a very attractive way (Deichmann, 2016). In the first part of the twentieth Century, the embryologist Conrad Waddington coined the term "Epigenetics" and, later on, funded the first "epigenetics laboratory."

The term may be used as an adjective or as a noun. Riggs et al. (1996) as quoted in Haig (2004) defined epigenetics (noun) as: "*the study of mitotically and/or meiotically heritable changes in gene function that cannot be explained by changes in DNA sequence*." A second definition was provided by Herring (1993) as quoted in Haig (2004): "*the entire series of interactions among cells and cell products which leads to morphogenesis and differentiation*." Then, epigenetic may be used as an adjective of any non-genetic mechanism underlying morphogenesis and differentiation. The last sentence in the abstract of the inspirational Felsenfeld (2014) review states: "*Recent discoveries about the role of these mechanisms in early development may make it desirable to return to the original definition of epigenetics*." As mentioned in Deichmann (2016), Waddington defined Epigenetics as "*the whole complex of developmental processes that lie between genotype and phenotype*." We think that this definition applies to both tissue-specific phenotypes under development and for mechanisms providing phenotypic diversity in adults, for instance, among genotype-identical twins that are subject to different environmental, life-styles, etc., constraints.

Surely, it is worth reading seminal papers and books on this matter (Waddington, 1939, 1942, 1956; Haig, 2004; Felsenfeld, 2014) some of which are quite old (i.e., pioneering) and for this reason not included in the PubMed database. In particular, one article with a suggestive title "*The (dual) origin of epigenetics*" (Haig, 2004) guides the reader on how to start confronting the diverse epigenetic faces. Recommendable is also to take into account the sections devoted to Epigenetics in the book on the "four dimensions" of Evolution by Jablonka and Lamb (2002).

EPIGENETIC FACTORS

Britannica encyclopedia's definition of epigenetics "*the study of the chemical modification of specific genes or gene-associated proteins of an organism*" beautifully summarizes today's more fashionable epigenetic traits, namely DNA methylation and histone acetylation. The first one is a chemical modification that regulates gene expression i.e., that contributes to turn genes on or off. Analogously, post-translational modification (acetylation but also methylation) of histones, which are proteins that directly interact with DNA, is a chemical mechanism with significant impact on gene regulation. These and other similar -though less studied- mechanisms operate in the nucleus, close to DNA. Quite unlikely for histone acetylation marks, DNA methylation patterns may be clonally inherited, i.e., they may pass to daughter cells, meaning that epigenetic factors in a liver cell are transmitted to another liver cell, or the other way around: upon mitosis of a kidney/muscle/etc. cell, some DNA methylation traits are maintained in the two arising cells, i.e., they are clonally inherited. Recent epigenetic markers impacting on gene expression regulation are exosomes and atypical RNAs: micro RNAs (miRNAs) and long non-coding RNAs. At present, it is not known whether these factors may be clonally inherited but, importantly, exosomes are acting as endocrine factors. miRNAs are described in mammalian body fluids and, by definition, they are also endocrine factors. By the same token, can classical endocrine factors, which do regulate gene expression in target cells, be considered epigenetic factors?

THE POOR KNOWLEDGE ON MECHANISMS

Today's fashionable epigenetic traits and the so-called epigenome are descriptors. A serious limitation to understand the real relevance of specific epigenetic traits is the lack of relevant information on mechanisms. For instance, why there are so many histone deacetylase genes and why, how and by whom DNA methyltransferases/demethylases and histone acetyltransferases/deacetylases become activated and deactivated. Also, the underlying mechanisms of the novel epigenetic mediators are still very obscure (Wiklund et al., 2010; Celluzzi and Masotti, 2016; Lange et al., 2017). We consider relevant that miRNAs and exosomes may act under endocrine paradigms. In fact, they are produced in a given organ/cell and reach another one by traveling via body fluids. In the case of exosomes, the gene regulation in the target cell(s) may be achieved by means of its RNA but also by other mediators that are contained in these vesicles. Accordingly, we find no reason to consider that hormonal regulation does not have epigenetic character, especially if we take into account that the endocrine regulation by which hormones act via receptors to affect gene expression is one of the best-known mechanisms of gene expression regulation.

THE CYTOCRIN SYSTEM. EPIGENETICS WITHIN A WHOLE-BODY FRAMEWORK

Hormonal regulation in mammals is categorized as endocrine, paracrine and/or autocrine. Regulation of cell phenotype in unicellular organisms by extracellular factors (hormones or nutrients) can only be autocrine, but the word is misleading since some of the regulators are produced by the cell while others are provided by the medium/environment. Actually, there is a need to denote the single-cell equivalent to endocrine system. Whereas, the suffix "crine" denotes something that is released to act from the outside, the cell machinery integrates and conveys all kind of extracellular signals to the cytoplasm and to the nucleus to regulate gene expression. We consider that the suffix

"crin," which refers to something that goes down as the crin of an animal, may be appropriate to describe this phenomenon in a general way. The underlying idea is to consider "crin" anything that goes from membranes inwards and can be applied to everything confined within a membrane (e.g., cell, nucleus, or mitochondria). Accordingly, the "cytocrin system" would describe the top-down effect of the different molecules impacting a unicellular organism or a single cell. Similarly, "nucleocrin" would describe the effect of the factors conveying cytoplasmic signals reaching the nucleus to be engaged in controlling gene expression. As mitochondria also has DNA, the equivalent word might be "mitochrin."

As indicated above, nutrients are key regulators despite not being produced by cells. Accordingly, mechanisms that regulate cell life in a general way (nutrients constitute again a convenient example) reach DNA and histones first in a cytocrin and later in a nucleocrin fashion. Following the reasoning and considering that each single cell in a mammal has its own internal machineries, "nucleocrin" could be used to describe mechanisms that end up activating/deactivating factors directly affecting the chromosomal structure and function. Note the difference between "nucleocrin" and "nucleocrine," which was a term coined by Radulescu (1995) to denote, in a cancer research context, how extracellular regulators may promote cell growth by interacting with nuclear proteins (tumor suppressors) (Radulescu, 1995, 2015). Moreover, we feel necessary to establish the mechanisms involved in transmitting extranuclear signals to the nucleus: directly (acting on transcription factors), and/or indirectly (acting on enzymes involved in managing epigenetic traits). We also consider more relevant to decipher the epigenetic mechanisms (triggers, activation/deactivation patterns, etc.,) than empirically describe methylation patterns, or that a given miRNA is increased in a given physiological circumstance or in a given disease (see below).

FROM EPIGENETICS IN UNICELLULAR ORGANISMS TO EPIGENETICS IN MAMMALS

Anything impacting on a unicellular organism is prone to provoke a reaction i.e., a specific phenotype. One of such factors is the carbon source needed for survival. Depending on the growth medium, the phenotype of a given organism with a given DNA sequence could change. Taking a naïve approach, nutrients are non-genetic (i.e., they may be considered epigenetic) factors. Indeed, nutrients may modify DNA methylation patterns or histone acetylation as they lead to expression of specific transcription factor(s) and trigger gene regulation programs. The effect of some nutrients on gene expression is mainly known after the seminal identification of the lactose operon in bacteria by Jacob and Monod (1961).

To our knowledge, the field of *mammalian* epigenetics tends to forget the overall phenotype of an individual, which results from a given genome but multiple epigenetic overlapping factors and mechanisms acting under short (even in hours) and long-term (homeostatic/permanent-like) paradigms and during development but also in the adult individual. Epigenetics seems to be restricted to the development of multicellular organisms, i.e., to explain how a body containing billions of cells and dozens of cell types (with the same DNA) arises from a single cell. We propose to forget this limitation and expand "epigenetic" to any factor that, without involvement of DNA alterations, is affecting the phenotype of a mammal (or any of its cell types). Daughter cells resulting from a single ovum (having the same DNA) start to be different very soon, just when molecules, mainly nutrients, impact cells unevenly. Surely, one of the first mechanisms of control of gene expression in a developing embryo arises from concentration gradients, for instance, when oxygen reaches more concentration in one cell than in another. Oxygen gradients are essential for development. Why oxygen may be an epigenetic factor during development but not in adult life? Similar to oxygen, and as indicated above for unicellular organisms, nutrients coming from placenta and also metabolites (ATP, adenosine, amino acids, etc.,) that appear in the extracellular space are essential for development. Cell surface receptors are mediators that trigger, in cells having the same genome but becoming to *differentiate* (i.e., to be *different*), varied gene transcription programs that ultimately depend on the concentration of the endogenous agonist. This non-genetic, i.e., epigenetic, mechanism may rely on differential DNA methylation patterns but differential gene regulation is probably a more likely mechanism. It is true that the interest to link cell surface receptor activation to epigenetic traits has been quite low. On the one hand, to expand epigenetic options may lead to a more complex scenario, but we feel the contrary, i.e., that it will serve to clarification and consensus. On the other hand, either nutrient-based and hormone-mediated gene regulation are considered epigenetic mechanisms, or solid reasons are needed to exclude these classical mechanisms while accepting those of atypical RNAs or exosomes.

BIOCHEMISTRY-BASED PROPOSAL FOR MORE EPIGENETIC FACTORS

The lack of consensus on a clear-cut operative definition on Epigenetics impacts on the whole field. In their excellent essay Deans and Maggert (2015) emphasize that the term has "*multiple meanings, describing vastly different phenomena.*" We consider that Epigenetics may be as wide-ranged as possible to, subsequently, look for new names to describe some specific factors/mediators/mechanisms. Our proposal to expand the epigenetic window necessarily leads to more epigenetic players (in mammals). Taking disease risk as an example, prediction do require to know: (a) the DNA sequence, (b) factors directly affecting DNA/chromosomal structure and (c) factors indirectly affecting the expression of phenotype(s). Until now only factors in (b) are considered epigenetic; we think that factors in (c) are also epigenetic. Epigenetic is, in our opinion, the adjective for genetic-independent variables that shape our phenotype and even disease risk, disease progression and therapeutic management.

From a biochemist perspective, the Chemical aspects of any Biological issue should be taken into account. First of all, chemical reactions, from those in test tube to those underlying epigenetic mechanisms in living animals, are ruled by Thermodynamic laws and depend on "state" variables. As usual, temperature and pressure are the first to consider. The gene expression pattern and the resulting phenotype for a given genome depend on whether the living being lives at sea level or in a high mountain, and at below 0° in Siberia or at 35° in the tropic. Water, which was highlighted by Aristotle as crucial for life, is another factor but mainly in terms of humidity, for example, life in a desert or in humid Amazonia.

A non-exhaustive enough list of epigenetic factors, mediators and traits is provided in **Table 1**. The list focusses in mammals and in factors that depend on the own characteristics of these animals. Briefly, anything impacting on the five senses (sight, smell, touch, taste, and hearing) is, to a greater or lesser degree, affecting gene expression and, consequently, the phenotype. Take for instance light exposure; surely, gene expression for a same individual is different if living in Sweden -with few daily hours in winter and many daily hours in summer- or in any country in the Earth equatorial region. Food and life styles, education and social interactions, are further factors that may help in identifying novel epigenetic players, mechanisms and traits. In addition, epigenetic features already accepted should be positioned within the bigger picture.

INHERITANCE AND TRANSGENERATIONAL TRANSMISSION ISSUES

Inheritance is at the center stage in Epigenetics. Waddington was interested in developmental mechanisms but did not care much on inheritability, i.e., it was not fundamental for his idea of Epigenetics. Holliday redefined Waddington's concepts and convinced many scientists that inheritance was a necessary aspect in Epigenetics (Holliday, 1984, 1990, 1993, 2005, 2006). In fact, the need of inheritable epigenetic characters is one of the problems in reaching consensus. On the one hand, epigenetic traits are first discovered and subsequently *forced* to be inheritable. On the other hand, it is doubtful that the novel epigenetic traits are inherited. The issue of inheritance is difficult to reconcile and, from a biochemist point of view, it should be secondary if not forgotten. Many of the differential traits found even in identical monozygotic twins must be considered as epigenetic and not necessarily acquired by inheritance mechanisms during development.

Despite DNA methylation patterns may be clonally inherited there is a reprograming of such patterns in the egg/embryo; they are erased except in few imprinted gene sequences (Seisenberger et al., 2012; Wasson et al., 2013; Monk, 2015; Zhou and Dean, 2015). Accordingly, histone modifications or DNA methylation are very unlikely transgenerational epigenetic mechanisms. In the absence of a breakthrough finding it will take time to confirm epigenetic transgenerational transmission and the underlying mechanisms. One of few examples in mammals derives from the study of phenotypic traits in humans conceived in the 1944–1945 Dutch famine (Veenendaal et al., 2013), in which health, weight, body mass index rate, etc., of individuals conceived from poorly feed parents or from well-feed parents were compared. One interesting finding was a higher adiposity in the offspring of prenatally undernourished fathers but not mothers (Veenendaal et al., 2013). The topic has provided reviews where potential mechanisms and myths on this topic are presented and discussed (Dias and Ressler, 2014; Heard and Martienssen, 2014). We raise the subject here because the candidates for transgenerational transmission are the novel epigenetic mediators: miRNAs and exosomes. They may travel from a given somatic cell to the ovum or the spermatozoon to achieve the transgenerational transmission. In this sense, these epigenetic mediators may be inherited once integrated in spermatozoon precursors but, very importantly, its epigenetic action is endocrine as they should reach the spermatozoon precursors from elsewhere in the human body. In the eventual case of maternal transmission, the inheritability of epigenetic traits is very unlikely as ovules do not divide but are present since early steps in mammalian life span, i.e., the epigenetic factors must reach ovules one by one from elsewhere in the female body.

EPIGENETIC-BASED THERAPY: TARGETING NON-INHERITED EPIGENETIC TRAITS?

Leaders in epigenetic research are expanding the sentence: "we are what we eat" to something like "we are what parents, grandparents, etc., ate." In fact, Sales et al. (2017) compile evidence to sustain that epigenetic transgenerational transmission may be the basis for "*non-genetic molecular legacy of prior environmental exposures and influence transcriptional regulation, developmental trajectories, and adult disease risk in offspring.*" The possibility of transmissible epigenetic factors that may impact on the disease risk of offspring, even across generations, is presented in several reviews (e.g., Nadeau, 2009; Somer and Thummel, 2014; Hur et al., 2017; Weber-Stadlbauer, 2017). However, in daily practice clinicians assume that the inherited risk of disease is due to DNAs inherited from father and/or mother. This assumption seems appropriate for a variety of diseases, for instance a higher risk of breast cancer in daughters from mothers having had the disease would be likely due to genetic factors. In other cases, where the genetic link is not so evident, the epigenetic one should be considered. Expecting to increase our knowledge on mechanisms linking epigenetic transmission and disease risk, the research has devoted to target epigenetic mechanisms to cure/combat diseases in gaining momentum. Accordingly, one of the most sought potential of Epigenetics is to translate preclinical research into "epigenetic" medicines.

The most studied paradigmatic case in epigenetic-based therapy is cancer. Evidence of epigenetic trait alterations in cancers was expectable and, in fact, provided in many studies. There are high expectations on targeting epigenetic DNA methylation or histone acetylation to combat cancer and in

TABLE 1 | Non-exhaustive list of Epigenetic factors, mediators and traits in mammals.

Factors		Observations	Example	Inheritability[b]	Endocrine-like	Underlying mechanism
	Temperature	Thermodynamic (state) variable[a]	Living in Gobi desert *vs.* living in Alaska	No	No	-
	Pressure	Thermodynamic (state) variable[a]	Living at sea level *vs.* living in high mountains	No	No	-
	Gravity	Physical factor[a]	Living on Earth surface *vs.* living in Space station	No	No	-
	Water	Humidity	Living in a desert *vs.* living in Amazonia	No	No	-
	Light	Circadian rhythms	Living in Sweden *vs.* living in Equator	No	Yes (partially)	Partly known
Mediators	Hormones/neuro-transmitters	Regulating gene expression	Steroids	No	Yes	Partly known
	Nutrients	Regulating gene expression	Lactose operon[c]	No	Yes	Partly known
	Covalent DNA modification	Affecting DNA structure	DNA methylases	No	No	Unknown
	Post-translational modification of histones	Affecting chromatin/chromosome structure	Histone deacetylases	No	No	Unknown
	Transcription factors	Regulating gene expression	-	No	No	Partly known
	Atypical RNAs	Regulating gene expression	miR-29 micro RNAs, long non-coding (ncRNAs)?	?	Yes	Unknown
	Prion proteins	Affecting cell fate	Scrapie prion protein	Yes	?	Partly known
Traits	Histone modifications	-	Histone acetylation	?	-	-
	DNA modifications	-	DNA methylation	Yes	-	-
	Other	To be discovered	To be discovered	-	-	-

Those that are currently more fashionable are highlighted in blue.

[a] *In the absence of other impacting factors, state variables (also gravity) affect biological processes in a way that does not depend on the steps but on the initial and final conditions.*

[b] *Clonal (not transgenerational) inheritability, i.e., from one parental to the two after-mitosis daughter cells. Inter- and transgenerational transmission are not considered in this article.*

[c] *Although not operating in mammals it was the first described mechanism of gene regulation in response to nutrient availability.*

a recent review Perri et al. (2017) describe how anti-cancer therapeutic approaches may take advantage of epigenetic control of cell expression. In practice and as superbly reviewed by Flavahan et al. (2017) fulfillment of expectations would require "*…test, validate (or refute) conceptual and mechanistic models for cancer epigenetics, and place them in context with prevailing genetic models.*" At present, epigenetic traits may help in better classification of cancer but the therapeutic prospects are poor.

The inheritability of epigenetic mechanisms should be put under a proper perspective; it appears as irrelevant in fighting cancer since anti-cancer therapy attempts to kill malignant cells before providing more daughter cancer cells. Epigenetic mechanisms cannot be inherited in cells that do not divide; neurons are the paradigm of such cells. Surely, there is now accepted that a certain degree of neural development exists in some restricted areas of the adult brain but, such possibility is very limited in the aged brain and very compromised in diseases of the central nervous system.

In our opinion, a fixation on cancer is limiting the advance in epigenetic-based therapies for other diseases, e.g., neurodegenerative, in which cells should survive instead of being killed. Epigenetic changes impacting on degenerating neurons do not have much chance to be transmitted to daughter cells. Current attempts to combat neurodegenerative diseases, mainly Alzheimer's, address a epigenetic mechanism (histone acetylation, see Cuadrado-Tejedor et al., 2013 for review) that is common to affected neurons and that is not necessarily transmitted from cell to cell. It is true that transcellular transmission of a pathogen triggering similar epigenetic responses in connected neurons cannot be ruled out. But even if this is the case, therapies based in epigenetic traits should not essentially assume that the targeted trait is inheritable/inherited or not. Other players may be identified in the future, that also will tell which ones are really operating in a physiologically relevant way and whether they may constitute targets to combat diseases.

AUTHOR CONTRIBUTIONS

GN and EM-P have searched for the literature and contributed to the writing. NF has contributed to the order of sections, subsections and Table construction, i.e., to the overall design. RF conceived the idea of the Perspective, contributed to the writing and did the coordination.

ACKNOWLEDGMENTS

We are deeply indebted to Prof. Jaume Baguñà, from the Genetics Department of the Faculty of Biology of the University of Barcelona for enlightening discussions on Epigenetics, a multifaceted fashionable topic.

REFERENCES

Celluzzi, A., and Masotti, A. (2016). How our other genome controls our epigenome. *Trends Microbiol.* 24, 777–787. doi: 10.1016/j.tim.2016.05.005

Cuadrado-Tejedor, M., Oyarzabal, J., Lucas, M. P., Franco, R., and García-Osta, A. (2013). Epigenetic drugs in Alzheimer's disease. *Biomol. Concepts* 4, 433–445. doi: 10.1515/bmc-2013-0012

Deans, C., and Maggert, K. A. (2015). What do you mean, "epigenetic"? *Genetics* 199, 887–896. doi: 10.1534/genetics.114.173492

Deichmann, U. (2016). Epigenetics: the origins and evolution of a fashionable topic. *Dev. Biol.* 416, 249–254. doi: 10.1016/j.ydbio.2016.06.005

Dias, B. G., and Ressler, K. J. (2014). Experimental evidence needed to demonstrate inter- and trans-generational effects of ancestral experiences in mammals. *Bioessays* 36, 919–923. doi: 10.1002/bies.201400105

Felsenfeld, G. (2014). A brief history of epigenetics. *Cold Spring Harb. Perspect. Biol.* 6:a018200. doi: 10.1101/cshperspect.a018200

Flavahan, W. A., Gaskell, E., and Bernstein, B. E. (2017). Epigenetic plasticity and the hallmarks of cancer. *Science* 357:eaal2380. doi: 10.1126/science.aal2380

Haig, D. (2004). The (dual) origin of epigenetics. *Cold Spring Harb. Symp. Quant. Biol.* 69, 67–70. doi: 10.1101/sqb.2004.69.67

Heard, E., and Martienssen, R. A. (2014). Transgenerational epigenetic inheritance: myths and mechanisms. *Cell* 157, 95–109. doi: 10.1016/j.cell.2014.02.045

Herring, S. W. (1993). Formation of the vertebrate face: epigenetic and functional influences. *Am. Zool.* 33:472. doi: 10.1093/icb/33.4.472

Holliday, R. (1984). The biological significance of meiosis. *Symp. Soc. Exp. Biol.* 38, 381–394.

Holliday, R. (1990). DNA methylation and epigenetic inheritance. *Philos. Trans. R. Soc. Lond. B. Biol. Sci.* 326, 329–338. doi: 10.1098/rstb.1990.0015

Holliday, R. (1993). Epigenetic inheritance based on DNA methylation. *EXS* 64, 452–468. doi: 10.1007/978-3-0348-9118-9_20

Holliday, R. (2005). DNA methylation and epigenotypes. *Biochemistry* 70, 500–504. doi: 10.1007/s10541-005-0144-x

Holliday, R. (2006). Dual inheritance. *Curr. Top. Microbiol. Immunol.* 301, 243–256. doi: 10.1007/3-540-31390-7_9

Hur, S. S. J., Cropley, J. E., and Suter, C. M. (2017). Paternal epigenetic programming: evolving metabolic disease risk. *J. Mol. Endocrinol.* 58, R159–R168. doi: 10.1530/JME-16-0236

Jablonka, E., and Lamb, M. J. (2002). The changing concept of epigenetics. *Ann. N. Y. Acad. Sci.* 981, 82–96. doi: 10.1111/j.1749-6632.2002.tb04913.x

Jacob, F., and Monod, J. (1961). Genetic regulatory mechanisms in the synthesis of proteins. *J. Mol. Biol.* 3, 318–356. doi: 10.1016/S0022-2836(61)80072-7

Lange, S., Gallagher, M., Kholia, S., Kosgodage, U., Hristova, M., Hardy, J., et al. (2017). Peptidylarginine deiminases—roles in cancer and neurodegeneration and possible avenues for therapeutic intervention via modulation of exosome and microvesicle (EMV) release? *Int. J. Mol. Sci.* 18:1196. doi: 10.3390/ijms18061196

Monk, D. (2015). Germline-derived DNA methylation and early embryo epigenetic reprogramming: the selected survival of imprints. *Int. J. Biochem. Cell Biol.* 67, 128–138. doi: 10.1016/j.biocel.2015.04.014

Nadeau, J. H. (2009). Transgenerational genetic effects on phenotypic variation and disease risk. *Hum. Mol. Genet.* 18, R202–R210. doi: 10.1093/hmg/ddp366

Perri, F., Longo, F., Giuliano, M., Sabbatino, F., Favia, G., Ionna, F., et al. (2017). Epigenetic control of gene expression: potential implications for cancer treatment. *Crit. Rev. Oncol. Hematol.* 111, 166–172. doi: 10.1016/j.critrevonc.2017.01.020

Radulescu, R. T. (1995). From insulin, retinoblastoma protein and the insulin receptor to a new model on growth factor specificity: the nucleocrine pathway. *J. Endocrinol.* 146, 365–368. doi: 10.1677/joe.0.1460365

Radulescu, R. T. (2015). The nucleocrine pathway comes of age. *Rom. J. Morphol. Embryol.* 56, 343–348.

Riggs, A., R. A., Martienssen, R., and Russo, V. (1996). *Introduction. In Epigenetic Mechanisms of Gene Regulation*. Cold Spring Harbour, NY: Cold Spring Harbour Laboratory Press.

Sales, V. M., Ferguson-Smith, A. C., and Patti, M.-E. (2017). Epigenetic mechanisms of transmission of metabolic disease across generations. *Cell Metab.* 25, 559–571. doi: 10.1016/j.cmet.2017.02.016

Seisenberger, S., Peat, J. R., Hore, T. A., Santos, F., Dean, W., and Reik, W. (2012). Reprogramming DNA methylation in the mammalian life cycle: building and breaking epigenetic barriers. *Philos. Trans. R. Soc. B Biol. Sci.* 368:20110330. doi: 10.1098/rstb.2011.0330

Somer, R. A., and Thummel, C. S. (2014). Epigenetic inheritance of metabolic state. *Curr. Opin. Genet. Dev.* 27, 43–47. doi: 10.1016/j.gde.2014.03.008

Veenendaal, M., Painter, R., de Rooij, S., Bossuyt, P., van der Post, J., Gluckman, P., et al. (2013). Transgenerational effects of prenatal exposure to the 1944-45 Dutch famine. *BJOG* 120, 548–554. doi: 10.1111/1471-0528.12136

Waddington, C. (1939). *An Introduction to Modern Genetics*. New York, NY: Macmillan Publishers Limited.

Waddington, C. (1942). The epigenome. *Endeavour* 1, 18–20.

Waddington, C. (1956). Embryology, epigenetics and biogenetics. *Nature* 177:1241. doi: 10.1038/1771241a0

Wasson, J. A., Ruppersburg, C. C., and Katz, D. J. (2013). Restoring totipotency through epigenetic reprogramming. *Brief. Funct. Genomics* 12, 118–128. doi: 10.1093/bfgp/els042

Weber-Stadlbauer, U. (2017). Epigenetic and transgenerational mechanisms in infection-mediated neurodevelopmental disorders. *Transl. Psychiatry* 7:e1113. doi: 10.1038/tp.2017.78

Wiklund, E. D., Kjems, J., and Clark, S. J. (2010). Epigenetic architecture and miRNA: reciprocal regulators. *Epigenomics* 2, 823–840. doi: 10.2217/epi.10.51

Zhou, L., and Dean, J. (2015). Reprogramming the genome to totipotency in mouse embryos. *Trends Cell Biol.* 25, 82–91. doi: 10.1016/j.tcb.2014.09.006

Conflict of Interest Statement: The authors declare that the research was conducted in the absence of any commercial or financial relationships that could be construed as a potential conflict of interest.

frontiers in Genetics

ORIGINAL RESEARCH
published: 19 June 2018
doi: 10.3389/fgene.2018.00203

High Fructose Intake During Pregnancy in Rats Influences the Maternal Microbiome and Gut Development in the Offspring

Stuart Astbury[1,2,3,4], Aleida Song[1], Mi Zhou[5], Brent Nielsen[1], Abha Hoedl[1], Benjamin P. Willing[5], Michael E. Symonds[2,3,4] and Rhonda C. Bell[1,6]**

[1] Division of Human Nutrition, Department of Agricultural, Food and Nutritional Science, University of Alberta, Edmonton, AB, Canada, [2] Early Life Research Unit, Division of Child Health, Obstetrics and Gynaecology, School of Medicine, The University of Nottingham, Nottingham, United Kingdom, [3] Nottingham Digestive Diseases Centre, School of Medicine, University of Nottingham, Nottingham, United Kingdom, [4] NIHR Nottingham Biomedical Research Centre, University of Nottingham and Nottingham University Hospitals NHS Trust, Nottingham, United Kingdom, [5] Division of Animal Science, Department of Agricultural, Food and Nutritional Sciences, University of Alberta, Edmonton, AB, Canada, [6] Women and Children's Health Research Institute, University of Alberta, Edmonton, AB, Canada

OPEN ACCESS

Edited by:
Jaap Joles,
Utrecht University, Netherlands

Reviewed by:
Joao Ricardo Diniz De Araujo,
Institut Pasteur, France
Maria Carmen Collado,
Instituto de Agroquímica y Tecnología de Alimentos (IATA), Spain
Michael T. Bailey,
The Ohio State University, United States

***Correspondence:**
Michael E. Symonds
michael.symonds@nottingham.ac.uk
Rhonda C. Bell
rhonda.bell@ualberta.ca

Specialty section:
This article was submitted to Epigenomics and Epigenetics, a section of the journal Frontiers in Genetics

Received: 24 January 2018
Accepted: 22 May 2018
Published: 19 June 2018

Citation:
Astbury S, Song A, Zhou M, Nielsen B, Hoedl A, Willing BP, Symonds ME and Bell RC (2018) High Fructose Intake During Pregnancy in Rats Influences the Maternal Microbiome and Gut Development in the Offspring. Front. Genet. 9:203. doi: 10.3389/fgene.2018.00203

Studies in pregnant women indicate the maternal microbiome changes during pregnancy so as to benefit the mother and fetus. In contrast, disruption of the maternal microbiota around birth can compromise normal bacterial colonisation of the infant's gastrointestinal tract. This may then inhibit development of the gut so as to increase susceptibility to inflammation and reduce barrier function. The impact of modulating fructose intake on the maternal microbiome through pregnancy is unknown, therefore we examined the effect of fructose supplementation on the maternal microbiome together with the immediate and next generation effects in the offspring. Wistar rat dams were divided into control and fructose fed groups that received 10% fructose in their drinking water from 8 weeks of age and throughout pregnancy (10–13 weeks). Maternal fecal and blood samples were collected pre-mating (9 weeks) and during early (gestational day 4–7) and late pregnancy (gestational day 19–21). We show supplementation of the maternal diet with fructose appears to significantly modulate the maternal microbiome, with a significant reduction in *Lactobacillus* and *Bacteroides*. In offspring maintained on this diet up to pregnancy and term there was a reduction in gene expression of markers of gut barrier function that could adversely affect its function. An exacerbated insulin response to pregnancy, reduced birth weight, but increased fat mass was also observed in these offspring. In conclusion dietary supplementation with fructose modulates the maternal microbiome in ways that could adversely affect fetal growth and later gut development.

Keywords: fructose, pregnancy, nutrition, microbiome, diabetes

INTRODUCTION

The intestinal microbiota is an important mediator of human metabolic health that can determine the onset of obesity and the metabolic syndrome (Turnbaugh et al., 2006). Dietary composition, rather than host genetics, can have a dominant role in modulating the microbiome (Carmody et al., 2015). This relationship could be especially important during pregnancy

when the maternal microbiome can undergo pronounced changes which are not dissimilar to those seen with obesity, becoming more pro-inflammatory and capable of inducing metabolic inflammation (Koren et al., 2012). Disruption of the maternal microbiota can affect microbial colonization in the offspring, potentially leading to increased intestinal permeability and reduced stomach growth (Fåk et al., 2008).

Although the impact of maternal diet (Payne et al., 2012; Cotillard et al., 2013; David et al., 2014), and specific dietary constituents (Gohir et al., 2015) on the microbiome has been examined, little is known about the impact of specific carbohydrates such as fructose. Globally, increased fructose intake has paralleled the prevalence of obesity and is widely recognized as a primary carbohydrate contributing to the rise in caloric consumption in Western diets (Lim et al., 2010). Although fructose in the form of high fructose corn syrup has been the focus of media and research attention (Bray et al., 2004; Goran et al., 2013), excessive consumption of fruit juices that are rich in fructose is also a public health concern (Faith et al., 2006). Fructose is metabolized differently to glucose, with the majority diverted toward hepatic lipogenesis, and has no effect on insulin release (Bezerra et al., 2000) while suppressing ghrelin secretion (Havel, 2005). Consumption of a high-fructose diet can induce insulin resistance (Bezerra et al., 2000; Huang et al., 2004), hypertension (Hwang et al., 1987), and dyslipidemia (Kazumi et al., 1997) in adult rodents.

Excess caloric intake in the form of a high-fat diet can adversely affect intestinal permeability, allowing components of the microbiota to pass into the systemic circulation and contribute to inflammation of adipose tissue (Lam et al., 2011). This type of chronic inflammation has subsequently been linked to the development of the metabolic syndrome (Lam et al., 2011). The impact of fructose on this process in the mother or offspring is unknown.

We have recently shown that although feeding a high fructose diet modulates the mother's metabolism, it has little impact on the offspring (Lineker et al., 2016) despite being smaller at birth. However, the maternal response appears to be amplified in the next generation when maintained on the same fructose supplemented diet (Song et al., 2017). Other groups have demonstrated that a high fructose intake during pregnancy will affect fetal endocrine function (Vickers et al., 2011) and lipid metabolism (Clayton et al., 2015). Young pigs and rats showing intrauterine growth restriction have a small intestine that is disproportionately affected with a reduced surface area (Younoszai and Ranshaw, 1973; Lebenthal et al., 1981; Xu et al., 1994) but effects on the microbiome remain to be defined. The aim of the present study was to determine whether pregnancy impacted on the maternal microbiome and was modifiable by fructose feeding. In addition, we examined whether female offspring born to dams fed a fructose-supplemented diet would show persistent differences within their small intestine that could further compromise glucose homeostasis in the next generation.

MATERIALS AND METHODS

Animal Study

The study protocol was approved by the Research Ethics Office of the University of Alberta, in accordance with regulations set by the Canadian Council on Animal Care.

Two generations of Wistar rats were used. Rats were obtained from Charles River Laboratories (Montreal, QC, Canada) at 7 weeks of age, and were allowed *ad libitum* access to chow (LabDiet 5001, Purina, MI, United States) and distilled water. At 8 weeks, female rats were randomly assigned to receive either 10% fructose solution or continue receiving distilled water. Rats were mated at 10 weeks of age and diets continued through pregnancy.

At gestational day (GD) 20, 10 control (Gen0-C) and 11 fructose-fed (Gen0-F) dams were euthanized using CO_2 for tissue collection. The remaining dams in each group were left to litter out and continued to receive their respective diets during lactation. Pups were placed on the control diet at weaning, until being placed on the same diet as their dam at 8 weeks of age, receiving either the 10% fructose (Gen1-F, $n = 10$) or distilled water (Gen1-C, $n = 10$). These diets continued through mating at 11 weeks and throughout pregnancy. Second generation dams were euthanized at GD20 for tissue collection. All rats from both generations were imaged via MRI (Echo Medical Systems, Houston, TX, United States) immediately prior to euthanasia for fat and lean mass measurements. An outline of the animal study is given in **Figure 1**.

Sample Collection and Measurement

All rats were weighed weekly. Blood samples were taken at four timepoints during the study: pre-diet (PD, 7 weeks), pre-mating (PM, 9 weeks), early pregnancy (EP, GD 4–7), and mid pregnancy (MP, GD 14–17). Whole blood was obtained from the tail vein and collected in K_2 EDTA microtainer tubes (BD, Franklin Lakes, NJ, United States). Plasma was separated from whole blood via centrifugation immediately following collection and stored at −20°C until analysis. Plasma glucose was determined via glucose (Trinder) assay (Genzyme Diagnostics, Charlottetown, PE, Canada). Plasma insulin concentrations were measured using the Insulin (Rat) Ultrasensitive ELISA Immunoassay kit (ALPCO Diagnostics, Salem, NH, United States). Plasma triglyceride concentrations were determined using the Triglyceride-SL assay kit (Genzyme Diagnostics).

Oral glucose tolerance tests (OGTTs) were carried out using 3 g glucose per kg of body weight administered by gavage to pregnant rats following a 4-h fast on GD19 [late pregnancy (LP)]. Blood samples were collected from the tail vein at 0, 15, 30, 45, 60, and 90 min intervals following administration of the oral glucose. Plasma glucose and insulin during OGTT were determined using the methods described above. OGTT results are presented as concentrations at each timepoint and incremental area under the curve (IAUC).

At dissection, the length of the small intestine (duodenum to cecum) was measured, and flushed with cold 10% phosphate buffered saline (PBS). Sections of ileum and jejunum were snap-frozen in liquid nitrogen for protein and RNA extraction.

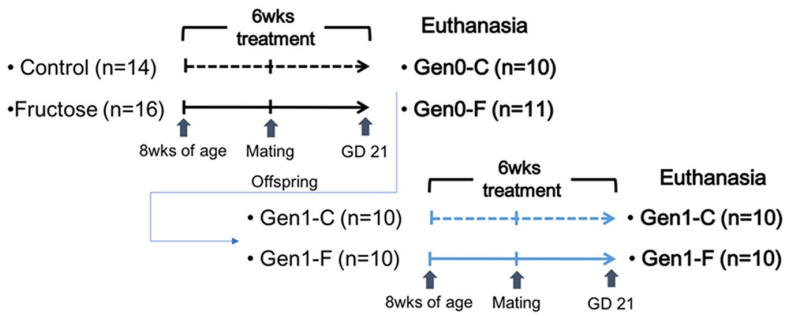

FIGURE 1 | Outline of the animal study.

All snap-frozen tissue was transferred to a −80°C freezer for storage. Sections of ileum and jejunum were also fixed in buffered zinc formalin (Z-Fix, Anatech Ltd., Battle Creek, MI, United States) for histology.

RNA Extraction and Quantitative PCR

A total of 60–80 mg of snap-frozen intestine and liver was homogenized in Tri-reagent (Ambion Diagnostics, Austin, TX, United States), and RNA extraction was carried out using the Qiagen RNeasy Mini Kit (Qiagen N.V., Hilden, Germany). RNA concentration and purity was confirmed via Nanodrop (Thermo Scientific, Waltham, MA, United States), and reverse transcription PCR carried out using the High Capacity cDNA reverse transcription kit (Applied Biosystems, Carlsbad, CA, United States). qPCR was then carried out using SYBR Green dye and the StepOne Plus PCR machine (Applied Biosystems). Primers were designed using Primer3 (Untergasser et al., 2007). All primers were designed to be intron-spanning to avoid amplification of genomic DNA. All qCPR results were adjusted to two reference genes (RPLP0 and GAPDH), using GeNorm software (Vandesompele et al., 2002) and are presented as fold change relative to the control group, calculated using the 2-ddCt method (Livak and Schmittgen, 2001). All sequences are included in Supplementary Table S1.

Histology

Approximately 2.5 cm length sections of ileum and jejunum were fixed in Z-Fix at dissection after flushing with cold 10% PBS. Four transverse sections of each sample were cut and embedded in paraffin blocks before sectioning at 4 μm and mounting, and were stained using hematoxylin and eosin. Villus height measurements were made using ImageJ, taking an average of measurements from 10 fields per section at 40x magnification.

Statistics

Glucose, triglyceride, insulin, and qPCR data were analyzed as follows. The four groups were compared using one-way analysis of variance (ANOVA) using contrast coefficients to compare both diet and generation or Kruskal–Wallis with *post hoc* tests depending on distribution. Data distribution was assessed with the Shapiro–Wilk test. All statistical analyses were carried out in SPSS v.21 (IBM Corp., Armonk, NY, United States) and presented using Prism 6 (GraphPad Software Inc., La Jolla, CA, United States).

Fecal DNA Extraction, Pyrosequencing, and Data Analysis

Fecal samples were collected at PM, EP, and LP and stored at −20°C until extraction; 180–220 mg of each sample was homogenized in a bead beater homogenizer (FastPrep 24, MP Biomedicals, Solon, OH, United States) and DNA extraction carried out using the QIAmp DNA Stool Mini Kit (Qiagen), following the standard protocol. The extracted DNA samples were quantified using a Nanodrop spectrophotometer (Thermo Fisher).

Universal 16s rRNA primers (27F and 519R) were used to generate amplicons from each fecal DNA sample. Each 20 μL reaction contained 0.4 U of Phusion Hot Start II High-Fidelity DNA Polymerase (Thermo Scientific), 1 × Phusion HF Buffer, 8 pmol of each primer, 4 mM dNTP, and 25 ng of DNA template. PCR was carried out under the following conditions: initial denaturing at 98°C for 1 min, followed by 30 cycles at 98°C for 10 s, 59°C for 30 s, and 72°C for 30 s, and a final extension at 72°C for 7 min. The PCR products were run on 1% agarose gels and excised using a scalpel. Agarose gel extractions were carried out using the QIAquick Gel Extraction Kit (Qiagen) and sample concentration and quality verified by Nanodrop. The same amount of each purified product (50 ng for PM/EP samples; 30 ng for LP samples) was pooled according to timepoint for 454 sequencing (McGill University and Génome Québec Innovation Centre, Montréal, QC, Canada).

All of the obtained pyrosequencing data were analyzed with the Quantitative Insights Into Microbial Ecology (QIIME) workflow (Caporaso et al., 2010) following the default settings. Samples with fewer than 1500 reads of raw data were removed. Operational taxonomic units (OTUs) were then assigned according to comparison with the Greengenes database (DeSantis et al., 2006) and alpha and beta diversities were calculated. Community composition was compared using analysis of similarity (ANOSIM) within QIIME, and abundance of each OTU and beta diversity of bacterial communities was compared between diets and pregnancy stages by ANOVA using SAS (version 9.2, SAS Institute, NC, United States). *Post hoc* pairwise comparisons were performed

using Tukey's HSD method. Significance was assumed at $P < 0.05$. Differential abundance analysis was performed for the identified phylotypes using zero-inflated log-normal mixture model within Metagenomeseq package. Raw *P*-values were used due to the small sample size. Sequence data are available from the NCBI Sequence Read Archive under project ID SRP143497.

RESULTS

Body Composition

There were no differences in body mass through pregnancy in the Gen0-F animals, but fat mass was raised with fructose feeding (**Table 1**). In the next generation, dams weighed more relative to Gen0 dams at the same timepoints, and fructose fed (Gen1-F) dams displayed significantly shorter small intestines relative to controls. Pancreas weight was also significantly reduced in Gen1-F dams relative to Gen1-C.

Glucose, Insulin, and Triglyceride Homeostasis Through Pregnancy

In the Gen0-F dams, plasma triglycerides were raised with fructose feeding from pre-mating (10 weeks) onward, an adaptation that was exacerbated in Gen1-F dams (**Table 2**). Plasma glucose was not different between groups throughout the OGTT in Gen0-F dams, and in Gen1-F, peak glucose was raised with fructose feeding but the area under the curve remained similar (**Figure 2A**). In contrast, plasma insulin was raised in Gen0-F dams 15 min following glucose administration and was accompanied with an increased IAUC, an adaptation that was amplified in the Gen1-F group (**Figure 2B**).

Gut Adaptations in the Offspring and Impact of Diet and Gestation on the Diversity of Fecal Bacteria

In Gen0-F dams, there was no change in expression of CLDN-3, ZO-1, JAMA, and OCLN between groups in either the jejunum or ileum (data not shown), whereas these were reduced in Gen1-F in the jejunum (**Figure 3**) but not ileum (data not shown). Villus height was significantly increased in the jejunum in Gen0-F, but unchanged between Gen1-F and Gen1-C in both ileum and jejunum (**Table 1**).

With respect to total fecal bacteria, our sample sequences (1970 ± 1085 seqs/sample) covered an estimated 86–98% of the total community (Supplementary Table S2) and were represented by OTUs (1004 ± 648 OTU/sample) that were assigned to 10 phyla, 15 classes, 22 orders, 40 families, 62 genera, and 100 species. The most abundant phyla were *Bacteroidetes* and *Firmicutes* (**Table 3**). Prior to pregnancy, control animals displayed a more diverse bacterial community compared to those fed fructose (Chao1 index 85 vs. 69, respectively). Prior to, and during LP, bacterial composition was different between diet groups and alpha and beta diversity were increased in the fructose group (**Figures 4**, **5**). At all sampling points, the differentially abundant OTUs at the species level (or proportions of OTUs) between diets are presented in **Table 4**.

Further comparison of the effect of pregnancy stage and diet on fecal bacterial communities indicated that pregnancy stage did not have significant influence on microbial profiles (**Figure 6A**), while the different diets resulted in a strong impact (**Figure 6B**). Individual species responded to host pregnancy stage and diet in different ways. As shown in **Table 4**, only five species were differentially abundant in different pregnancy stages: along with pregnancy stage, *Parabacteroides* sp., *Lactobacillus reuteri*, and sp. of order RF39 were decreased, *Prevotella* sp. was increased, while sp. of *Clostridiales* was lowered during EP and recovered gradually during LP. The effect of diet was more obvious, with 15 species differentially abundant between control and fructose diets, among which sp. of Bacteroidales, *Parabacteroides* sp., *Lactobacillus reuteri*, and sp. of Lachnospiraceae were exclusively observed in rats given the control diet. Association analyses were performed between physiology parameters and the relative abundance of individual bacterial species; however, no correlations were seen (data not shown).

DISCUSSION

The present study extends our previous findings that increased consumption of fructose negatively impacts on lipid and

TABLE 1 | Body composition measurements. All values mean ± SEM, $^{*}p < 0.05$, $^{**}p < 0.01$, one-way ANOVA with contrasts (Gen0-C vs. Gen0-F and Gen1-C vs. Gen1-F).

	Gen0-C (*n* = 9)	Gen0-F (*n* = 6)	Gen1-C (*n* = 10)	Gen1-F (*n* = 10)
Birth weight (g)	–	–	3.86 ± 0.7	3.26 ± 0.6*
Weight at GD20 (g)	422.2 ± 8.7	434.8 ± 12.3	454.4 ± 19.9	468.5 ± 19.2
Percentage fat	10.3 ± 1.4	12.9 ± 1.9	11.4 ± 0.5	16.8 ± 1.3**
Percentage lean	75.6 ± 0.9	73.3 ± 1.4	75.8 ± 0.3	71.4 ± 1.0**
Small intestinal length (cm)	124.8 ± 3.4	126.5 ± 2.6	128.5 ± 1.8	123.8 ± 0.4*
Liver (g)	18.7 ± 0.6	19.6 ± 0.8	21.1 ± 0.5	21.9 ± 1.4
Pancreas (g)	1.14 ± 0.1	1.15 ± 0.1	1.34 ± 0.1	1.08 ± 0.1*
Ileum villus height (μm)	416 ± 15	490 ± 33	662 ± 28	663 ± 38
Jejunum villus height (μm)	492 ± 42	668 ± 35*	592 ± 27	606 ± 16

TABLE 2 | Plasma glucose, insulin, and triglycerides.

	Gen0-C (n = 9)	Gen0-F (n = 6)	Gen1-C (n = 10)	Gen1-F (n = 10)
Glucose (mmol/L)				
Pre-diet	7.86 ± 0.6	8.01 ± 0.8	7.29 ± 0.7	7.30 ± 0.5
Pre-mating	7.99 ± 0.7	7.98 ± 1.1	7.00 ± 0.4	8.57 ± 0.9*
Early pregnancy	7.45 ± 0.9	8.27 ± 0.8*	6.80 ± 0.6	7.73 ± 0.5*
Mid pregnancy	6.53 ± 0.7	6.64 ± 0.3	5.55 ± 0.5	6.72 ± 0.8*
Late pregnancy	5.36 ± 0.6	6.32 ± 0.5	5.69 ± 0.3	6.01 ± 0.1
Insulin (ng/mL)				
Pre-diet	0.86 ± 0.5	0.78 ± 0.3	0.87 ± 0.5	1.03 ± 0.5
Pre-mating	0.97 ± 0.7	1.01 ± 0.5	1.37 ± 0.6	2.31 ± 1.2*
Early pregnancy	0.83 ± 0.5	1.07 ± 0.2	1.27 ± 1.0	2.76 ± 1.6*
Mid pregnancy	0.62 ± 0.2	1.47 ± 0.5	0.95 ± 0.5	2.78 ± 1.7*
Late pregnancy	0.86 ± 0.7	1.68 ± 0.4	0.86 ± 0.2	1.69 ± 0.5*
Triglyceride (mmol/L)				
Pre-diet	3.58 ± 1.2	3.26 ± 0.9	3.88 ± 1.5	3.71 ± 1.3
Pre-mating	4.41 ± 1.8	7.09 ± 2.2*	4.72 ± 1.0	17.58 ± 5.1*
Early pregnancy	5.19 ± 1.1	9.49 ± 3.2*	4.51 ± 1.3	14.11 ± 4.2*
Mid pregnancy	11.01 ± 4.7	18.39 ± 1.6*	10.42 ± 2.7	21.28 ± 6.7*
Late pregnancy	12.14 ± 1.0	20.32 ± 1.5*	11.42 ± 3.2	23.43 ± 3.1*

*All values mean ± SEM, *$p < 0.05$, (Gen0-C vs. Gen0-F and Gen1-C vs. Gen1-F), one-way ANOVA with contrasts.*

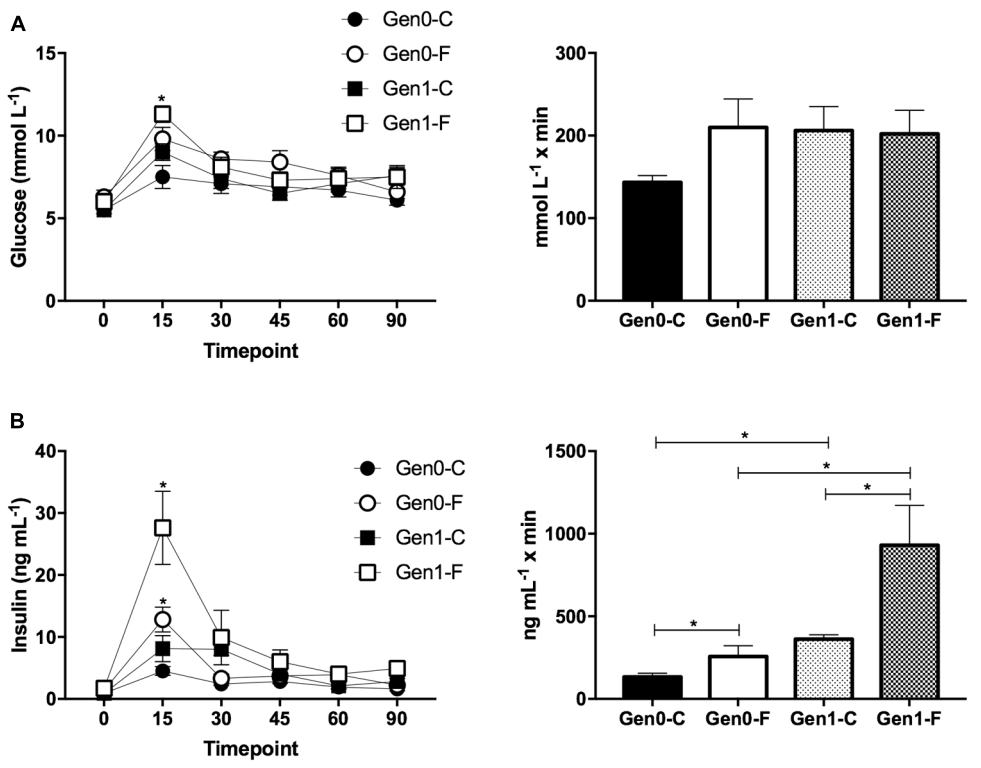

FIGURE 2 | (A) OGTT for glucose (L) and incremental area under the curve for first and second generation dams at GD19. *$p < 0.05$ Gen1-C vs. Gen1-F, one way ANOVA with contrasts. **(B)** Plasma insulin OGTT (L) and incremental area under the curve (R) at GD19. (L) *$p < 0.05$ Gen0-C vs. Gen0-F and Gen1-C vs. Gen1-F, Unpaired t-test, (R) *$p < 0.05$, one way ANOVA with contrasts.

carbohydrate metabolism due to insulin resistance (Lineker et al., 2016; Song et al., 2017). Importantly, this adverse adaptation only becomes apparent during pregnancy and is amplified in the next generation. Here we show that one factor contributing to the negative impact of fructose on maternal metabolism could be maladaptation of the microbiome. Fructose is known

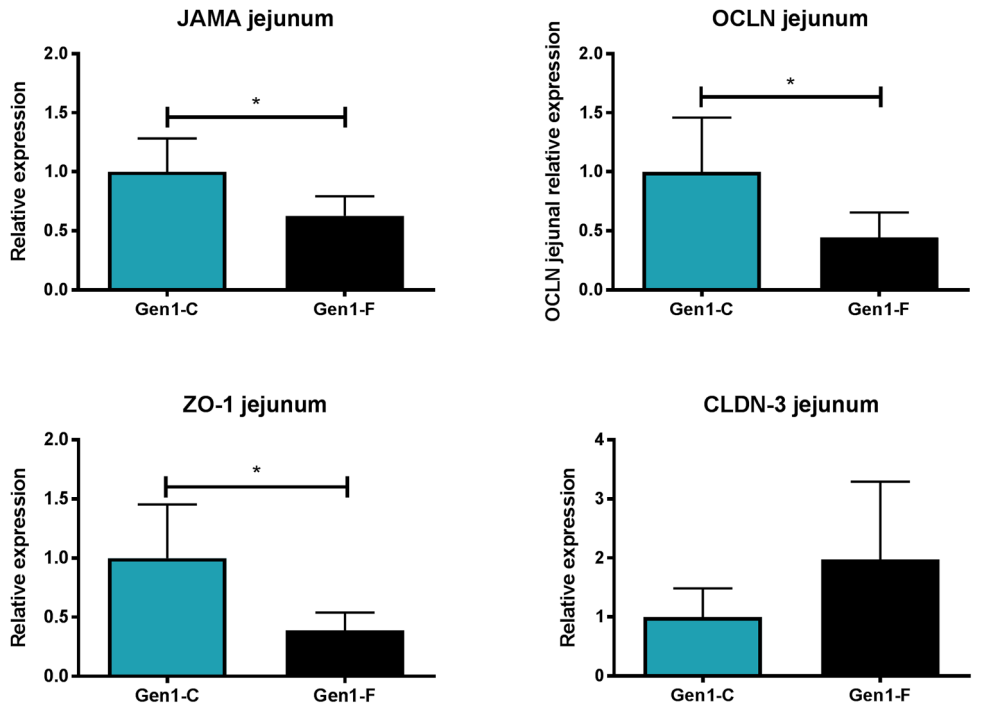

FIGURE 3 | Second generation jejunum gene expression results. All values mean ± SEM, $*p < 0.05$, one way ANOVA with contrasts.

TABLE 3 | Relative abundance of the identified bacteria phyla.

	PM		EP		LP			P		
Phyla	**C**	**F**	**C**	**F**	**C**	**F**	**SEM**	**Period**	**Diet**	**Period * Diet**
Actinobacteria	0.20*	0.43	0.45	0.64	0.39	1.00	0.12	0.363	0.157	0.733
Bacteroidetes	42.00	33.15	49.02	47.45	61.93	44.69	2.37	0.024	0.041	0.379
Cyanobacteria	0.78	0.00	0.14	0.19	0.01	0.00	0.15	0.524	0.386	0.459
Deferribacteres	0.08	0.00	0.00	0.00	0.00	0.02	0.01	0.402	0.421	0.286
Firmicutes	54.31	63.07	49.36	46.28	36.95	50.61	2.39	0.038	0.153	0.335
Proteobacteria	1.74	1.01	0.78	4.06	0.62	3.53	0.49	0.730	0.078	0.173
TM7	0.24	0.00	0.00	0.01	0.01	0.09	0.05	0.591	0.592	0.364
Tenericutes	0.40	0.15	0.08	0.11	0.08	0.00	0.03	0.006	0.087	0.200
Verrucomicrobia	0.25	2.19	0.16	1.26	0.00	0.06	0.36	0.438	0.147	0.558

*PM, pre-mate; EP, early pregnancy; LP, late pregnancy; C, Control; F, Fructose. *Data presented in proportion.*

to affect the microbiota (Pachikian et al., 2013; Wagnerberger et al., 2013; Vos, 2014) and when the maternal microbiota is compromised with antibiotic exposure, intestinal development in the offspring is adversely affected in conjunction with the appearance of an *Enterobacteriaceae*-rich microbiome (Fåk et al., 2008). Previously, the influence of pregnancy on the microbiome has not been examined in an animal model. During pregnancy, substantial changes in maternal hormones, immune function, and metabolism occur (Mor and Cardenas, 2010; Newbern and Freemark, 2011) that could impact on the microbiome which in some human studies has been suggested to result in a more obesogenic profile (Collado et al., 2008; Moreira et al., 2012).

Birth weight was significantly reduced in Gen1-F rats; in conjunction with this, we also observed significantly shorter small intestines and dysregulation of epithelial tight junction gene expression relative to controls. This is consistent with previous work associating growth restriction and impaired small intestinal development in rats (Baserga et al., 2004), pigs (Morise et al., 2008; Wang et al., 2008), and humans (Indrio et al., 2013). The reduction we found in three of the four epithelial tight junctions studied (JAMA, OCLN, and ZO-1) in Gen1-F suggests that intestinal permeability is affected either by the fructose diet directly or through maternal gut related adaptations. There is some evidence to support both hypotheses that fructose is known to adversely affect intestinal permeability (Spruss and Bergheim, 2009) and disruption of the maternal microbiota can lead to altered offspring gut development (Fåk et al., 2008). In

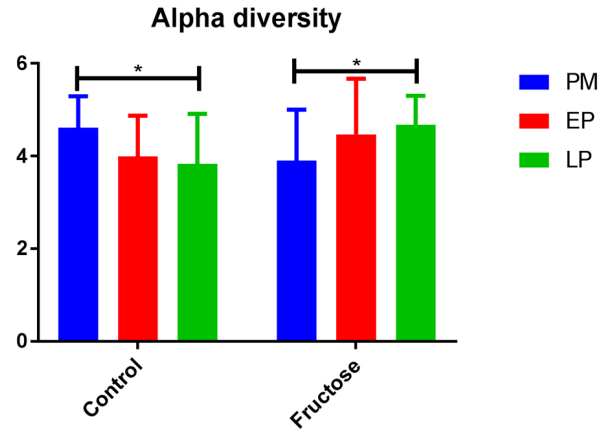

FIGURE 4 | Alpha diversity (Shannon index) of bacterial communities between diets at each pregnancy timepoint.

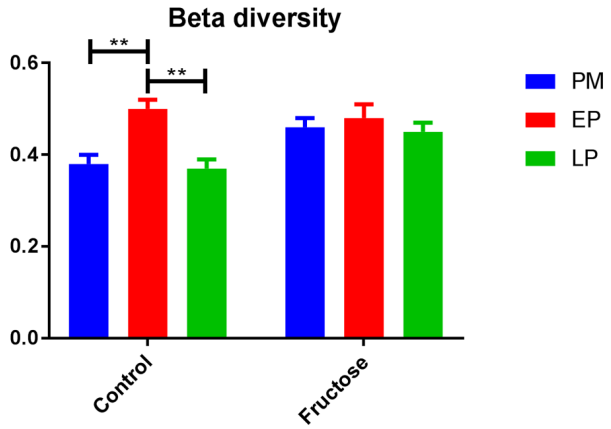

FIGURE 5 | Beta diversity (Bray–Curtis dissimilarity indices) of bacterial communities between diets at each pregnancy timepoint.

the case of this study, fructose is potentially adversely affecting offspring gut development via both of the above mechanisms. Further work such as a crossover design in which offspring born to fructose-fed mothers were switched to a control diet would be required to determine the relative significance of diet and the microbiota passed from the mother.

Previous work in humans has shown that regardless of pre-pregnancy body mass index, the diversity of bacterial species within an individual declines with gestation, but diversity of species between individuals increases (Koren et al., 2012). As a caveat dietary changes throughout gestation in this study were not detailed and it is known that dietary intake can adapt early in pregnancy (Rifas-Shiman et al., 2006). We observed different trends in our control animals with bacterial alpha (within individual) diversity declining by the end of pregnancy but beta (inter-individual) diversity remaining unchanged. This is potentially due to the difference in environmental exposure between rats and humans, and illustrates the potential issues of using the rat microbiome as a model for humans.

Although fructose fed animals had a less diverse (numerically but not statistically different) microbiome to begin with, the opposite trend in diversity was observed during pregnancy, with alpha diversity increasing throughout pregnancy but beta diversity remaining unchanged. Importantly, these adaptations occurred despite no change in total energy intake as the increased consumption of fructose in drinking water was compensated for by a reduced intake of food (Erlanson-Albertsson and Lindqvist, 2010; Vickers et al., 2011; Gray et al., 2013).

Chronic consumption of fructose (but not glucose) can induce endotoxemia in mice (Bergheim et al., 2008) and gene expression of claudin-4 is reduced *in vitro* with the addition of fructose (Johnson et al., 2013). In rats, disruption of the maternal microbiota has been shown to adversely affect intestinal permeability in the offspring (Fåk et al., 2008), and therefore it is possible that a microbiota deficient in *Bacteroides*, *Prevotella*, and *Ruminococcaceae* as demonstrated with fructose feeding is passed on to the offspring. There is some parallel between our study and those using *Lactobacillus* as a probiotic intervention to slow progression of type II diabetes (Yadav et al., 2007) and liver steatosis (Wagnerberger et al., 2013) in fructose fed mice and rats, suggesting that a microbiome deficient in *Lactobacillus* is part of the adverse effects caused by a high-fructose diet. However, there is currently no evidence to suggest a direct link between changes in bacterial abundance and intestinal permeability. Further studies measuring intestinal permeability directly and relevant end organs are now required to ascertain if the changes in tight junction gene expression observed in our model contribute to further adverse effects. Studies of a high fructose diet in germ-free mice, while not representing normal physiological or environmental conditions, would be worthwhile to determine whether the changes observed in this study are a direct effect of fructose or are indirectly caused by changes to the microbiome.

CONCLUSION

We have shown that fructose consumption during pregnancy affects microbial diversity in the mother, with a shift toward a microbiome that is more diverse, that appears to be the opposite of changes in a normal pregnancy. Further studies into how this maternal microbiome will influence colonization in the offspring, either those continuing on a fructose supplemented diet or switching to a control diet, would be informative. Continuation of the fructose-supplemented diet by the offspring adversely affects epithelial tight junctions and therefore potentially intestinal permeability, with these effects not being apparent in the first generation.

To our knowledge, this is the first account of both these microbial changes and the offspring effects being demonstrated

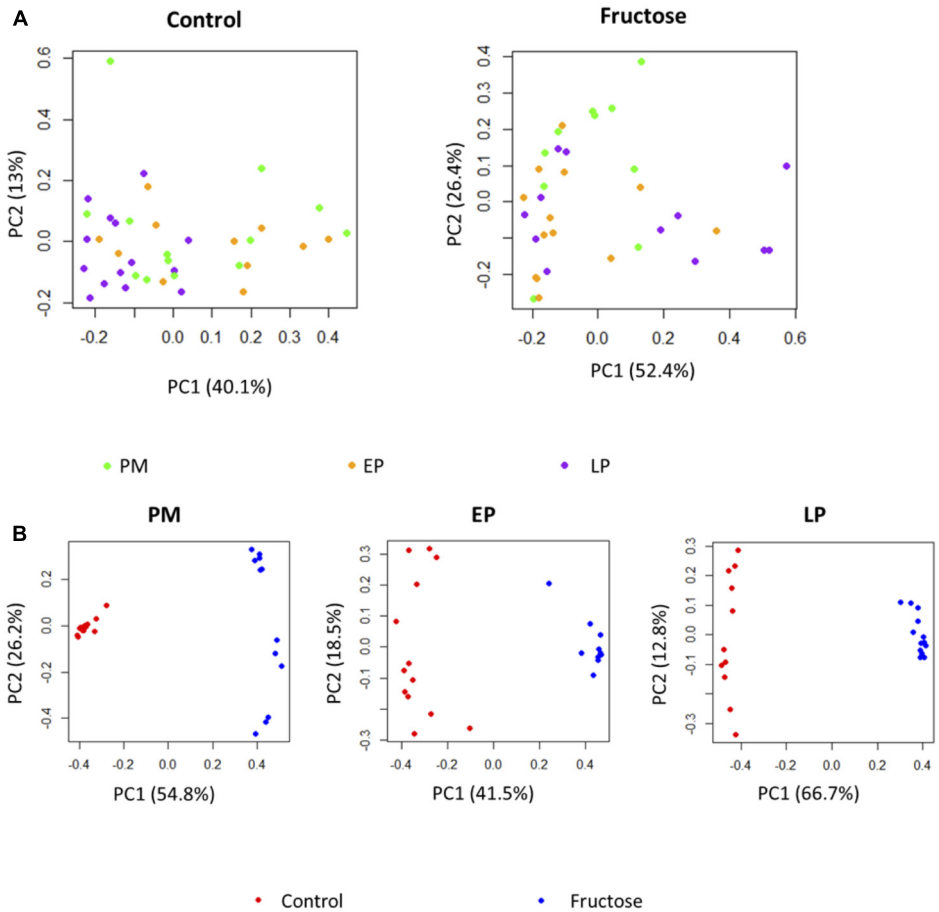

FIGURE 6 | PCoA plots of bacterial profiles at species level based on Bray–Curtis dissimilarity analysis. **(A)** Pregnancy status did not affect the clustering of the bacterial profiles either under Control diet or under Fructose diet. **(B)** At each pregnancy stage, bacterial profiles clustered based on the diets they receive.

TABLE 4 | Relative abundance of the identified bacteria species.

	PM		EP		LP			P		
Species	**C**	**F**	**C**	**F**	**C**	**F**	**SEM**	**Period**	**Diet**	**Period * Diet**
sp. of Bacteroidales	0.08	0.00	0.07	0.00	0.17	0.00	0.02	0.441	<0.001	0.269
Bacteroides sp.	0.92	0.01	1.82	0.01	0.66	0.04	0.25	0.477	0.027	0.595
Parabacteroides sp.	0.31	0.00	0.19	0.00	0.05	0.00	0.02	0.011	<0.001	0.026
Prevotella sp.	7.81	0.01	18.32	0.03	29.46	0.00	1.70	0.005	<0.001	0.001
sp. of family S24-7	34.12	0.47	28.44	0.22	28.83	0.23	2.16	0.225	<0.001	0.607
Lactobacillus sp.	5.84	0.00	6.09	0.02	5.50	0.01	0.80	0.879	<0.001	0.988
Lactobacillus reuteri	9.62	0.00	1.25	0.00	0.91	0.00	0.74	0.003	0.002	0.007
Turicibacter sp.	1.50	9.08	1.45	11.42	0.82	8.90	0.92	0.917	<0.001	0.818
sp. of Clostridiales	1.96	0.00	9.96	0.02	2.16	0.01	0.88	0.032	0.006	0.080
sp. of Lachnospiraceae	0.47	0.00	0.25	0.00	0.34	0.00	0.04	0.209	<0.001	0.280
sp. of Peptostreptococcaceae	0.01	2.17	0.11	2.86	0.03	2.03	0.19	0.642	<0.001	0.490
Oscillospira sp.	2.45	0.16	2.01	0.51	2.72	0.39	0.19	0.962	<0.001	0.463
Ruminococcus sp.	0.69	0.90	0.71	2.42	0.61	1.53	0.19	0.346	0.018	0.267
Anaeroplasma sp.	0.03	0.18	0.00	0.19	0.00	0.04	0.02	0.055	<0.001	0.080
sp. of order RF39	0.58	0.00	0.09	0.01	0.11	0.04	0.04	<0.001	<0.001	<0.001

*PM, pre-mate; EP, early pregnancy; LP, late pregnancy; C, control; F, fructose. *Data presented in proportion.*

with a relatively low supplementation of fructose, and this may have implications for the effects of fructose consumption as part of the Western diet.

AUTHOR CONTRIBUTIONS

All authors contributed to the research and reviewed the manuscript. SA, AS, and RB designed the study. SA, AS, BN, and AH carried out all animal husbandry, sample collection, and laboratory work. MZ and BW carried out analysis of 16s sequencing data. SA, AS, MZ, BW, MS, and RB drafted the manuscript. All authors discussed the analysis, interpretation, and presentation of the results.

FUNDING

This work was supported by the University of Alberta Faculty of Medicine and Dentistry Emerging Team Grant (with the Women and Children's Health Research Institute), the Natural Sciences and Engineering Research Council of Canada, the Alberta Diabetes Institute, and The Faculty of Medicine and Health Sciences, University of Nottingham.

ACKNOWLEDGMENTS

The authors would like to thank Nicole Coursen for assistance with all aspects of the animal study.

SUPPLEMENTARY MATERIAL

The Supplementary Material for this article can be found online at: https://www.frontiersin.org/articles/10.3389/fgene.2018.00203/full#supplementary-material

REFERENCES

Baserga, M., Bertolotto, C., Maclennan, N. K., Hsu, J. L., Pham, T., Laksana, G. S., et al. (2004). Uteroplacental insufficiency decreases small intestine growth and alters apoptotic homeostasis in term intrauterine growth retarded rats. *Early Hum. Dev.* 79, 93–105. doi: 10.1016/j.earlhumdev.2004.04.015

Bergheim, I., Weber, S., Vos, M., Krämer, S., Volynets, V., Kaserouni, S., et al. (2008). Antibiotics protect against fructose-induced hepatic lipid accumulation in mice: role of endotoxin. *J. Hepatol.* 48, 983–992. doi: 10.1016/j.jhep.2008.01.035

Bezerra, R. M., Ueno, M., Silva, M. S., Tavares, D. Q., Carvalho, C. R., and Saad, M. J. (2000). A high fructose diet affects the early steps of insulin action in muscle and liver of rats. *J. Nutr.* 130, 1531–1535. doi: 10.1093/jn/130.6.1531

Bray, G. A., Nielsen, S. J., and Popkin, B. M. (2004). Consumption of high-fructose corn syrup in beverages may play a role in the epidemic of obesity. *Am. J. Clin. Nutr.* 79, 537–543. doi: 10.1093/ajcn/79.4.537

Caporaso, J. G., Kuczynski, J., Stombaugh, J., Bittinger, K., Bushman, F. D., Costello, E. K., et al. (2010). QIIME allows analysis of high-throughput community sequencing data. *Nat. Methods* 7, 335–336. doi: 10.1038/nmeth.f.303

Carmody, R. N., Gerber, G. K., Luevano, JM Jr, Gatti, D. M., Somes, L., Svenson, K. L., et al. (2015). Diet dominates host genotype in shaping the murine gut microbiota. *Cell Host Microbe* 17, 72–84. doi: 10.1016/j.chom.2014.11.010

Clayton, Z. E., Vickers, M. H., Bernal, A., Yap, C., and Sloboda, D. M. (2015). Early life exposure to fructose alters maternal, fetal and neonatal hepatic gene expression and leads to sex-dependent changes in lipid metabolism in rat offspring. *PLoS One* 10:e0141962. doi: 10.1371/journal.pone.0141962

Collado, M. C., Isolauri, E., Laitinen, K., and Salminen, S. (2008). Distinct composition of gut microbiota during pregnancy in overweight and normal-weight women. *Am. J. Clin. Nutr.* 88, 894–899. doi: 10.1093/ajcn/88.4.894

Cotillard, A., Kennedy, S. P., Kong, L. C., Prifti, E., Pons, N., Le Chatelier, E., et al. (2013). Dietary intervention impact on gut microbial gene richness. *Nature* 500, 585–588. doi: 10.1038/nature12480

David, L. A., Maurice, C. F., Carmody, R. N., Gootenberg, D. B., Button, J. E., Wolfe, B. E., et al. (2014). Diet rapidly and reproducibly alters the human gut microbiome. *Nature* 505, 559–563. doi: 10.1038/nature12820

DeSantis, T. Z., Hugenholtz, P., Larsen, N., Rojas, M., Brodie, E. L., Keller, K., et al. (2006). Greengenes, a chimera-checked 16S rRNA gene database and workbench compatible with ARB. *Appl. Environ. Microbiol.* 72, 5069–5072. doi: 10.1128/AEM.03006-05

Erlanson-Albertsson, C., and Lindqvist, A. (2010). Fructose affects enzymes involved in the synthesis and degradation of hypothalamic endocannabinoids. *Regul. Pept.* 161, 87–91. doi: 10.1016/j.regpep.2010.01.003

Faith, M. S., Dennison, B. A., Edmunds, L. S., and Stratton, H. H. (2006). Fruit juice intake predicts increased adiposity gain in children from low-income families: weight status-by-environment interaction. *Pediatrics* 118, 2066–2075. doi: 10.1542/peds.2006-1117

Fåk, F., Ahrné, S., Molin, G., Jeppsson, B., and Weström, B. (2008). Microbial manipulation of the rat dam changes bacterial colonization and alters properties of the gut in her offspring. *Am. J. Physiol. Gastrointest. Liver Physiol.* 294, G148–G154. doi: 10.1152/ajpgi.00023.2007

Gohir, W., Whelan, F. J., Surette, M. G., Moore, C., Schertzer, J. D., and Sloboda, D. M. (2015). Pregnancy-related changes in the maternal gut microbiota are dependent upon the mother's periconceptional diet. *Gut Microbes* 6, 310–320. doi: 10.1080/19490976.2015.1086056

Goran, M. I., Ulijaszek, S. J., and Ventura, E. E. (2013). High fructose corn syrup and diabetes prevalence: a global perspective. *Glob. Public Health* 8, 55–64. doi: 10.1080/17441692.2012.736257

Gray, C., Long, S., Green, C., Gardiner, S. M., Craigon, J., and Gardner, D. S. (2013). Maternal fructose and/or salt intake and reproductive outcome in the rat: effects on growth, fertility, sex ratio, and birth order. *Biol. Reprod.* 89:51. doi: 10.1095/biolreprod.113.109595

Havel, P. J. (2005). Dietary fructose: implications for dysregulation of energy homeostasis and lipid/carbohydrate metabolism. *Nutr. Rev.* 63, 133–157. doi: 10.1111/j.1753-4887.2005.tb00132.x

Huang, B.-W., Chiang, M.-T., Yao, H.-T., and Chiang, W. (2004). The effect of high-fat and high-fructose diets on glucose tolerance and plasma lipid and leptin levels in rats. *Diabetes Obes. Metab.* 6, 120–126. doi: 10.1111/j.1462-8902.2004.00323.x

Hwang, I. S., Ho, H., Hoffman, B. B., and Reaven, G. M. (1987). Fructose-induced insulin resistance and hypertension in rats. *Hypertension* 10, 512–516. doi: 10.1161/01.HYP.10.5.512

Indrio, F., Maggio, L., and Raimondi, D. F. (2013). "Feeding the preterm neonate with intrauterine growth restriction," in *Nutrition for the Preterm Neonate*, ed. S. Patole (Berlin: Springer), 391–404.

Johnson, R. J., Rivard, C., Lanaspa, M. A., Otabachian-Smith, S., Ishimoto, T., Cicerchi, C., et al. (2013). Fructokinase, fructans, intestinal permeability, and metabolic syndrome: an equine connection? *J. Equine Vet. Sci.* 33, 120–126. doi: 10.1016/j.jevs.2012.05.004

Kazumi, T., Odaka, H., Hozumi, T., Ishida, Y., Amano, N., and Yoshino, G. (1997). Effects of dietary fructose or glucose on triglyceride production and lipogenic enzyme activities in the liver of Wistar fatty rats, an animal model of NIDDM. *Endocr. J.* 44, 239–245. doi: 10.1507/endocrj.44.239

Koren, O., Goodrich, J. K., Cullender, T. C., Spor, A., Laitinen, K., Kling Bäckhed, H., et al. (2012). Host remodeling of the gut microbiome and metabolic changes during pregnancy. *Cell* 150, 470–480. doi: 10.1016/j.cell.2012.07.008

Lam, Y. Y., Mitchell, A. J., Holmes, A. J., Denyer, G. S., Gummesson, A., Caterson, I. D., et al. (2011). Role of the gut in visceral fat inflammation and metabolic disorders. *Obesity* 19, 2113–2120. doi: 10.1038/oby.2011.68

Lebenthal, E., Nitzan, M., Lee, P. C., Chrzanowski, B. L., and Krasner, J. (1981). Effect of intrauterine growth retardation on the activities of fetal intestinal enzymes in rats. *Neonatology* 39, 14–21. doi: 10.1159/000241387

Lim, J. S., Mietus-Snyder, M., Valente, A., Schwarz, J.-M., and Lustig, R. H. (2010). The role of fructose in the pathogenesis of NAFLD and the metabolic syndrome. *Nat. Rev. Gastroenterol. Hepatol.* 7, 251–264. doi: 10.1038/nrgastro.2010.41

Lineker, C., Kerr, P. M., Nguyen, P., Bloor, I., Astbury, S., Patel, N., et al. (2016). High fructose consumption in pregnancy alters the perinatal environment without increasing metabolic disease in the offspring. *Reprod. Fertil. Dev.* 28, 2007–2015. doi: 10.1071/RD15119

Livak, K. J., and Schmittgen, T. D. (2001). Analysis of relative gene expression data using real-time quantitative PCR and the 2-ΔΔCT method. *Methods* 25, 402–408. doi: 10.1006/meth.2001.1262

Mor, G., and Cardenas, I. (2010). The immune system in pregnancy: a unique complexity. *Am. J. Reprod. Immunol.* 63, 425–433. doi: 10.1111/j.1600-0897.2010.00836.x

Moreira, A. P., Texeira, T. F., Ferreira, A. B., Peluzio Mdo, C., and Alfenas Rde, C. (2012). Influence of a high-fat diet on gut microbiota, intestinal permeability and metabolic endotoxaemia. *Br. J. Nutr.* 108, 801–809. doi: 10.1017/S0007114512001213

Morise, A., Louveau, I., and Le Huërou-Luron, I. (2008). Growth and development of adipose tissue and gut and related endocrine status during early growth in the pig: impact of low birth weight. *Animal* 2, 73–83. doi: 10.1017/S175173110700095X

Newbern, D., and Freemark, M. (2011). Placental hormones and the control of maternal metabolism and fetal growth. *Curr. Opin. Endocrinol. Diabetes Obes.* 18, 409–416. doi: 10.1097/MED.0b013e32834c800d

Pachikian, B. D., Essaghir, A., Demoulin, J.-B., Catry, E., Neyrinck, A. M., Dewulf, E. M., et al. (2013). Prebiotic approach alleviates hepatic steatosis: Implication of fatty acid oxidative and cholesterol synthesis pathways. *Mol. Nutr. Food Res.* 57, 347–359. doi: 10.1002/mnfr.201200364

Payne, A. N., Chassard, C., and Lacroix, C. (2012). Gut microbial adaptation to dietary consumption of fructose, artificial sweeteners and sugar alcohols: implications for host–microbe interactions contributing to obesity. *Obes. Rev.* 13, 799–809. doi: 10.1111/j.1467-789X.2012.01009.x

Rifas-Shiman, S. L., Rich-Edwards, J. W., Willett, W. C., Kleinman, K. P., Oken, E., and Gillman, M. W. (2006). Changes in dietary intake from the first to the second trimester of pregnancy. *Paediatr. Perinat. Epidemiol.* 20, 35–42. doi: 10.1111/j.1365-3016.2006.00691.x

Song, A., Astbury, S., Hoedl, A., Nielsen, B., Symonds, M. E., and Bell, R. C. (2017). Lifetime exposure to a constant environment amplifies the impact of a fructose-rich diet on glucose homeostasis during pregnancy. *Nutrients* 9:E327. doi: 10.3390/nu9040327

Spruss, A., and Bergheim, I. (2009). Dietary fructose and intestinal barrier: potential risk factor in the pathogenesis of nonalcoholic fatty liver disease. *J. Nutr. Biochem.* 20, 657–662. doi: 10.1016/j.jnutbio.2009.05.006

Turnbaugh, P. J., Ley, R. E., Mahowald, M. A., Magrini, V., Mardis, E. R., and Gordon, J. I. (2006). An obesity-associated gut microbiome with increased capacity for energy harvest. *Nature* 444, 1027–1031. doi: 10.1038/nature05414

Untergasser, A., Nijveen, H., Rao, X., Bisseling, T., Geurts, R., and Leunissen, J. A. (2007). Primer3Plus, an enhanced web interface to Primer3. *Nucleic Acids Res.* 35, W71–W74. doi: 10.1093/nar/gkm306

Vandesompele, J., De Preter, K., Pattyn, F., Poppe, B., Van Roy, N., De Paepe, A., et al. (2002). Accurate normalization of real-time quantitative RT-PCR data by geometric averaging of multiple internal control genes. *Genome Biol.* 3:RESEARCH0034. doi: 10.1186/gb-2002-3-7-research0034

Vickers, M. H., Clayton, Z. E., Yap, C., and Sloboda, D. M. (2011). Maternal fructose intake during pregnancy and lactation alters placental growth and leads to sex-specific changes in fetal and neonatal endocrine function. *Endocrinology* 152, 1378–1387. doi: 10.1210/en.2010-1093

Vos, M. B. (2014). Nutrition, nonalcoholic fatty liver disease and the microbiome: recent progress in the field. *Curr. Opin. Lipidol.* 25, 61–66. doi: 10.1097/MOL.0000000000000043

Wagnerberger, S., Spruss, A., Kanuri, G., Stahl, C., Schröder, M., Vetter, W., et al. (2013). *Lactobacillus casei* Shirota protects from fructose-induced liver steatosis: a mouse model. *J. Nutr. Biochem.* 24, 531–538. doi: 10.1016/j.jnutbio.2012.01.014

Wang, J., Chen, L., Li, D., Yin, Y., Wang, X., Li, P., et al. (2008). Intrauterine growth restriction affects the proteomes of the small intestine, liver, and skeletal muscle in newborn pigs. *J. Nutr.* 138, 60–66. doi: 10.1093/jn/138.1.60

Xu, R. J., Mellor, D. J., Birtles, M. J., Reynolds, G. W., and Simpson, H. V. (1994). Impact of intrauterine growth retardation on the gastrointestinal tract and the pancreas in newborn pigs. *J. Pediatr. Gastroenterol. Nutr.* 18, 231–240. doi: 10.1097/00005176-199402000-00018

Yadav, H., Shalini, J., and Sinha, P. R. (2007). Antidiabetic effect of probiotic dahi containing *Lactobacillus acidophilus* and *Lactobacillus casei* in high fructose fed rats. *Nutrition* 23 62–68. doi: 10.1016/j.nut.2006.09.002

Younoszai, M. K., and Ranshaw, J. (1973). Gastrointestinal growth in the fetus and suckling rat pups: effects of maternal dietary protein. *J. Nutr.* 103, 454–461. doi: 10.1093/jn/103.3.454

Conflict of Interest Statement: The authors declare that the research was conducted in the absence of any commercial or financial relationships that could be construed as a potential conflict of interest.

frontiers in Cell and Developmental Biology

ORIGINAL RESEARCH
published: 21 June 2017
doi: 10.3389/fcell.2017.00063

At Term, XmO and XpO Mouse Placentas Show Differences in Glucose Metabolism in the Trophectoderm-Derived Outer Zone

Nannan He[1], Shujing J. Lim[1†], Joana C. Moreira de Mello[2], Injerreau Navarro[1], Monika Bialecka[1], Daniela C. F. Salvatori[1,3], Lucette A. J. van der Westerlaken[4], Lygia V. Pereira[2] and Susana M. Chuva de Sousa Lopes[1,5]**

[1] Department of Anatomy and Embryology, Leiden University Medical Center, Leiden, Netherlands, [2] Department of Genetics and Evolutionary Biology, University of São Paulo, São Paulo, Brazil, [3] Central Laboratory Animal Facility, Leiden University Medical Center, Leiden, Netherlands, [4] Department of Gynaecology, Leiden University Medical Center, Leiden, Netherlands, [5] Department for Reproductive Medicine, Ghent University Hospital, Ghent, Belgium

OPEN ACCESS

Edited by:
Rafael Franco,
University of Barcelona, Spain

Reviewed by:
Ravi Goyal,
Loma Linda University, United States
Antonius Plagge,
University of Liverpool,
United Kingdom

***Correspondence:**
Lygia V. Pereira
lpereira@usp.br
Susana M. Chuva de Sousa Lopes
lopes@lumc.nl

†Present Address:
Shujing J. Lim,
College of Medicine and Veterinary Medicine, University of Edinburgh, Edinburgh, United Kingdom

Specialty section:
This article was submitted to Epigenomics and Epigenetics, a section of the journal Frontiers in Cell and Developmental Biology

Received: 03 April 2017
Accepted: 06 June 2017
Published: 21 June 2017

Citation:
He N, Lim SJ, Moreira de Mello JC, Navarro I, Bialecka M, Salvatori DCF, van der Westerlaken LAJ, Pereira LV and Chuva de Sousa Lopes SM (2017) At Term, XmO and XpO Mouse Placentas Show Differences in Glucose Metabolism in the Trophectoderm-Derived Outer Zone. Front. Cell Dev. Biol. 5:63. doi: 10.3389/fcell.2017.00063

Genetic mouse model (39,XO) for human Turner Syndrome (45,XO) harboring either a single maternally inherited (Xm) or paternally inherited (Xp) chromosome show a pronounced difference in survival rate at term. However, a detailed comparison of XmO and XpO placentas to explain this difference is lacking. We aimed to investigate the morphological and molecular differences between XmO and XpO term mouse placentas. We observed that XpO placentas at term contained a significantly larger area of glycogen cells (GCs) in their outer zone, compared to XmO, XX, and XY placentas. In addition, the outer zone of XpO placentas showed higher expression levels of lactate dehydrogenase (*Ldha*) than XmO, XX, and XY placentas, suggestive of increased anaerobic glycolysis. In the labyrinth, we detected significantly lower expression level of trophectoderm (TE)-marker keratin 19 (*Krt19*) in XpO placentas than in XX placentas. The expression of other TE-markers was comparable as well as the area of TE-derived cells between XO and wild-type labyrinths. XpO placentas exhibited specific defects in the amount of GCs and glucose metabolism in the outer zone, suggestive of increased anaerobic glycolysis, as a consequence of having inherited a single Xp chromosome. In conclusion, the XpO genotype results in a more severe placental phenotype at term, with distinct abnormalities regarding glucose metabolism in the outer zone.

Keywords: X chromosome, mouse, placenta, trophoblast cells, glucose metabolism, Turner Syndrome

INTRODUCTION

Turner Syndrome is the most common sex chromosome disorder affecting 1 in 2,000 live births. It is caused by the loss of genetic material from one of the sex chromosomes and the retained single X chromosome can be inherited either from the mother (Xm) or the father (Xp) (Saenger, 1996). In humans, 99% of the XO fetuses are lost during pregnancy (Cockwell et al., 1991; Ranke and Saenger, 2001). By contrast, in mice, 90% of embryos with a single Xm survive to term, whereas 40% of embryos with a single Xp are resorbed due to severe placental abnormalities (Burgoyne et al., 1983a,b; Hunt, 1991). This suggests that the transcription of a single Xm or Xp in mouse placentas

is not equivalent and influences development differently, reflecting either a different genome-wide epigenetic landscape between Xp and Xm or the existence of certain paternally imprinted X-linked genes in the mouse placenta.

X chromosome inactivation (XCI) is better understood in mice than in humans (Payer and Lee, 2008, 2014; Okamoto et al., 2011; Deng et al., 2014; Petropoulos et al., 2016) due to the existence of well-studied genetic sub-strains of mice. In mice, in female (XX) late blastocysts, the trophectoderm (TE), and primitive endoderm (PE) show imprinted XCI (with an obligatory active Xm) and the epiblast (EPI) shows random XCI (in each cell either the Xm or Xp is active; Payer and Lee, 2008; Silva et al., 2009; Okamoto et al., 2011). In the placenta, the TE-derived cells [trophoblast giant cells (TGCs), spongiotrophoblasts and glycogen cells (GCs) in the outer zone; mononuclear trophoblast cells and syncytiotrophoblast cells in the labyrinth] maintain imprinted XCI (active Xm). By contrast, the chorionic plate and the embryonic endothelial cells of the labyrinth are derived from EPI, therefore showing random XCI.

In humans, there may not be imprinted XCI in the placenta (de Mello et al., 2010; Penaherrera et al., 2012; Hamada et al., 2016). By the end of the first trimester, the placental volume of XO and control placenta seemed comparable (Wegrzyn et al., 2005); and the birth weight of XmO and XpO new-born babies was similar (Mathur et al., 1991). Nevertheless, there is a higher incidence of XpO human fetuses lost during pregnancy (Jacobs et al., 1989) and the percentage of patients retaining the XmO is 60%–80% (Monroy et al., 2002; Uematsu et al., 2002; Sagi et al., 2007; Ko et al., 2010; Álvarez-Nava et al., 2013).

The placenta is a crucial organ during mammalian development, ensuring the selective and directional transport of gases, nutrients and waste products between the maternal blood and the embryonic blood (Jansson, 2016). In mice, the GCs may serve as a potential additional energy source, due to their high glycogen content and sensitivity to glucagon signaling (Coan et al., 2006). The placenta is a highly regulative organ that adapts constantly to the maternal environment, for example oxygen tension and hypoxia (Adelman et al., 2000; Higgins et al., 2016), availability of nutrients or calorie restriction (Ganguly et al., 2012) and exposure to maternal hormones (Fowden et al., 2009; Dimasuay et al., 2016) to sustain optimal embryonic growth throughout pregnancy.

Interestingly, (epi)genetic abnormalities that affect placental development trigger an adaptive response in the placenta to suppress the decreased efficiency to support embryonic growth (Hemberger, 2002; Lefebvre, 2012; Sandovici et al., 2012; Himes et al., 2013). In the case of XO embryos, embryonic day (E)8.5 XpO embryos had been shown to have small ectoplacental cones (Jamieson et al., 1998). However, by E14, XpO placentas had caught up in size and some showed a larger outer zone (Zechner et al., 1997). At E18.5, XpO placentas were significantly heavier than XX controls (Burgoyne et al., 1983b). But in a later study, XmO, XpO, and XY placentas were found heavier than XX placentas (Ishikawa et al., 2003).

To date, a detailed comparison of XmO and XpO term placentas, in particular the TE-derived part of the placenta, is missing. Here, we show that E18.5 XpO placentas exhibited significantly larger area occupied by GCs in outer zone when compared to XmO, XX, and XY placentas. Moreover, the expression of *Ldha*, coding for the enzyme that converts lactate to pyruvate through anaerobic glycolysis, was significantly higher in outer zone of XpO placentas than the XmO, XX, and XY placentas, suggesting increased anaerobic glycolysis and underlying possible defects in oxygen availability in XpO placentas. In conclusion, the XpO genotype results in a more severe placental phenotype at term, with distinct abnormalities regarding glucose metabolism in the outer zone.

MATERIALS AND METHODS

Mice and Genotyping

All animal tissues used in this work were a generous gift from P. Burgoyne in accordance with the United Kingdom Animals Scientific Procedures Act 1986 and approved by the local ethical committee of the National Institute of Medical Research, London. MF1 mice bearing XX and XY embryos were from XX × XY crossings. XmO and XpO mice were generated as previously described (Ishikawa et al., 2003). Briefly, XmO animals were produced by crossing XX females with $X^{Y}O$ males, and identified by visual detection of female genitalia; the $X^{Y}O$ males were generated by crossing $X^{Paf}O$ females with XY* males. The XpO animals were generated by crossing $In(X)^{Paf}/X$ females with XY males. All females [In(X)/X, XX^{Paf}, and XpO] were karyotyped with trypsin-Giemsa banding using fresh liver to identify the XpO embryos (with 39 chromosomes as opposed to 40 chromosomes).

Placenta Collection and Histology

From a total of 12 litters, E18.5 embryos were isolated in phosphate buffer saline (PBS) and separated into males and females by morphology and genotyped as above. The placentas were dissected into quarters and some quarters were collected for RNA isolation after removal of the outer zone (Jz, TGCs, and decidua), whereas others were fixed in 4% paraformaldehyde (PFA, Merck, Darmstadt, Germany) at 4°C overnight (o/n), washed in PBS and dehydrated through increasing concentrations of ethanol and finally xylene, embedded in paraffin and serially sectioned (5 μm) in the sagittal plane using a microtome (Leica RM2055, Nussloch, Germany) in the medial-to-lateral direction ($N = 3$ XX, $N = 3$ XY, $N = 5$ XmO, $N = 4$ XpO).

Prior to Periodic acid-Shiff (PAS) staining, sections were deparaffinised in xylene, rehydrated through a series of ethanol solutions and incubated 30 min at 56°C in pre-heated 1% periodic acid (Sigma-Aldrich, St. Louis, USA), rinsed in water, immersed in Schiff's reagent (Klinipath, Duiven, The Netherlands) 30 min at room temperature (RT), rinsed in water and counterstained with Mayer's haematoxylin (Merck, Darmstadt, Germany). Congo red, Masson's trichrome and Hematoxylin-eosin staining were performed using standard histological procedures. Stained sections were washed in water, dehydrated through a series of ethanol, xylene, and mounted in Entellan (Merck, Darmstadt, Germany).

Quantitative Reverse-Transcription Polymerase Chain Reaction (QPCR)

QPCR was performed on placental quarters after removal of the outer zone and analyzed as described (de Melo Bernardo et al., 2015); or on RNA material isolated from 5x paraffin sections of the outer zone using RecoverAll total nucleic acid isolation kit (AM1975, Ambion, Carlsbad, CA, USA) following the manufacturer's protocol. For normalization, the ΔΔCt method was used with the reference genes *Ubc* and *B2m*, stably expressed in mouse placenta (Solano et al., 2016). All individual placentas were analyzed in technical triplicates. The fold change in expression was calculated relative to the XX1 placenta. Briefly, the average ΔCt value from the technical triplicates of the XX1 (Ave ΔCt XX1) was calculated. Next, we subtracted Ave ΔCt XX1 from each ΔCt (ΔΔCt) and the relative fold change $[2^{-(\Delta\Delta Ct)}]$ calculated. The fold change of each of the triplicate values per placenta was then averaged (mean) and the standard deviation was calculated. The primers used are listed in Supplementary Table 1.

Immunofluorescence

Paraffin sections were deparaffinised and used for immunofluorescence as previously described (Heeren et al., 2015). Primary antibodies used were rabbit anti-KRT19 (or keratin 19) (1:250; ab52625, Abcam, Cambridge, UK) and rat anti-EMCN (or endomucin) (1:150; sc-65495, Santa Cruz Biotechnology, Santa Cruz, CA, USA). Afterwards, sections were washed in 0.05% Tween-20/PBS, treated with 0.3% Sudan Black B (Edward Gurr Ltd, London, UK) in 70% ethanol for 5 min to eliminate background autofluorescence from red blood cells (Romijn et al., 1999) and incubated with secondary antibodies diluted in blocking solution for 1 h at RT. Secondary antibodies were Alexa Fluor 488 goat anti-rabbit (1:500; A-11034, Life Technologies, Eugene, OR, USA) and Alexa Fluor 555 goat anti-rat (1:500; A-21434, Life Technologies, Eugene, OR, USA). Nuclei were stained with 4′,6-diamidino-2-phenylindole (DAPI) (Vector Laboratories, Peterborough, UK) and sections were mounted in Prolong Gold anti-fade reagent (Life technologies, Eugene, OR, USA). Slides used for isotype controls were treated as above using rabbit immunoglobulin fraction (1:250; X0903, Dako, Heverlee, Belgium) and rat IgG2a (1:150, MAB006, R&D Systems, Minneapolis, MN, USA) instead of the primary antibodies.

Imaging and Quantification

Bright-field images were taken on an Olympus AX70 microscope (Olympus, Zoeterwoude, Netherlands) equipped with a digital camera (Olympus XC50, Tokyo, Japan). Fluorescence images were acquired on a Leica DMRA fluorescence microscope (Leica, Wetzlar, Germany) with a CoolSnap HQ2 camera (Photometrics, Tucson, USA) or a Leica AF6000 fluorescence microscope with a Hamamatsu EM-CCD C9100 camera (Leica Microsystems, Wetzlar, Germany). Quantification was performed in ImageJ 1.48 (http://imagej.nih.gov/ij).

Statistical Analysis

The statistical analyses of the proportion of glycogen cells area in the outer zone of the placentas, the percentage of fetal vascular space, the area occupied by TE-derived cells in the labyrinth and differential gene expression per genotype were performed using one-way ANOVA with the Tukey-HSD applied for *post-hoc* testing, using statistical software package SPSS 20.0 (SPSS Inc., Chicago, IL, USA). $P < 0.05$ was considered significant.

RESULTS

At Term, XpO Placentas Showed Larger Area Occupied by GCs in the Outer Zone

We investigated the placental morphology of the four genotypes ($N = 3$ XX, $N = 3$ XY, $N = 5$ XmO, $N = 3$ XpO) at E18.5 using PAS-staining. This allowed us to distinguish the outer zone from the labyrinth (**Figure 1A**). We observed the presence of a broader outer zone in the lateral part of XmO ($N = 2$ in 5, 40%) and XpO ($N = 3$ in 3, 100%) placentas (**Figure 1A**). To quantify the area occupied by GCs in the outer zone, the ratio of the area occupied by GCs in the outer zone was calculated on individual placental sections ($n = 3$–5 medial sections per placenta, containing a visible connection to the umbilical cord; **Figures 1B,C**). The XpO placentas contained a significantly larger area occupied by GCs in the outer zone when compared to XX, XY, and XmO placentas ($P = 0.004$, 0.008, and 0.045, respectively, **Figure 1C**). In contrast, the area occupied by GCs in the outer zone of XmO placentas was comparable to that of XX and XY placentas (**Figure 1C**).

At Term, XpO Placentas Showed Increased *Ldha* Expression in the Outer Zone

The larger area of GCs in outer zone of XpO placentas led us to investigate defects in gene expression related to glucagon signaling and glucose metabolism (**Figure 2A**) in the outer zone. The expression level of glucagon receptor (*Gcgr*) as well as of glucose transporter *Slc2a1*, which mediate passive glucose uptake in cells (Zhao and Keating, 2007) was similar between XmO, XpO, and XX placentas (**Figure 2B**, Supplementary Table 2).

Two X-linked genes, *G6pdx* and *Pgk1*, encode essential enzymes in the conversion of glucose to pyruvate (Semenza et al., 1994; Tuttle et al., 2000). In the outer zone, *G6pdx* showed significantly lower expression in both XmO and XpO placentas compared to the XX placentas (XmO vs. XX: $P = 0.028$; XpO vs. XX: $P = 0.007$; **Figure 2B,** Supplementary Table 2). However, expression of *Pgk1* was significantly higher in XpO placentas than in XmO placentas ($P = 0.009$, **Figure 2B,** Supplementary Table 2).

Under normal oxygen supply (aerobic glycolysis), pyruvate is catabolized into acetyl-CoA to be used in the tricarboxylic acid (TCA) cycle to produce energy efficiently (**Figure 2A**). One of the enzymes of the TCA cycle, encoded by X-linked gene *Idh3g*, showed similar expression between XO and wild-type placentas (**Figure 2B,** Supplementary Table 2). However, if oxygen supply is low, pyruvate is metabolized to lactate (anaerobic glycolysis). In anaerobic glycolysis, the key enzyme that converts pyruvate into lactate is encoded by the *Ldha* gene. The expression levels

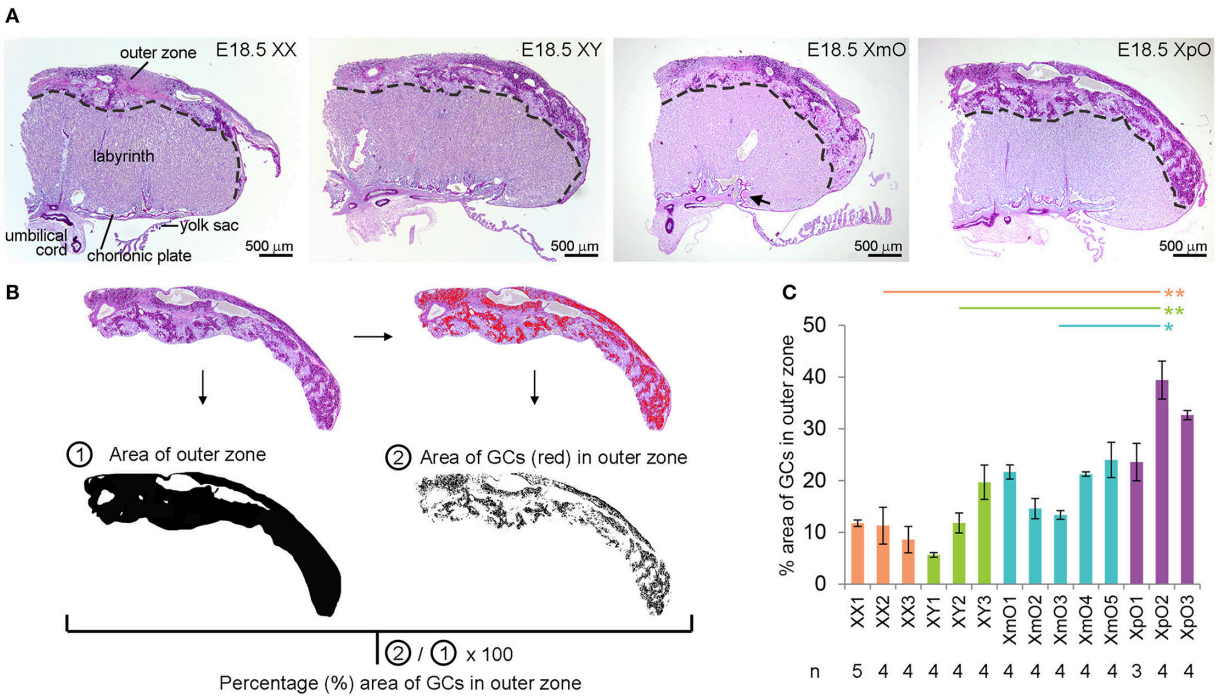

FIGURE 1 | XpO placentas have a larger area occupied by glycogen cells in the outer zone. **(A)** Representative PAS-stained medial placental sections of the different genotypes (XX, XY, XmO, XpO). **(B)** From the images acquired by microscopy, the outer zone of the placenta is digitally selected, then converted to black-and-white on Image J to provide the total area of the outer zone. From the selected outer zone of the placenta, the dark PAS-stained glycogen cells (GCs) are identified digitally (red cells) by selecting a threshold on Image J. The percentage of the GCs in the outer zone of each placenta section is obtained by using the ratio of the area of GCs ②/total area of the outer zone ① . **(C)** Graph depicting the percentage (%) area of outer zone occupied by GCs in the different genotypes (XX, XY, XmO, XpO). Significant *P*-values between XpO placentas and the other genotypes are indicated by $^{*}P < 0.05$ and $^{**}P < 0.01$.

of *Ldha* in the outer zone of XpO placentas were significantly higher than in the other placentas (XpO vs. XX: $P = 0.007$; XpO vs. XY: $P = 0.015$; XpO vs. XmO: $P < 0.001$; **Figure 2B,** Supplementary Table 2), suggesting higher levels of anaerobic respiration specifically in the outer zone of the XpO placentas, where a higher incidence of GCs was found.

The Labyrinths of XO and Wild-Type Placentas Were Comparable

Next, we determined the relative expression of TE markers [keratin 19 (*Krt19*), syncytin b (*Synb*), glial cells missing homolog 1 (*Gcm1*)] and endothelial markers [endoglin (*Eng*), platelet/endothelial cell adhesion molecule 1 (*Pecam1*)] in the labyrinth of the four types of placentas.

The expression levels of TE-marker *Krt19* in the labyrinth of XpO placenta were significantly lower than that in XX placenta ($P = 0.024$, **Figure 2C,** Supplementary Table 2). However, the TE-markers *Synb* and *Gcm1* were similarly expressed in the four types of placentas (**Figure 2C,** Supplementary Table 2). There was also no difference in the expression of endothelial-markers *Eng* and *Pecam1* in the labyrinth (**Figure 2C,** Supplementary Table 2). Together, the data suggests that the labyrinth of XO placentas may be similar to wild-type placentas.

To further confirm that, we quantified the area occupied by (EMCN-positive) fetal capillaries and (KRT19-positive) TE-derived cells in the labyrinth ($n = 3$–5 sections per individual placenta; $N = 3$ XX, $N = 3$ XY, $N = 5$ XmO, $N = 4$ XpO; **Figure 3**). For the quantification, single channel images of the labyrinth zone from medial placental sections immunostained for anti-EMCN (red) and anti-KRT19 (green), and DAPI (details shown in **Figures 3B,D,E**) were used. The area of the fetal vasculature (**Figure 3B**), considered the area occupied by the EMCN-positive fetal capillaries, was similar between XO and wild-type labyrinths (**Figure 3C,** left panel). Moreover, the vascular density, calculated as the number of fetal capillaries per image, was also comparable between XO and wild-type labyrinths (**Figure 3C,** right panel).

To quantify the area of occupied by TE-derived cells, the nuclei area (DAPI-positive) was merged with the KRT19-positive cytoplasmic staining of the TE derived cells. However, to exclude the nuclear area of the fetal vasculature, we subtracted the fetal vascular area (**Figures 3B,D,E**). In this way, we obtained the area occupied solely by TE-derived cells (cytoplasm and nuclei). We concluded that the area occupied by TE-derived cells in labyrinth was similar between XO and wild-type placentas (**Figure 3E**).

At Term, XpO Placentas Showed Decreased *Xlr4b/4c* in the Labyrinth Zone

The X-linked *Xlr3b* has previously been identified as differentially expressed in XmO and XpO brains, but not in the placentas (Davies et al., 2005). In addition to *Xlr3b*, *Xlr4b/4c* were also reported to be differentially expressed between XmO and XpO

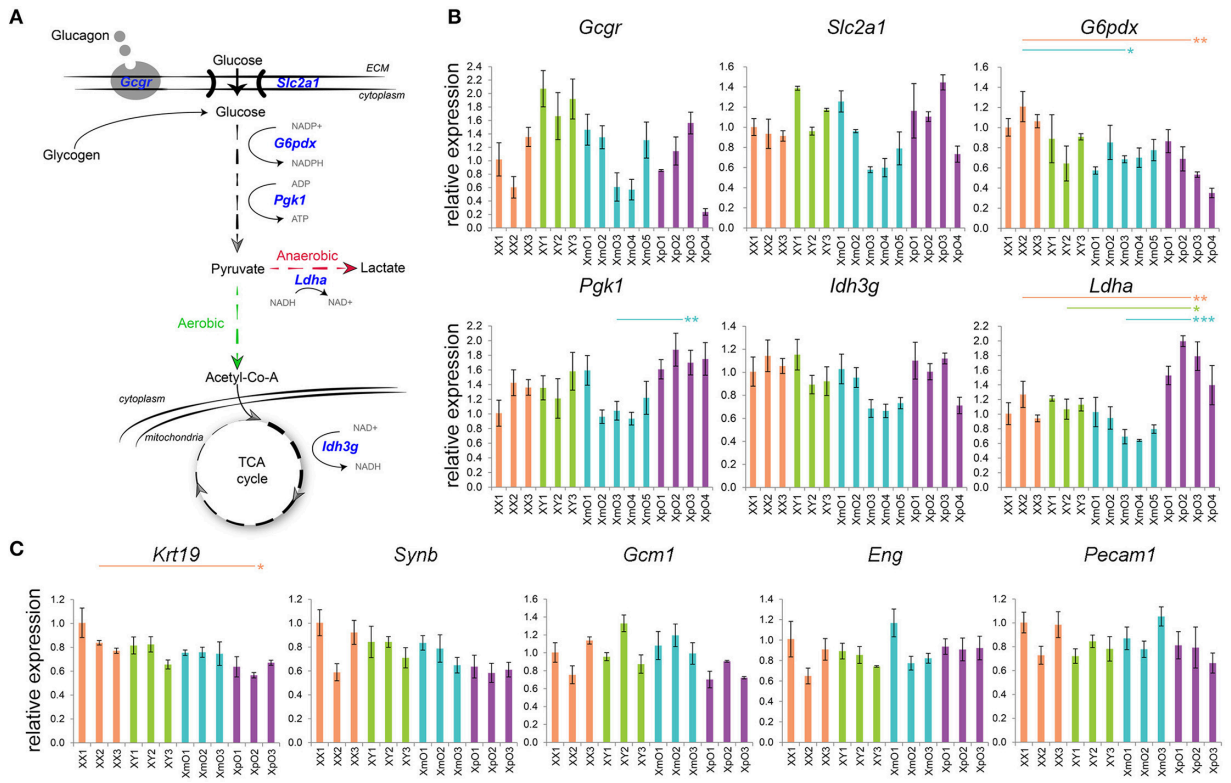

FIGURE 2 | Expression of genes related to glucose metabolism in the outer zone and expression of genes related to TE and vasculature in the labyrinth. **(A)** Scheme of glucose metabolism cascade, with the genes analyzed in blue. **(B)** Relative expression of the depicted genes in the outer zone of XX, XY, XmO, XpO placentas. Each bar represents mean ± standard deviation of technical triplicates of a different individual placenta. *P*-values were calculated between the different genotype-groups using one-way ANOVA with the Tukey-HSD. Significant *P*-values between genotypes are indicated by $^{*}P < 0.05$, $^{**}P < 0.01$, and $^{***}P < 0.001$. **(C)** Relative expression of the depicted genes in the labyrinth of XX, XY, XmO, XpO placentas. Each bar represents mean ± standard deviation of technical triplicates of a different individual placenta. Significant *P*-value between XX and XpO is indicated by $^{*}P < 0.05$.

brains, but at least *Xlr4c* not in placentas (Raefski and O'Neill, 2005). However, whole placentas were used for analysis and a possible regional regulation could have been missed. We therefore investigated the expression of *Xlr3b* and *Xlr4b/4c* separately in outer zone and labyrinth zone of term placenta.

We did not observe significantly differential expression of *Xlr3b* and *Xlr4b/4c* in the XpO and XmO outer zones (**Figure 4A,** Supplementary Table 2), even though XpO outer zones had significantly lower *Xlr3b* than XY outer zones ($P = 0.030$; **Figure 4A,** Supplementary Table 2). In the labyrinth zone, the expression levels of *Xlr3b* were comparable between genotypes (**Figure 4B**, Supplementary Table 2), but surprisingly XpO labyrinth zone had significantly lower expression levels of *Xlr4b/4c* than the other placentas (XpO vs. XX: $P = 0.006$; XpO vs. XY: $P < 0.001$; XpO vs. XmO: $P = 0.003$; **Figure 4B,** Supplementary Table 2).

At Term, XmO Placentas Contained Higher Incidence of Fibrin Nodules in the Maternal Arterial Sinuses Adjacent to the Chorionic Plate

Interestingly, the XmO placentas contained small nodules, partially occluding some maternal arterial sinuses proximal of the chorionic plate (black arrow in **Figure 1A**). After Congo red, Masson's trichrome and Hematoxylin-eosin staining, we concluded that those were fibrin deposits (**Figure 5A**).

To quantify the incidence of fibrin nodules in the different placentas ($N = 3$ XX, $N = 3$ XY, $N = 5$ XmO, $N = 4$ XpO), we manually counted the number of fibrin nodules present in medial placental sections. All XmO placentas contained fibrin deposits in most sections analyzed, whereas the nodules were not observed in most of the other placentas (XmO vs. XX: $P = 0.0007$; XmO vs. XY: $P = 0.0007$; XmO vs. XpO: $P = 0.0019$; **Figure 5B**). On average, per section one or two nodules were observed (**Figures 5A,C**).

DISCUSSION

The lack of a second sex chromosome in XO mouse embryos leads to the development of smaller trophectoderm ectoplacental cones and, in some cases, pregnancy loss (Burgoyne et al., 1983b; Hunt, 1991; Thornhill and Burgoyne, 1993; Jamieson et al., 1998; Ishikawa et al., 2003). Our study on XO placental abnormalities in mice shows that inheriting the single X chromosome from the paternal or maternal side leads to different placental phenotypes: E18.5 XpO placentas contained a larger

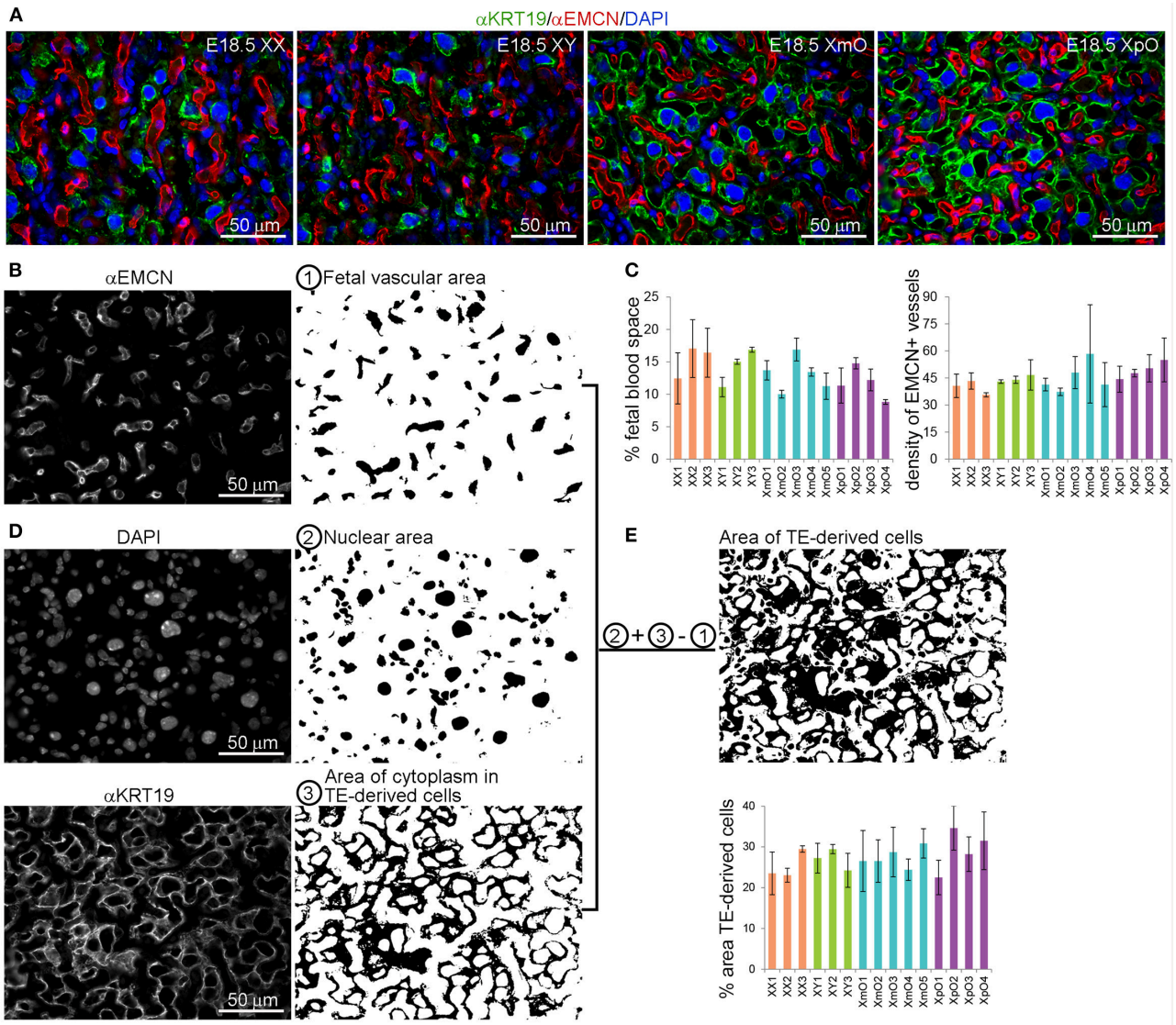

FIGURE 3 | XO placentas show comparable fetal vascular area and TE-derived cell area in the labyrinth. **(A)** Representative medial placental sections from the different genotypes (XX, XY, XmO, XpO) immunostained for KRT19 and EMCN show the organization of the fetal vasculature and maternal blood space in the labyrinth. **(B)** To quantify the fetal vascular area and density, single channel images for EMCN-positive fetal capillaries are filled with black area ① and either the number of vessels counted (density of fetal vessels in that area) or the percentage of fetal vascular area is quantified (sum of the area of EMCN-positive blood vessels/total area of the image × 100). **(C)** Graph depicting the percentage (%) of area occupied by fetal vasculature and the density of EMCN-positive fetal blood vessels in the different genotypes analyzed (XX, XY, XmO, XpO). **(D)** To calculate the percentage of area occupied by TE-derived cells, the single channel images for DAPI ② and KRT19 ③ are converted to black-and-white, added digitally and finally from that area (②+③) the fetal capillary area is subtracted (②+③−①) (sum of the resulting black area/total area of the image × 100). **(E)** Graph depicts the percentage (%) of area occupied by TE-derived cells in the different genotypes analyzed (XX, XY, XmO, XpO).

area of GCs in the outer zone with a possible consequent increase in anaerobic glycolysis and/or oxygen availability. This does not seem to be the case in XmO placentas. By contrast, XmO placentas show increased incidence of small fibrin nodules in maternal arterial sinuses proximal of the chorionic plate.

The placenta is sensitive to defects in epigenetic regulation, such as regulation of imprinted genes and imprinted X inactivation (Hemberger, 2002; Lefebvre, 2012; Himes et al., 2013). As such, it is not surprising that many imprinted and X-linked genes are expressed in the placenta and regulate metabolism and growth (Hemberger, 2002; Lefebvre, 2012; Sandovici et al., 2012). The higher incidence of GCs in the outer zone of XpO placentas may be such an adaptive response to placental insufficiency. Studies in mice show that XpO fetuses have a higher risk of being lost during pregnancy, whereas XmO fetuses generally have a better chance of surviving to term (Hunt, 1991; Jamieson et al.,

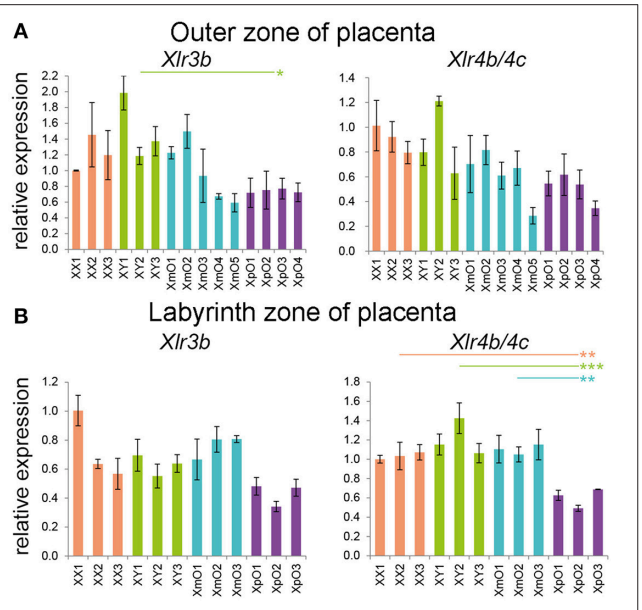

FIGURE 4 | *Xlr* genes expression in the outer zone and labyrinth zone of term placentas. **(A,B)** Relative expression of *Xlr3b* and *Xlr4b/4c* in the outer zone **(A)** and labyrinth zone **(B)** of XX, XY, XmO, XpO placentas. Each bar represents mean ± standard deviation of technical triplicates of a single placenta. Significant *P*-values between genotypes are indicated by $^{*}P < 0.05$, $^{**}P < 0.01$, and $^{***}P < 0.001$.

1998). In XX fetuses, the Xp is preferentially inactivated in the TE-derived tissues (Harper et al., 1982). Thus, in both females and males, it is the Xm that is active in TE-derived tissues during placental development. Epigenetic differences between Xp and Xm, including genome-wide differences in chromatin condensation or the existence of X-linked paternally imprinted genes in the placenta, could explain why XpO embryos have a higher risk of being lost during pregnancy.

Alternatively, as a smaller trophectoderm ectoplacental cone in XO embryos is often associated with a delay in embryonic development (Thornhill and Burgoyne, 1993; Jamieson et al., 1998; Ishikawa et al., 2003), the alteration observed in GCs in outer zone of XpO placentas could reflect a general small delay in development instead of an (active) adaptive response. Interestingly, it has been shown that both the number of GCs and the volume of the junctional zone increases during gestation, peaks at E16.5, followed by reduction until birth (Coan et al., 2004, 2006). Therefore, if the physiological regression of GCs in XpO placentas was delayed, this would result in relatively more GCs and increased size of the outer zone at E18.5 compared to wild-type placentas.

Abnormal GC numbers, related to impaired glucose transport and glycogen metabolism in placenta (Redline et al., 1993; Sibley et al., 2004), have been reported in several mutant mouse placentas, including that of X-linked and imprinted genes, and usually result in runting. Opposite phenotypes regarding GCs numbers can still develop in mouse mutants showing a normal placenta at E10.5. As the XpO phenotype, maternally inherited defects in X-linked *Evx1* also showed higher numbers of GCs, spongiotrophoblasts and secondary TGCs by E14.5 and the mutant pups were smaller at birth (Li and Behringer, 1998). By contrast, *Cited2 KO* and the imprinted (paternally-expressed) *Igf2* KO mice show severe reduction of numbers of GCs, spongiotrophoblasts and secondary TGCs at E12.5–13.5 (Lopez et al., 1996; Withington et al., 2006), but this also resulted in reduced weight at birth (Sibley et al., 2004); whereas the imprinted (maternally-expressed) *Cdkn1c* (or $p57^{Kip2}$) KO showed placentomegaly, with larger labyrinth zone and excess of spongiotrophoblasts, but normal number of GCs and TGCs and no difference in the weight of embryos (Takahashi et al., 2000).

The detected significantly higher expression of *Ldha* in outer zone of XpO placentas indicates a switch from aerobic to anaerobic glycolysis in outer zone of XpO placentas. *Ldha* expression is reported to be increased in human primary placental trophoblast cells under hypoxic conditions (Kay et al., 2007). Interestingly, transcriptomics analysis between XX and XO human fibroblasts revealed differences in glucose metabolism (Rajpathak et al., 2014), but the parental origin of the X chromosome was unclear. Moreover, women with Turner syndrome are characterized by increased size of type IIa muscle fibers in addition to impaired glucose tolerance and insulin resistance, indicating diminished oxygen and substrate supply for metabolic processes (Gravholt et al., 2001). It is also reported that Turner syndrome women have increased anaerobic glycolysis and lactic acid production during exercise, compared to a control group (Wells et al., 2013).

It is unclear whether Xlr factors are directly involved in glucose metabolism, but they could impact on cell differentiation in the outer zone toward GC cells. We observed similar expression of *Xlr3b* and *Xlr4b/4c* in XpO and XmO outer zones suggesting that these genes are not involved in the production of GCs and are not imprinted in the (TE-derived) outer zone. However, the biological significance of the specific decrease in *Xlr4b/4c* in XpO labyrinth remains to be investigated. If this decrease is not due to imprinting in TE-derived labyrinth cells (mononuclear trophoblast and syncytiotrophoblast cells), then perhaps *Xlr4b/c* could be imprinted and silenced on the Xp in the EPI-derived endothelial cells of the labyrinth, in line with the reported imprint in the brain (Raefski and O'Neill, 2005). This could explain the 40% reduction in expression observed.

Small fibrin nodules, most probably from maternal blood-clots, were observed in the maternal sinus of all XmO placentas, but not in most of the other placentas. Interestingly, TE-derived cells at the fetal-maternal interface in both mouse and human exhibit endothelial-like properties (endovascular extravillous trophoblast cells and syncytiotrophoblast cells in humans; syncytiotrophoblast cells in mice) and seem to be involved in the regulation of coagulation during pregnancy (Sood et al., 2006). Fibrin deposits are occasionally described in the labyrinth and spongiotrophoblast area of mouse placentas (Vogt et al., 1996; Redecha et al., 2009); and in the perivillous space, associated with local syncytial denudation, in human placentas (Nelson et al.,

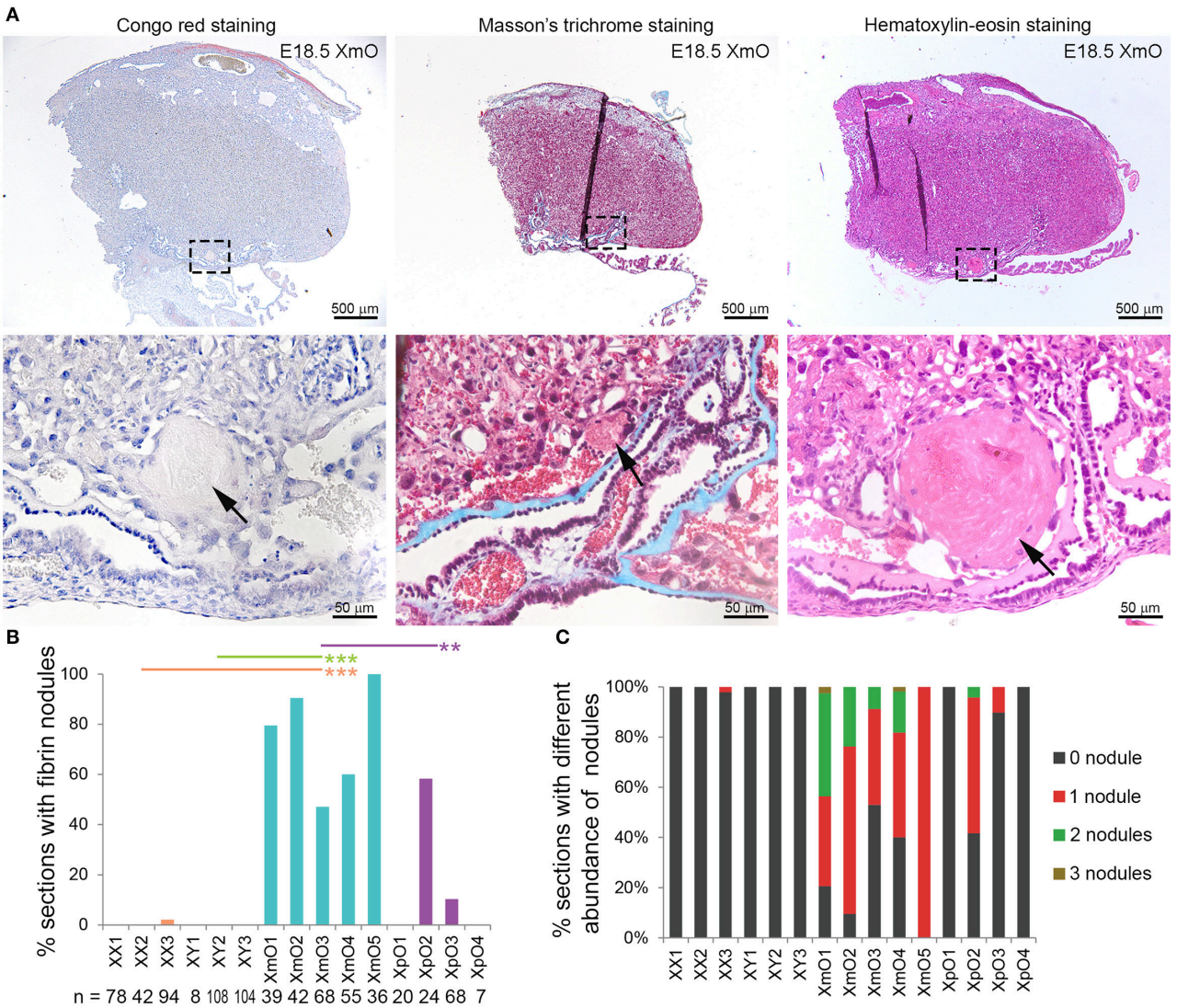

FIGURE 5 | Identifications and quantification of fibrin deposits in term placentas. **(A)** Representative medial XmO placenta sections with Congo red, Masson's trichrome and Hematoxylin-Eosin staining. The dashed boxes in top panels are shown as magnification in bottom panels. Black arrows point to fibrin deposits. **(B)** Graph depicting the percentage (%) of placental sections with fibrin nodules per histological section (*n*) in different genotypes. Significant *P*-values between XmO placentas and the other genotypes are indicated by $^{**}P < 0.01$ and $^{***}P < 0.001$. **(C)** Graph depicting the percentage (%) of placental sections with different abundance of fibrin nodules per histological section (n in **B**) in different genotypes.

1990; Khan et al., 2011). Excessive fibrin deposits at the fetal-maternal interface early during development, such as in *Procr* (or *Epcr*) KO embryos results in severe placental thrombosis and lethality at E10.5 (Gu et al., 2002); whereas in *Wnt2* KO embryos showed fibrin deposits between E14 and E18 with maternal blood accumulation in the labyrinth zone, resulting in 50% viability and smaller pups at birth (Monkley et al., 1996). The fibrin deposits in XmO placentas indicate excessive activation of the coagulation cascade in the maternal circulation, but this obstruction was not as severe as in *Wnt2* KO mice and, as such, does not seem to be pathological.

In conclusion, mouse embryos with a single Xp have a lower chance than XmO embryos to survive to term due to placental insufficiency. Here, we show that XmO and XpO term placentas differ significantly in the amount of GCs in the outer zone and that XpO placentas may have shifted toward anaerobic glycolysis. This shift in glucose metabolism does not seem to be a direct consequence of altered expression of X-linked genes involved in this metabolism (although *Pgk1* expression differs between XmO and XpO outer zones), but rather a consequence of an altered cellular composition of the XpO outer zone (large GCs area) due to placental adaptive response earlier during development. Our findings highlight the need to investigate glucose metabolism in the placenta of human Turner patients, which may provide individual potential therapeutic strategies for Turner Syndrome.

AUTHORS CONTRIBUTIONS

NH, SL, JC, DS, LP, SC designed the study. NH, SL, JC, IN, MB, DS, LV, LP, SC performed experiments and/or analyzed data. NH, SL, SC wrote the manuscript. All authors contributed critical comments and corrections and gave approval for publication.

FUNDING

NH is funded by the China Scholarship Council (CSC) [NO.201307040026]; JC is funded by Fundação de Amparo à Pesquisa do Estado de São Paulo (FAPESP) [2009/17481-6; 2015/03610-0] and LP by Fundação de Amparo à Pesquisa do Estado de São Paulo (FAPESP) [CEPID 13/08135-2]; SC is funded by the Interuniversity Attraction Poles-Phase VII, Belgium [IUAP/PAI P7/14].

ACKNOWLEDGMENTS

We would like to express our gratitude to A. Ojarikre, and P. Burgoyne, MRC National Institute for Medical Research, the Ridgeway, Mill Hill, London, UK for the work involved in mouse husbandry, the logistics of the crossings and timed mattings and for performing the genotyping/karyotyping of the embryos; L. van Iperen for histology; B. Reinius for isolating RNA; J. Goeman for advise on the statistical test to use and A. Zwijsen and N. Criem for useful discussions.

SUPPLEMENTARY MATERIAL

The Supplementary Material for this article can be found online at: http://journal.frontiersin.org/article/10.3389/fcell.2017.00063/full#supplementary-material

REFERENCES

Adelman, D. M., Gertsenstein, M., Nagy, A., Simon, M. C., and Maltepe, E. (2000). Placental cell fates are regulated *in vivo* by HIF-mediated hypoxia responses. *Genes Dev.* 14, 3191–3203. doi: 10.1101/gad.853700

Álvarez-Nava, F., Lanes, R., Quintero, J. M., Miras, M., Fideleff, H., Mericq, V., et al. (2013). Effect of the parental origin of the X-chromosome on the clinical features, associated complications, the two-year-response to growth hormone (rhGH) and the biochemical profile in patients with turner syndrome. *Int. J. Pediatr. Endocrinol.* 2013:10. doi: 10.1186/1687-9856-2013-10

Burgoyne, P. S., Evans, E. P., and Holland, K. (1983a). XO monosomy is associated with reduced birthweight and lowered weight gain in the mouse. *J. Reprod. Fertil.* 68, 381–385. doi: 10.1530/jrf.0.0680381

Burgoyne, P. S., Tam, P. P., and Evans, E. P. (1983b). Retarded development of XO conceptuses during early pregnancy in the mouse. *J. Reprod. Fertil.* 68, 387–393. doi: 10.1530/jrf.0.0680387

Coan, P. M., Conroy, N., Burton, G. J., and Ferguson-Smith, A. C. (2006). Origin and characteristics of glycogen cells in the developing murine placenta. *Dev. Dyn.* 235, 3280–3294. doi: 10.1002/dvdy.20981

Coan, P. M., Ferguson-Smith, A. C., and Burton, G. J. (2004). Developmental dynamics of the definitive mouse placenta assessed by stereology. *Biol. Reprod.* 70, 1806–1813. doi: 10.1095/biolreprod.103.024166

Cockwell, A., MacKenzie, M., Youings, S., and Jacobs, P. (1991). A cytogenetic and molecular study of a series of 45,X fetuses and their parents. *J. Med. Genet.* 28, 151–155. doi: 10.1136/jmg.28.3.151

Davies, W., Isles, A., Smith, R., Karunadasa, D., Burrmann, D., Humby, T., et al. (2005). Xlr3b is a new imprinted candidate for X-linked parent-of-origin effects on cognitive function in mice. *Nat. Genet.* 37, 625–629. doi: 10.1038/ng1577

de Mello, J. C. M., de Araujo, E. S. S., Stabellini, R., Fraga, A. M., de Souza, J. E. S., Sumita, D. R., et al. (2010). Random X inactivation and extensive mosaicism in human placenta revealed by analysis of allele-specific gene expression along the X chromosome. *PLoS ONE* 5:e10947. doi: 10.1371/journal.pone.0010947

de Melo Bernardo, A., Heeren, A. M., van Iperen, L., Fernandes, M. G., He, N., Anjie, S., et al. (2015). Meiotic wave adds extra asymmetry to the development of female chicken gonads. *Mol. Reprod. Dev.* 82, 774–786. doi: 10.1002/mrd.22516

Deng, X., Berletch, J. B., Nguyen, D. K., and Disteche, C. M. (2014). X chromosome regulation: diverse patterns in development, tissues and disease. *Nat. Rev. Genet.* 15, 367–378. doi: 10.1038/nrg3687

Dimasuay, K. G., Boeuf, P., Powell, T. L., and Jansson, T. (2016). Placental responses to changes in the maternal environment determine fetal growth. *Front. Physiol.* 7:12. doi: 10.3389/fphys.2016.00012

Fowden, A. L., Sferruzzi-Perri, A. N., Coan, P. M., Constancia, M., and Burton, G. J. (2009). Placental efficiency and adaptation: endocrine regulation. *J. Physiol.* 587(Pt 14), 3459–3472. doi: 10.1113/jphysiol.2009.173013

Ganguly, A., Collis, L., and Devaskar, S. U. (2012). Placental glucose and amino acid transport in calorie-restricted wild-type and Glut3 null heterozygous mice. *Endocrinology* 153, 3995–4007. doi: 10.1210/en.2011-1973

Gravholt, C. H., Nyholm, B., Saltin, B., Schmitz, O., and Christiansen, J. S. (2001). Muscle fiber composition and capillary density in Turner syndrome: evidence of increased muscle fiber size related to insulin resistance. *Diabetes Care* 24, 1668–1673. doi: 10.2337/diacare.24.9.1668

Gu, J.-M., Crawley, J. T., Ferrell, G., Zhang, F., Li, W., Esmon, N. L., et al. (2002). Disruption of the endothelial cell protein C receptor gene in mice causes placental thrombosis and early embryonic lethality. *J. Biol. Chem.* 277, 43335–43343. doi: 10.1074/jbc.M207538200

Hamada, H., Okae, H., Toh, H., Chiba, H., Hiura, H., Shirane, K., et al. (2016). Allele-specific methylome and transcriptome analysis reveals widespread imprinting in the human placenta. *Am. J. Hum. Genet.* 99, 1045–1058. doi: 10.1016/j.ajhg.2016.08.021

Harper, M. I., Fosten, M., and Monk, M. (1982). Preferential paternal X inactivation in extraembryonic tissues of early mouse embryos. *J. Embryol. Exp. Morphol.* 67, 127–135.

Heeren, A. M., van Iperen, L., Klootwijk, D. B., de Melo Bernardo, A., Roost, M. S., Gomes Fernandes, M. M., et al. (2015). Development of the follicular basement membrane during human gametogenesis and early folliculogenesis. *BMC Dev. Biol.* 15:4. doi: 10.1186/s12861-015-0054-0

Hemberger, M. (2002). The role of the X chromosome in mammalian extra embryonic development. *Cytogenet. Genome Res.* 99, 210–217. doi: 10.1159/000071595

Higgins, J. S., Vaughan, O. R., Fernandez de Liger, E., Fowden, A. L., and Sferruzzi-Perri, A. N. (2016). Placental phenotype and resource allocation to fetal growth are modified by the timing and degree of hypoxia during mouse pregnancy. *J. Physiol.* 594, 1341–1356. doi: 10.1113/JP271057

Himes, K. P., Koppes, E., and Chaillet, J. R. (2013). Generalized disruption of inherited genomic imprints leads to wide-ranging placental defects and dysregulated fetal growth. *Dev. Biol.* 373, 72–82. doi: 10.1016/j.ydbio.2012.10.010

Hunt, P. A. (1991). Survival of XO mouse fetuses: effect of parental origin of the X chromosome or uterine environment? *Development* 111, 1137–1141.

Ishikawa, H., Rattigan, A., Fundele, R., and Burgoyne, P. S. (2003). Effects of sex chromosome dosage on placental size in mice. *Biol. Reprod.* 69, 483–488. doi: 10.1095/biolreprod.102.012641

Jacobs, P., Hassold, T., Harvey, J., and May, K. (1989). The origin of sex chromosome aneuploidy. *Prog. Clin. Biol. Res.* 311, 135.

Jamieson, R. V., Tan, S. S., and Tam, P. P. (1998). Retarded postimplantation development of X0 mouse embryos: impact of the parental origin of the monosomic X chromosome. *Dev. Biol.* 201, 13–25. doi: 10.1006/dbio.1998.8972

Jansson, T. (2016). Placenta plays a critical role in maternal-fetal resource allocation. *Proc. Natl. Acad. Sci. U.S.A.* 113, 11066–11068. doi: 10.1073/pnas.1613437113

Kay, H. H., Zhu, S., and Tsoi, S. (2007). Hypoxia and lactate production in trophoblast cells. *Placenta* 28, 854–860. doi: 10.1016/j.placenta.2006.11.011

Khan, H. M., Khan, M. Y., and Minhas, L. A. (2011). Histological study of the developing mouse placenta. *J. Rawalpindi Med. Coll.* 15, 116–119.

Ko, J. M., Kim, J. M., Kim, G. H., Lee, B. H., and Yoo, H. W. (2010). Influence of parental origin of the X chromosome on physical phenotypes and GH responsiveness of patients with Turner syndrome. *Clin. Endocrinol.* 73, 66–71. doi: 10.1111/j.1365-2265.2010.03782.x

Lefebvre, L. (2012). The placental imprintome and imprinted gene function in the trophoblast glycogen cell lineage. *Reprod. Biomed. Online* 25, 44–57. doi: 10.1016/j.rbmo.2012.03.019

Li, Y., and Behringer, R. R. (1998). Esx1 is an X-chromosome-imprinted regulator of placental development and fetal growth. *Nat. Genet.* 20, 309–311. doi: 10.1038/3129

Lopez, M., Dikkes, P., Zurakowski, D., and Villa-Komaroff, L. (1996). Insulin-like growth factor II affects the appearance and glycogen content of glycogen cells in the murine placenta. *Endocrinology* 137, 2100–2108. doi: 10.1210/endo.137.5.8612553

Mathur, A., Stekol, L., Schatz, D., MacLaren, N., Scott, M., and Lippe, B. (1991). The parental origin of the single X chromosome in Turner syndrome: lack of correlation with parental age or clinical phenotype. *Am. J. Hum. Genet.* 48, 682.

Monkley, S. J., Delaney, S. J., Pennisi, D. J., Christiansen, J. H., and Wainwright, B. J. (1996). Targeted disruption of the Wnt2 gene results in placentation defects. *Development* 122, 3343–3353.

Monroy, N., López, M., Cervantes, A., García-Cruz, D., Zafra, G., Canún, S., et al. (2002). Microsatellite analysis in Turner syndrome: parental origin of X chromosomes and possible mechanism of formation of abnormal chromosomes. *Am. J. Med. Genet.* 107, 181–189. doi: 10.1002/ajmg.10113

Nelson, D. M., Crouch, E. C., Curran, E. M., and Farmer, D. R. (1990). Trophoblast interaction with fibrin matrix. Epithelialization of perivillous fibrin deposits as a mechanism for villous repair in the human placenta. *Am. J. Pathol.* 136, 855–865.

Okamoto, I., Patrat, C., Thepot, D., Peynot, N., Fauque, P., Daniel, N., et al. (2011). Eutherian mammals use diverse strategies to initiate X-chromosome inactivation during development. *Nature* 472, 370–374. doi: 10.1038/nature09872

Payer, B., and Lee, J. T. (2008). X chromosome dosage compensation: how mammals keep the balance. *Annu. Rev. Genet.* 42, 733–772. doi: 10.1146/annurev.genet.42.110807.091711

Payer, B., and Lee, J. T. (2014). Coupling of X-chromosome reactivation with the pluripotent stem cell state. *RNA Biol.* 11, 798–807. doi: 10.4161/rna.29779

Penaherrera, M., Jiang, R., Avila, L., Yuen, R., Brown, C., and Robinson, W. (2012). Patterns of placental development evaluated by X chromosome inactivation profiling provide a basis to evaluate the origin of epigenetic variation. *Hum. Reprod.* 27, 1745–1753. doi: 10.1093/humrep/des072

Petropoulos, S., Panula, S. P., Schell, J. P., and Lanner, F. (2016). Single-cell RNA sequencing: revealing human pre-implantation development, pluripotency and germline development. *J. Intern. Med.* 280, 252–264. doi: 10.1111/joim.12493

Raefski, A. S., and O'Neill, M. J. (2005). Identification of a cluster of X-linked imprinted genes in mice. *Nat. Genet.* 37, 620–624. doi: 10.1038/ng1567

Rajpathak, S. N., Vellarikkal, S. K., Patowary, A., Scaria, V., Sivasubbu, S., and Deobagkar, D. D. (2014). Human 45, X fibroblast transcriptome reveals distinct differentially expressed genes including long noncoding RNAs potentially associated with the pathophysiology of Turner syndrome. *PLoS ONE* 9:e100076. doi: 10.1371/journal.pone.0100076

Ranke, M. B., and Saenger, P. (2001). Turner's syndrome. *Lancet* 358, 309–314. doi: 10.1016/S0140-6736(01)05487-3

Redecha, P., van Rooijen, N., Torry, D., and Girardi, G. (2009). Pravastatin prevents miscarriages in mice: role of tissue factor in placental and fetal injury. *Blood* 113, 4101–4109. doi: 10.1182/blood-2008-12-194258

Redline, R. W., Chernicky, C. L., Tan, H. Q., Ilan, J., and Ilan, J. (1993). Differential expression of insulin-like growth factor-II in specific regions of the late (post day 9.5) murine placenta. *Mol. Reprod. Dev.* 36, 121–129. doi: 10.1002/mrd.1080360202

Romijn, H. J., van Uum, J. F., Emmering, J., Goncharuk, V., and Buijs, R. M. (1999). Colocalization of VIP with AVP in neurons of the human paraventricular, supraoptic and suprachiasmatic nucleus. *Brain Res.* 832, 47–53. doi: 10.1016/S0006-8993(99)01468-7

Saenger, P. (1996). Turner's syndrome. *N. Engl. J. Med.* 335, 1749–1754. doi: 10.1056/NEJM199612053352307

Sagi, L., Zuckerman-Levin, N., Gawlik, A., Ghizzoni, L., Buyukgebiz, A., Rakover, Y., et al. (2007). Clinical significance of the parental origin of the X chromosome in turner syndrome. *J. Clin. Endocrinol. Metab.* 92, 846–852. doi: 10.1210/jc.2006-0158

Sandovici, I., Hoelle, K., Angiolini, E., and Constancia, M. (2012). Placental adaptations to the maternal-fetal environment: implications for fetal growth and developmental programming. *Reprod. Biomed. Online* 25, 68–89. doi: 10.1016/j.rbmo.2012.03.017

Semenza, G. L., Roth, P. H., Fang, H. M., and Wang, G. L. (1994). Transcriptional regulation of genes encoding glycolytic enzymes by hypoxia-inducible factor 1. *J. Biol. Chem.* 269, 23757–23763.

Sibley, C., Coan, P., Ferguson-Smith, A., Dean, W., Hughes, J., Smith, P., et al. (2004). Placental-specific insulin-like growth factor 2 (Igf2) regulates the diffusional exchange characteristics of the mouse placenta. *Proc. Natl. Acad. Sci. U.S.A.* 101, 8204–8208. doi: 10.1073/pnas.0402508101

Silva, J., Nichols, J., Theunissen, T. W., Guo, G., van Oosten, A. L., Barrandon, O., et al. (2009). Nanog is the gateway to the pluripotent ground state. *Cell* 138, 722–737. doi: 10.1016/j.cell.2009.07.039

Solano, M. E., Thiele, K., Kowal, M. K., and Arck, P. C. (2016). Identification of suitable reference genes in the mouse placenta. *Placenta* 39, 7–15. doi: 10.1016/j.placenta.2015.12.017

Sood, R., Kalloway, S., Mast, A. E., Hillard, C. J., and Weiler, H. (2006). Fetomaternal cross talk in the placental vascular bed: control of coagulation by trophoblast cells. *Blood* 107, 3173–3180. doi: 10.1182/blood-2005-10-4111

Takahashi, K., Kobayashi, T., and Kanayama, N. (2000). p57Kip2 regulates the proper development of labyrinthine and spongiotrophoblasts. *Mol. Hum. Reprod.* 6, 1019–1025. doi: 10.1093/molehr/6.11.1019

Thornhill, A. R., and Burgoyne, P. S. (1993). A paternally imprinted X chromosome retards the development of the early mouse embryo. *Development* 118, 171–174.

Tuttle, S., Stamato, T., Perez, M. L., and Biaglow, J. (2000). Glucose-6-phosphate dehydrogenase and the oxidative pentose phosphate cycle protect cells against apoptosis induced by low doses of ionizing radiation. *Radiat. Res.* 153, 781–787. doi: 10.1667/0033-7587(2000)153[0781:GPDATO]2.0.CO;2

Uematsu, A., Yorifuji, T., Muroi, J., Kawai, M., Mamada, M., Kaji, M., et al. (2002). Parental origin of normal X chromosomes in Turner syndrome patients with various karyotypes: implications for the mechanism leading to generation of a 45, X karyotype. *Am. J. Med. Genet.* 111, 134–139. doi: 10.1002/ajmg.10506

Vogt, E., Ng, A.-K., and Rote, N. S. (1996). A model for the antiphospholipid antibody syndrome: monoclonal antiphosphatidylserine antibody induces intrauterine growth restriction in mice. *Am. J. Obstet. Gynecol.* 174, 700–707. doi: 10.1016/S0002-9378(96)70453-2

Wegrzyn, P., Faro, C., Falcon, O., Peralta, C., and Nicolaides, K. (2005). Placental volume measured by three-dimensional ultrasound at 11 to 13+ 6 weeks of gestation: relation to chromosomal defects. *Ultrasound obstet. Gynecol.* 26, 28–32. doi: 10.1002/uog.1923

Wells, G. D., O'Gorman, C. S., Rayner, T., Caterini, J., Thompson, S., Bradley, T., et al. (2013). Skeletal muscle abnormalities in girls and adolescents with Turner syndrome. *J. Clin. Endocrinol. Metab.* 98, 2521–2527. doi: 10.1210/jc.2012-4016

Withington, S., Scott, A., Saunders, D., Floro, K. L., Preis, J., Michalicek, J., et al. (2006). Loss of Cited2 affects trophoblast formation and vascularization of the mouse placenta. *Dev. Biol.* 294, 67–82. doi: 10.1016/j.ydbio.2006.02.025

Zechner, U., Reule, M., Burgoyne, P. S., Schubert, A., Orth, A., Hameister, H., et al. (1997). Paternal transmission of X-linked placental dysplasia in mouse interspecific hybrids. *Genetics* 146, 1399–1405.

Zhao, F. Q., and Keating, A. F. (2007). Functional properties and genomics of glucose transporters. *Curr. Genomics* 8, 113–128. doi: 10.2174/138920207780368187

Conflict of Interest Statement: The authors declare that the research was conducted in the absence of any commercial or financial relationships that could be construed as a potential conflict of interest.

frontiers in Genetics

ORIGINAL RESEARCH
published: 10 April 2017
doi: 10.3389/fgene.2017.00042

Characterization of X-Chromosome Gene Expression in Bovine Blastocysts Derived by *In vitro* Fertilization and Somatic Cell Nuclear Transfer

*Byungkuk Min, Jung Sun Park, Kyuheum Jeon and Yong-Kook Kang **

Development and Differentiation Research Center, Korea Research Institute of Bioscience Biotechnology, Daejeon, South Korea

To better understand X-chromosome reactivation (XCR) during early development, we analyzed transcriptomic data obtained from bovine male and female blastocysts derived by *in-vitro* fertilization (IVF) or somatic-cell nuclear transfer (SCNT). We found that X-linked genes were upregulated by almost two-fold in female compared with male IVF blastocysts. The upregulation of X-linked genes in female IVFs indicated a transcriptional dimorphism between the sexes, because the mean autosomal gene expression levels were relatively constant, regardless of sex. X-linked genes were expressed equivalently in the inner-cell mass and the trophectoderm parts of female blastocysts, indicating no imprinted inactivation of paternal X in the trophectoderm. All these features of X-linked gene expression observed in IVFs were also detected in SCNT blastocysts, although to a lesser extent. A heatmap of X-linked gene expression revealed that the initial resemblance of X-linked gene expression patterns between male and female donor cells turned sexually divergent in host SCNTs, ultimately resembling the patterns of male and female IVFs. Additionally, we found that sham SCNT blastocysts, which underwent the same nuclear-transfer procedures, but retained their embryonic genome, closely mimicked IVFs for X-linked gene expression, which indicated that the embryo manipulation procedure itself does not interfere with XCR in SCNT blastocysts. Our findings indicated that female SCNTs have less efficient XCR, suggesting that clonal reprogramming of X chromosomes is incomplete and occurs variably among blastocysts, and even among cells in a single blastocyst.

Keywords: X chromosome reactivation (XCR), X chromosome inactivation (XCI), SCNT, RNA-seq, bovine embryos

OPEN ACCESS

Edited by:
Rafael Franco, University of Barcelona, Spain

Reviewed by:
Montserrat Corominas, University of Barcelona, Spain
Andrea Cerase, European Molecular Biology Laboratory, Italy

****Correspondence:***
Yong-Kook Kang
ykkang@kribb.re.kr

Specialty section:
This article was submitted to Epigenomics and Epigenetics, a section of the journal Frontiers in Genetics

Received: *02 January 2017*
Accepted: *24 March 2017*
Published: *10 April 2017*

Citation:
Min B, Park JS, Jeon K and Kang Y-K (2017) Characterization of X-Chromosome Gene Expression in Bovine Blastocysts Derived by In vitro Fertilization and Somatic Cell Nuclear Transfer. Front. Genet. 8:42. doi: 10.3389/fgene.2017.00042

INTRODUCTION

X-chromosome inactivation (XCI) has evolved in female mammals to compensate for sex-chromosome dosage differences by suppressing gene expression from one X chromosome, and to render all cells as functionally monosomic for the X chromosome, a process considered to be important for normal embryonic development (Monk and Harper, 1979; Penny et al., 1996).

The current understanding of XCI during early embryogenesis largely originates from studies in mice, partially because XCI occurs during a very early developmental window when the embryo is accessible. In female mice, dosage compensation takes place within a continual cycle of XCI and reversal, also known as X-chromosome reactivation (XCR) (Lee and Bartolomei, 2013). Inactivation of the paternal X chromosome occurs progressively during the first days of post-fertilization cleavage until the morula stage (Okamoto and Heard, 2006; Kalantry et al., 2009; Namekawa et al., 2010). At the late blastocyst stage, XCR is observed within cells from the inner cell mass (ICM) that will form the embryo proper (i.e., two active X chromosomes are present in these cells), whereas cells of the trophectoderm (TE), which will form the placenta, maintain imprinted inactivation of the paternal X chromosome (Mak et al., 2004; Okamoto et al., 2004; Patrat et al., 2009). At the onset of gastrulation, embryonic lineage cells randomly undergo XCI again without a parent-of-origin bias, and once random X-inactivation is initiated, all the progeny cells maintain the same X-inactivation status (Lyon, 1961). In contrast to embryonic lineage cells, extra-embryonic cells (i.e., TE cells) maintain the silenced paternal X chromosome throughout embryogenesis. Meanwhile, XCR can be induced during reprogramming of differentiated cells toward pluripotency by nuclear transfer, cell fusion, or ectopic expression of reprogramming factors (for a review, see Pasque and Plath, 2015; Payer, 2016; Vallot et al., 2016). Recently, it was shown that during the early period of reprogramming in hybrid cells between human fibroblasts and mouse embryonic stem cells, human nuclei undergo a loss of *XIST* and XCI-associated histone marks from the inactive X chromosome to accomplish XCR, although some regions on the X chromosome are refractory to reprogramming (Cantone et al., 2016).

However, species-specific differences are found in the patterns of X-inactivation and reactivation in mammals. Early human and rabbit embryos have different XCI initiation strategies compared with mice (Okamoto et al., 2011; Deng et al., 2014). Furthermore, in these species, *XIST* was not imprinted, and both X chromosomes remained active in the ICM and TE of blastocysts. In addition, several studies found that the paternal X chromosome does not undergo imprinted X inactivation in human embryos and in extra-embryonic tissues (Skuse et al., 1997; Skuse, 2005; Moreira de Mello et al., 2010; Penaherrera et al., 2012; Tachibana et al., 2012). Similarly, XCI does not occur in bovine blastocysts. Early studies found upregulation of X-linked genes such as *XIAP, G6PD*, and *HPRT* in female bovine blastocysts, despite strong *XIST* expression (Gutierrez-Adan et al., 2000; Peippo et al., 2002; Wrenzycki et al., 2002; Morton et al., 2007). Allelic expression analysis of the X-linked polymorphic *MAOA* gene showed preferential inactivation of the paternal X chromosome in bovine fetal placentae at approximately 100 days of gestation (Xue et al., 2002); however, more definitive studies with earlier stage embryos have not been reported. A microarray study using pooled *in vitro*-produced bovine blastocysts of known sexes showed that X-linked transcripts were mostly upregulated (Bermejo-Alvarez et al., 2010), which indicated that XCI does not occur at the blastocyst stage. Studies on XCI in non-rodent mammalian species demonstrated that X inactivation in mice might not apply to other species; therefore, determining the similarities and differences in XCI among mammalian species is very important.

Global gene expression studies using bovine pre-implantation embryos are scarce, and investigations into X-inactivation/reactivation using transcriptomic data from early embryos are scarcer still. This is mostly because of the major technical barrier in dealing with a limited number of embryos in a minuscule volume. In this study, we generated RNA-seq data derived from *in vitro* bovine male and female blastocysts to identify and characterize gender-specific expression patterns of genes from the X chromosome and autosomes. To investigate differences between embryos of different origins, we included male and female somatic cell nuclear transfer (SCNT) embryos in the RNA-seq analysis. Furthermore, our RNA-seq data were obtained from single male and female blastocysts, which enabled analysis of individual blastocysts to investigate the variability in X chromosome gene expression profiles. Knowledge regarding XIC in non-rodent pre-implantation embryos is extremely limited; therefore, our study using bovine embryos will provide insights into the evolutionary and molecular aspects of X inactivation and reactivation that occurs in early mammalian embryos, including humans.

MATERIALS AND METHODS

Generation of Bovine Blastocyst Samples and Sexing

This study was carried out in strict accordance with the recommendations in the Guide for the Care and Use of Laboratory Animals of the National Livestock Research Institute of Korea. The protocol was approved by the Committee on the Ethics of Animal Experiments of the Korea Research Institute of Bioscience and Biotechnology.

The procedures for generation of bovine IVF and SCNT blastocysts were described in detail elsewhere (Kwon et al., 2015b). Briefly, single donor cell was injected into enucleated oocyte by a micromanipulator with an inverted microscope (Leitz), and each donor-oocyte complex was fused by an Electro Cell Manipulator 2001 (BTX). The fused eggs were activated 4 h after. Blastocysts were generated 6–8 days post-NT. The quality of each blastocyst was assessed by Hoechst staining, and only high quality embryos with 60–80 blastomeres were chosen for transcriptomic analysis. We used male and female bovine ear skin fibroblasts as donor cells which were passaged three times before SCNT.

For generation of sham SCNT blastocysts, 18–22 h post-IVF, the zygote with two parental pronuclei was chosen for manipulation (Park et al., 2007). To exactly mimic the physical damage of enucleation, zona pellucida was partially ripped and the polar body and a part of the underlying ooplasm were removed using a micropipette without touching either male or female pronucleus. After 2 h of incubation, the reconstructed oocytes were activated using 5 μM ionomycin (Sigma) for 5 min, followed by treatment with 2.5 mM 6-dimethyl-aminopurine

(DMAP, Sigma) in CR1aa culture media supplemented with 0.3% BSA for 3.5 h. The oocytes were then *in vitro* cultured to the blastocyst stage.

Sexes of IVF or sham-SCNT blastocysts were determined by PCR with Y-specific primers (BY; 5′-CTCAGCAAAGCA CACCAGAC-3′ and 5′-GAACTTTCAAGCAGCTGAGGC-3′) and bovine-specific primers (BSP; 5′-TTTACCTTAGAACAA ACCGAGGCAC-3′ and 5′-TACGGAAAGGAAAGATGACCT GACC-3′) as previously reported (Rattanasuk et al., 2011). One-tenth volume of genomic DNA extracted from single blastocysts was amplified by PCR using AccuPower PCR PreMix (Bioneer) and PCR product was resolved on 2% agarose gel.

Transcriptome Amplification of Single Blastocysts by Pico-Profiling

Transcriptomic materials were extracted from total 35 blastocysts (6 male IVF, 6 male SCNT, 6 male sham, 6 female IVF, 6 female SCNT, 5 sham) and male/female donor cells and amplified by the pico-profiling method. The pico-profiling procedure was described in detail elsewhere (Min et al., 2015, 2016). Briefly, from each bovine blastocyst, poly-A tailed RNAs were extracted using Dynabeads mRNA DIRECT kit (Invitrogen) and reverse transcribed using 200 units of SuperScript III (Invitrogen). Pico-profiling was done using random primer harboring MlyI restriction enzyme site. The pico-profiled cDNA fragments were amplified using 5′ anchor primer by PCR with 20 cycles of 94°C for 2 min, 70°C for 5 min. Adapters were removed from amplicons by overnight digestion with MlyI restriction enzyme to produce double strand cDNA fragments suitable for Illumina NGS library generation.

Preparation of NGS Libraries

Illumina NGS libraries were generated using TruSeq DNA Sample Preparation kit (Illumina) according to the supplier's guide with several minor modifications. End-repair was performed using the whole pico-profiling amplicons (20 μl) by incubating with 25 μl End Repair Mix (Illumina) and 5 μl DW at 30°C for 2 h. The reactions were purified with AMPure XP beads (Beckman) and DNA was eluted in 12.5 μl DW. Then, 12.5 μl A-Tailing Mix (Illumina) and 5 μl DW were added into each sample, and the mixtures were incubated at 37°C for 2 h. Next, 1 μl barcoded adapter was added into each 3' end adenylated DNA sample with 2.5 μl Ligation Mix (Illumina) and 6.5 μl DW, and the mixtures was overnight incubated at 16°C. Ligates were purified twice using AMPure XP bead (Bechman) and eluted into 30 μl DW. For size selection, adapter ligated DNA samples were mixed with 10 μl loading solution (Sage Science) and loaded onto Pippin Prep (Sage Science). DNA samples were enriched by 18 cycles of PCR reaction comprising 5 μl size selected DNA fragments, 25 μl PCR Master Mix(Illumina), 1 μl PCR Primer Cocktail (Illumina), and 19 ul DW. Finally, enriched DNA fragments were purified and sequenced using HiSeq2500. Male and female samples were separately pooled and sequenced using two flow cells of HiSeq2500 system.

Bioinformatic Analyses

Raw reads from HiSeq2500 (100 bp, PE) were preprocessed using "trim_galore" to remove Illumina adapter sequences and low quality bases, and the trimmed reads were aligned on *Bos taurus* UMD3.1 (NCBI) with TopHat2 (Trapnell et al., 2012; Kim et al., 2013). We followed the Tuxedo suit pipeline (TopHat, Cufflinks, and CummeRbund) with default parameters for mapping, expression estimation and differential expression (DE) analysis (Trapnell et al., 2012). For the estimation of gene expression levels, Cufflinks with -G option was used to calculate the abundance of only known transcripts due to the incomplete genomic annotation of the bovine genome.

For sliding window analyses, each chromosome was binned into 1 megabase windows. FPKM values of genes in each window were summed up, and relative expression levels against mean expression levels of male IVF blastocysts were calculated. In order to plot the calculated relative expression, FPKM values were smoothened by averaging 30 windows moving along each chromosome. All plots in this study were generated using in-house R scripts, Origin (OriginLab), or Excel (Microsoft).

RESULTS

Experimental Scheme and Validation of Pico-Profiling-Sequencing Method through a Pilot Experiment

We extracted mRNA and genomic DNA from single bovine IVF blastocysts (IVF-BLs) for pico-profiling of transcripts (Min et al., 2015, 2016) and gender identification, as illustrated in **Figure 1A**. Complementary DNA (cDNA) amplicons from six male and six female IVF-BLs were used for RNA-seq library construction. First, we evaluated the pico-profiling-sequencing (Pip-seq) method in a preliminary experiment, using total RNA from a pool of four IVF-BLs that was divided into four parts for Pip-seq library construction (**Figure 1B**). The sequencing results showed that the distributions of normalized counts in the four replicates were comparable (**Figure 1C**), and the correlation was higher among the replicates ($r = 0.98$) compared with those between other IVF-BLs ($r = 0.86$–0.90; **Figure 1D**). In addition, we found that the replicates had significantly less variable FPKM (fragments per kilobase of exon per million mapped fragments) values for housekeeping genes such as *GAPDH* and *ACTB* compared to those found in a separate RNA-seq dataset derived from single blastocysts (**Figure 1E**). These results demonstrated that Pip-seq is a reliable method of cDNA amplification for use with minute samples, such as individual preimplantation embryos. In addition to IVF-BLs, we included SCNT blastocysts (SCNT-BLs) in our analysis, which were generated from adult ear skin fibroblasts under standardized SCNT conditions (Kwon et al., 2015a). As a reference, we included sham nuclear transfer blastocysts (sham NT-BLs) that mimicked SCNT-BLs because they underwent the same nuclear transfer procedure except that they retained their intact genomic material (**Figure 1F**). From Pip-seq, we obtained 37 transcriptomes from 35 blastocysts and two donor cells (see **Supplementary Table S3** for the details of samples

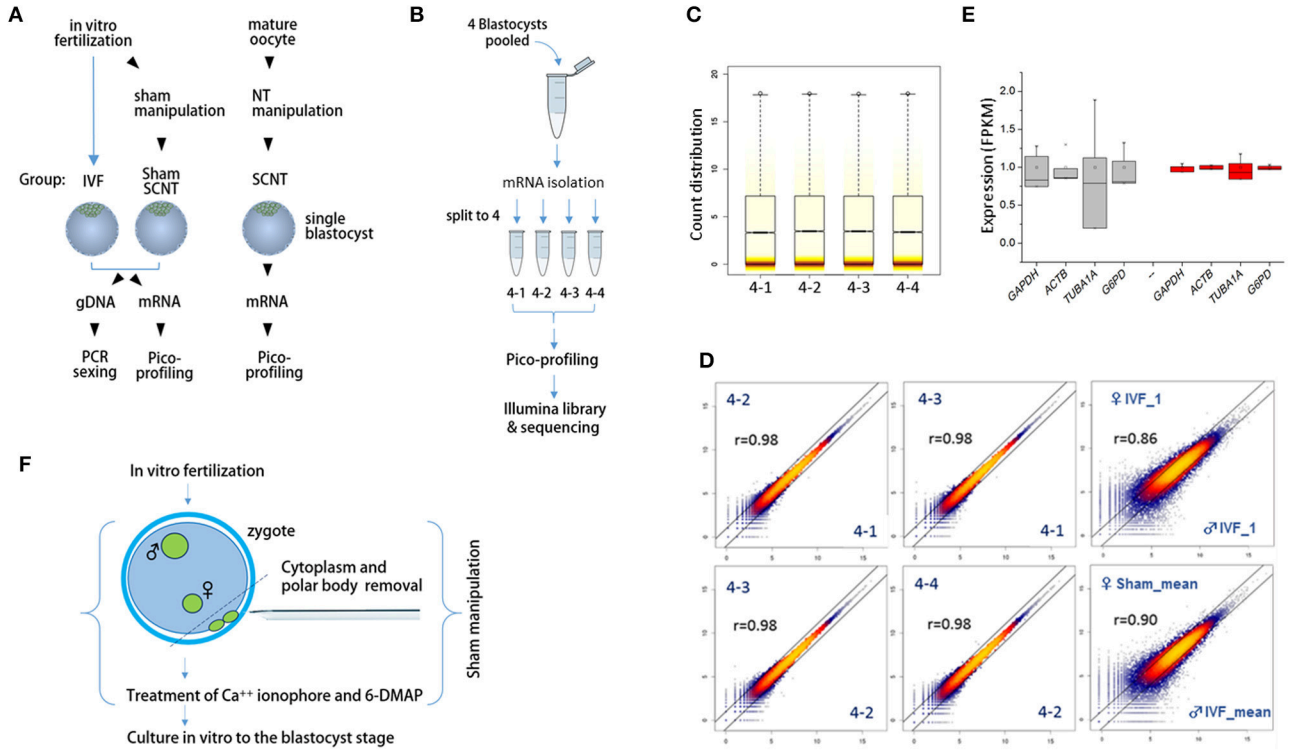

FIGURE 1 | Schematics of the sample preparation and pico-profiling processes for deep sequencing. (A) Preparation of bovine blastocyst samples for sexing and pico-profiling. Blastocysts were derived by *in vitro*-fertilization (IVF) or somatic cell nuclear transfer (SCNT). Adult ear skin fibroblasts were used as donor cells to obtain SCNT embryos. Genomic DNA and mRNA were extracted from single IVF and sham nuclear transfer (NT) blastocysts for sexing and pico-profiling. **(B–E)** Validation of the pico-profiling method. In **(B)**, there is an overview of the experimental strategy for validation using four identical replicates of pooled blastocyst samples. In **(C)** and **(D)**, sequencing results are presented. Box plot in **(C)** shows the distribution of total gene expression levels [$\log_2$(FPKM)] for each replicate. Colored stripes indicate gene density within a specific expression level. Scatter plots in **(D)** show the correlation between replicates. For comparison, other non-technical replicates (i.e., male IVF and female IVF blastocyst samples) are included. Pearson correlation coefficients (r) are denoted on each plot. In E, expression levels of housekeeping genes are compared between replicate groups (red) and other independent sample groups (gray). Note significantly less variability in the expression levels of the replicates compared to that found in other sample groups. **(F)**, Generation of sham NT embryos. Sixteen to 18 h after IVF, a zygote with maternal and paternal pronuclei was manipulated to remove the polar bodies plus a portion of cytoplasm underneath them, followed by a standard nuclear transfer protocol to develop to the blastocyst stage.

and sequencing results). We found that *XIST* was expressed abundantly in female blastocysts, and male-specific genes such as *UTY*, *DDX3Y*, and *EIF2S3Y* were expressed exclusively in male blastocysts (**Supplementary Figure S1**).

X-Linked Genes Were Upregulated in Bovine Female Blastocysts

We calculated the mean expression levels of individual genes in each group of blastocysts. Plotting the relative mean expression levels for each group to the mean expression levels for the male IVF group against chromosome, we found that X-linked genes were upregulated specifically in the female blastocyst groups (**Figure 2A**). In a comparison of the mean expression levels between male and female X-linked genes, we found a clear distinction between the sexes in each blastocyst group, in which female blastocysts had high and variable expression, whereas male blastocysts had relatively low and constant expression (**Figure 2B**). The mean female to male X-linked gene expression ratios were estimated as 1.8, 1.5, and 1.9 in the IVF, SCNT, and sham groups, respectively (**Figure 2C**). The almost two-fold higher abundance of X-linked gene transcripts indicated that both maternal and paternal X chromosomes are active in bovine female blastocysts, despite the presence of *XIST* transcripts, and suggested a late onset of XCI, similar to that observed in humans (Okamoto et al., 2004).

Plotting X-linked gene expression along the chromosome, we found that the expression patterns were very similar in all blastocyst groups (sham groups omitted), with an overall higher level of expression in the female groups, which indicated that upregulation of X-linked genes in female blastocysts does not occur locally, but is chromosome-wide (**Figure 2D**). Notably, female SCNT-BLs exhibited a lower profile compared to that found in female IVF-BLs, which is consistent with the lower FPKMs of X-linked genes found in female SCNT-BLs compared with that found in female IVF-BLs (**Figure 2C**). In addition, although the expression levels of X-linked genes differed between male and female SCNT-BLs, their expressions were very similar in male and female donor cells (**Supplementary Figure S2**), which

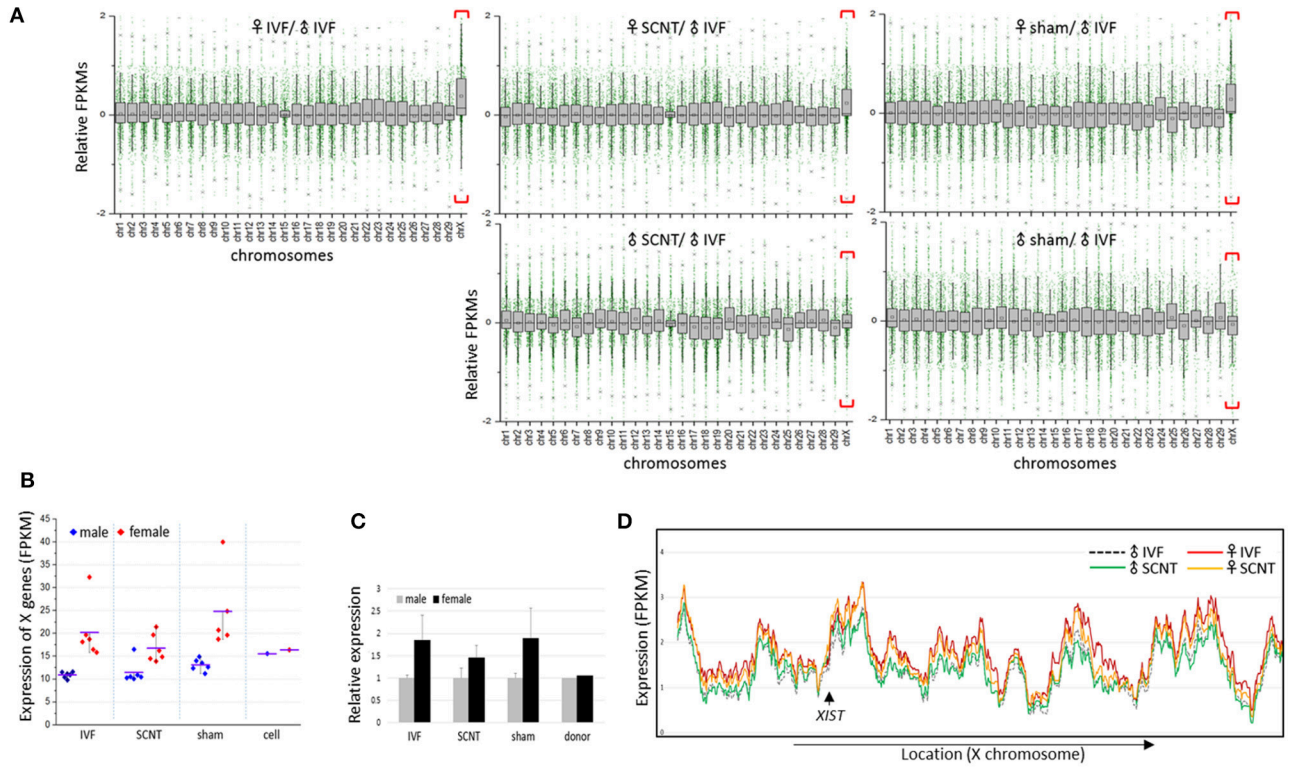

FIGURE 2 | Upregulation of X-chromosome genes in bovine female blastocysts. (A) Box plots showing relative gene expression levels in FPKMs (fragments per kilobase of exon per million mapped fragments) of IVF, SCNT, and sham NT blastocysts plotted from chromosome 1 to X (excluding the Y chromosome) against the mean FPKM of male IVF blastocysts. X chromosomes are distinguished by higher mean expression levels (red brackets). Upper panel, females; lower panel, males. **(B)** Mean FPKMs of X-chromosome genes (X-linked genes) in individual embryos (dots) from IVF, SCNT, and sham NT groups. Donor cells (cell) are included. Blue, male; red, female; black line, group mean FPKM. **(C)**, Relative expression of X-linked genes in female blastocysts (black) compared to that in male blastocysts (gray). Error bars, standard deviation. **(D)** Comparison of chromosome-scale X-linked gene expression patterns using sliding window analysis between male and female samples, and between IVF and SCNT groups. Mean expression of X-linked genes in IVF and SCNT groups are plotted in order of genomic location. The location of the *XIST* gene is indicated (arrow).

suggested sexual differentiation in transcriptomes during SCNT development.

The Distribution of Female-to-Male Ratios of X-Linked Genes Was Female-Biased in Both IVF-BLs and SCNT-BLs

Next, we examined the distribution of female-to-male (F:M) ratios of the expression levels of X-linked genes in IVF-BLs and SCNT-BLs (**Figure 3A**). Overall, we found that the distribution was female-biased in both groups. However, in contrast to the SCNT group, donor cell populations had a relatively balanced distribution, which suggested that the symmetric F:M distribution pattern of donor cells drifted to an asymmetric, female-biased pattern in SCNT-BLs, as in IVF-BLs. Non-parametric analysis using the Mann-Whitney (MW) test and the two-sample Kolmogov-Smirnov (KS) test showed that distributions of the F:M ratios of X-linked genes with FPKMs > 1 were significantly different in SCNT vs. donor cells, and in IVF vs. donor cells (both $p < 0.05$), but not between IVF vs. SCNT groups (MW test: $p = 0.860$).

The numbers of X-linked genes expressed in IVF-BLs, SCNT-BLs, sham NT-BLs, and donor cells were 668, 666, 628, and 479, respectively. We used volcano plots to display the mean F:M levels of individual X-linked genes in each blastocyst group (**Figure 3B**), which showed that the majority of X-linked genes were upregulated in female blastocysts. Notably, however, the SCNT group still had a considerable number of X-linked genes that were expressed at higher levels in males. Proportions of X-linked genes that were highly expressed (F:M > 1) in female blastocysts were 78.7, 66.7, 78.1, and 51.2%, and those with an F:M ratio > 2 were 46.7, 36.2, 33.1, and 24.2% in IVF-BLs, SCNT-BLs, sham NT-BLs, and donor cells, respectively.

Expressions Levels of Autosomal Genes Are Balanced between Bovine Female and Male Blastocysts

We compared the mean expression levels of X-linked genes and autosomal genes (A-genes) in individual blastocysts, and found that the expressions of A-genes were relatively constant in all blastocysts, irrespective of the different X-linked gene expressions observed between the sexes (**Figure 3C**). Furthermore, we found

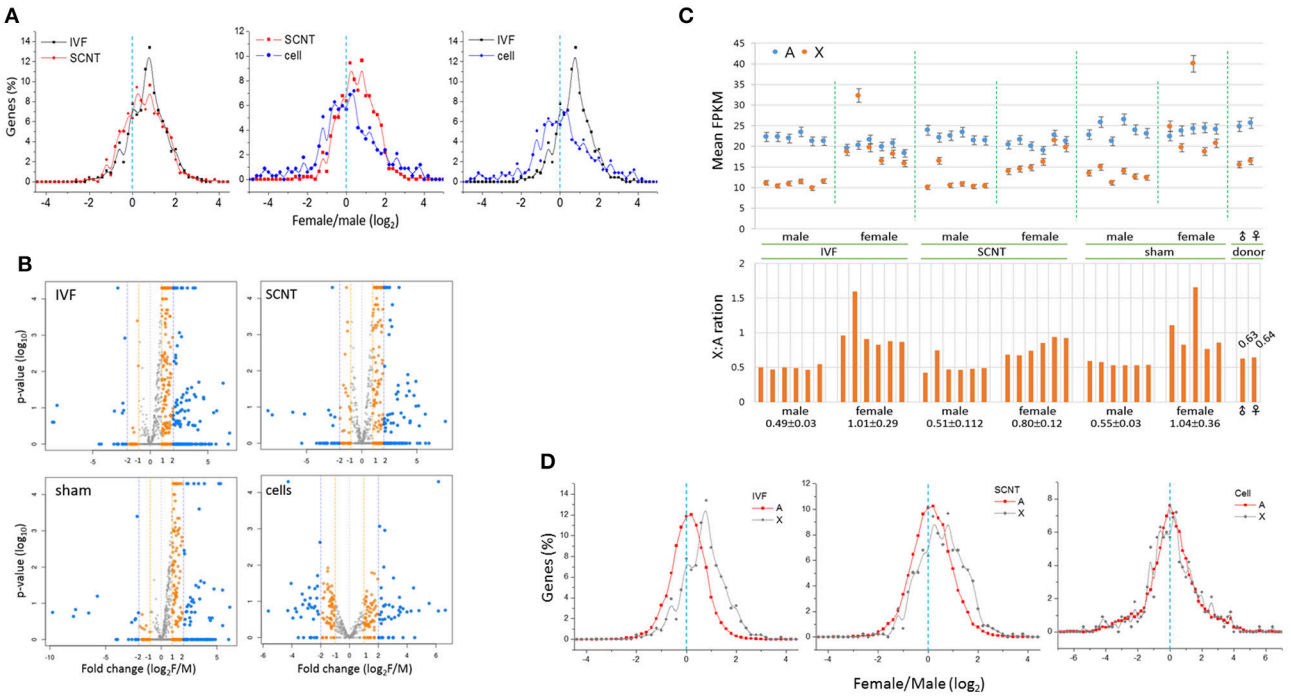

FIGURE 3 | Distribution of female-to-male ratios of X-chromosome gene expression levels in bovine blastocysts. (A) Distribution of female-to-male (F:M) ratios of expression levels of X-chromosome genes (X-linked genes) in bovine IVF (black) and SCNT (red) blastocysts, and donor cells (blue). The dotted line (cyan) denotes an F:M ratio of 1 [$\log_2$(F:M) ratio = 0]. Bin size, 0.2 in $\log_2$(FPKM). **(B)** Volcano plots showing mean F:M levels of individual X-linked genes against *p*-values and fold changes in each blastocyst group. Genes with different F:M fold changes are denoted in different colors. **(C)** Comparison of expression (mean FPKM ± STD) in autosomal (A, blue) and X-chromosome genes (X, orange) between males and females in IVF, SCNT, and sham-NT blastocysts. The X:A ratio that denotes the FPKM level in each blastocyst is provided in the lower panel; the mean X:A ratios (± STD) of individual groups are denoted below. Donor cells are included for reference. **(D)** Distribution of female-to-male ratios in autosomal (A, black) and X-chromosome genes (X, red) in IVF and SCNT blastocysts. A dotted line (cyan) denotes an F:M ratio of 1 [$\log_2$(F:M) ratio = 0]. Bin size, 0.2 in $\log_2$(FPKM). Donor cell samples are included for reference.

that the male IVF group had a mean X:A ratio of 0.49 compared with a mean of 1.01 found in the female IVF group, revealing a significant difference between the sexes (Wilcoxon signed rank test; $p = 6.0e\text{-}09$). We found X:A ratios of 0.51 and 0.80 in male and female SCNT-BLs, respectively, which were similar to those found in IVF-BLs, although slightly lower in female SCNT-BLs compared with those in female IVF-BLs.

We compared the distributions of F:M ratios of A-gene expression levels in IVF and SCNT blastocysts, and donor cell groups (**Figure 3D**). The F:M distribution was not skewed for A-genes in these groups, centering on an F:M ratio of 1 ($\log_2$ ratio = 0). Using an MW test, we found that the F:M distributions between X- and A-genes were significantly different between the IVF and SCNT groups ($p < 0.002$), but not in the donor cells ($p > 0.05$). In addition, examining autosomal differentially expressed genes (aDEGs; $p < 0.05$) between the sexes, we found that the number of male-high or female-high aDEGs was similar in both IVF (51.0 vs. 49.0%, respectively; $n = 2{,}020$) and SCNT (48.8 vs. 51.2%; $n = 3{,}051$) groups. This probably indicated that X chromosomes impose an extensive transcriptional regulation on A-genes in both IVF and SCNT blastocysts, as previously suggested (Bermejo-Alvarez et al., 2010).

Features of X-Linked Differentially Expressed Genes and in the De-Repression of X-Linked Genes

A heatmap of X-linked gene expression revealed a gender-specific pattern in blastocysts, with higher levels found in female blastocysts (**Figure 4A**). The heatmap pattern of female SCNT-BLs differed from that of male SCNT-BLs, and resembled that observed in female IVF-BLs. In addition, we found that male and female donor cells had similar X-linked gene expression patterns, but neither the pattern observed in female SCNT-BLs nor that found in male SCNT-BLs was similar to the pattern found in donor cells. **Figure 4B** shows a cluster analysis of X-linked gene expression, in which each cluster presents the pattern of change in gene expression between donor cells and SCNT-BLs, using the pattern seen in IVF-BLs as a reference. The genes that belong to each category are listed in the **Supplementary Table S1**.

Next, we detected and evaluated differentially expressed X-linked genes (xDEGs; $p < 0.05$) between the sexes (**Figure 4C**). In the IVF group, we found 182 xDEGs, of which 94% (171/182) were highly expressed in female blastocysts (**Supplementary Table S2**). We found that only a small proportion (6%) of xDEGs, including *GYG2*, *CD99*, *GDPD2*, *ZBED1*, *XIAP*, *TM9SF2*, and LOC100848605 were highly

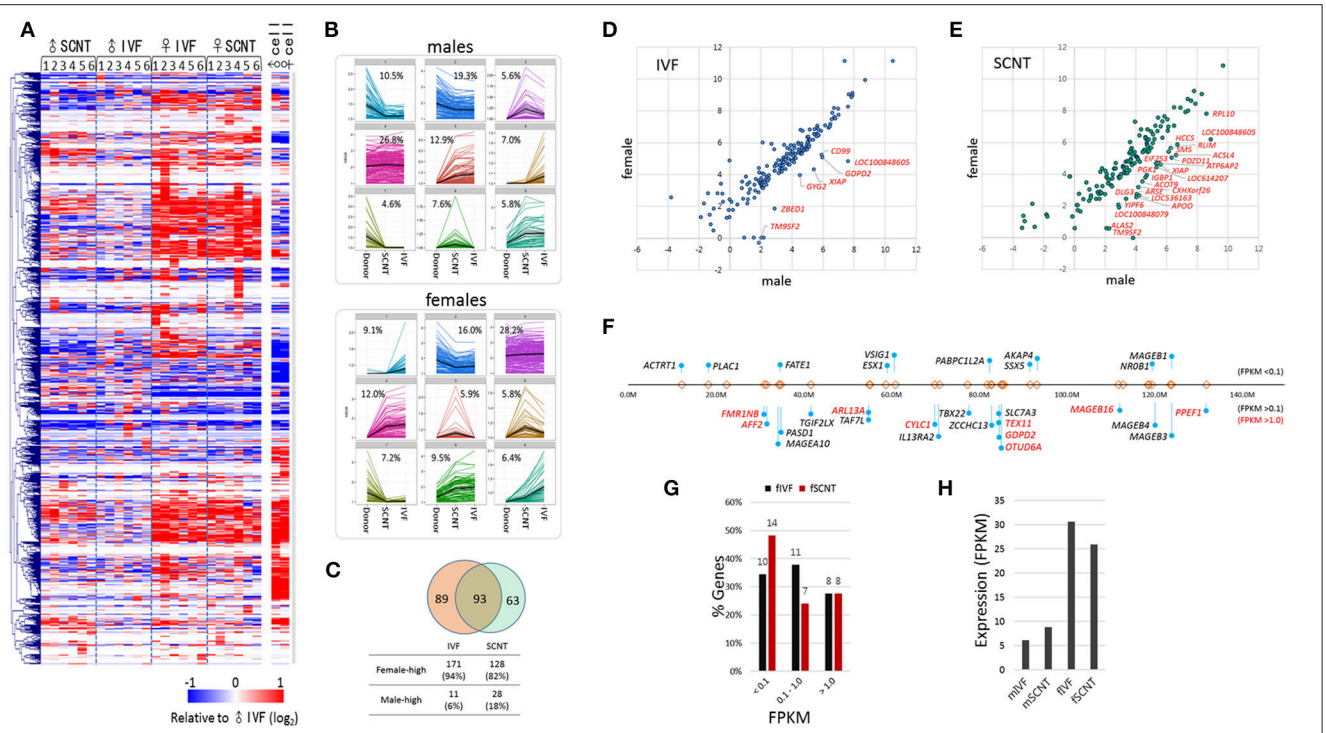

FIGURE 4 | Features of X-chromosome gene expression in IVF and SCNT blastocysts. (A) Heatmap of relative X-chromosome gene (X-linked gene) expression in individual IVF and SCNT blastocysts vs. the mean expression level of the male IVF blastocyst group. Donor cells are included for reference. Genes are hierarchically clustered. **(B)** *k*-mean clustering ($k = 9$) of X-chromosome genes among donor cell, SCNT, and IVF blastocyst groups. The frequency of each cluster is denoted in the panel. Upper panel, males; lower panel, females. **(C)** Venn diagram showing the overlap between 182 IVF X-linked differentially expressed genes (xDEGs, $p < 0.05$; orange) and 156 SCNT xDEGs (green). **(D–E)** Scatter plots of xDEGs in IVF **(D)** and SCNT **(E)** blastocyst groups. Most xDEGs are highly expressed in females, and high-expressing xDEGs in males (male-high) are partly denoted with gene symbols. **(F–H)** Respective location **(F)** and expression **(G–H)** of 29 X-linked genes in bovine IVF and SCNT blastocysts specifically expressed in human and mouse testes. In **(F)** the relative positions and distances of genes on the X chromosome are indicated by "lollipops." Genes are categorized by expression level where a FPKM < 0.1 indicates a none-to-weak level of expression, a FPKM > 0.1 indicates weak-to-moderate expression, and a FPKM > 0.5 (red) indicates moderate-to-high expression. Comparison of the expression of 29 testes-specific genes between female IVF and SCNT groups **(G)**, and between males and females **(H)**.

expressed in male IVFs (**Figure 4D**). Of these genes, *ZBED1* and *CD99* are located in the pseudoautosomal region 1 (PAR1) and therefore, are present on both the X and Y chromosomes. We propose that this male-biased expression resulted from partial spreading of XCI in females (Johnston et al., 2008). Furthermore, *GYG2* is known to have a short truncated version on the Y chromosome in humans (Zhai et al., 2000).

By contrast, in the SCNT group, we found 156 xDEGs (**Supplementary Table S2**), of which 18% (28/156) were highly expressed in males (**Figure 4E**). This proportion was larger than that observed in the IVF group, and it would interesting to determine whether these genes reside at loci that are refractory to X-chromosome reprogramming. We found that 93 xDEGs were common to IVF-BLs and SCNT-BLs (**Figure 4C**), and among them, *XIAP*, *TM9SF2*, and LOC100848605 were identified to be male-high. The regulatory mechanism involved in the expression of these male-high X-linked genes is currently unknown.

Certain male-specific X-linked genes are expressed specifically in the testes, the majority of which are expressed predominantly or exclusively at both pre- and post-meiotic stages (Wang et al., 2001; Mueller et al., 2008). Using previously reported data (Wang et al., 2008) as a reference, we selected 68 X-linked genes that have testes-specific expression in humans and mice, and identified annotations for 29 of these genes in the bovine genome browser (**Figure 4F**). We found that these genes are not localized at specific loci or regions, but are distributed over the entire X chromosome. In our blastocyst samples, we found that more than half of these 29 genes were expressed at an FPKM > 0.1 (**Figure 4G**), and that their expression levels were 3–5 times higher than that found in female blastocysts (**Figure 4H**). Therefore, our findings indicated that upregulation of the X chromosome or XCR leads to a de-repression of a large number of X-linked genes, including testes-specific genes, which are not necessary at the blastocyst stage. Furthermore, the data suggest a randomness and non-selectiveness in the de-repression of X-linked genes during XCR.

X Chromosome Genes Were Similarly Expressed in Inner Cell Mass Cells and Trophectoderm Cells

Blastocysts contain cells of two different lineages, the ICM cells and trophectoderm (TE) cells. These two groups of cells might, as in mouse blastocyst (Mak et al., 2004; Okamoto et al., 2004; Patrat et al., 2009), have different strategies to express

X-linked genes: ICM cells having both maternal and paternal active X chromosomes, and TE cells having active maternal and inactive paternal X chromosomes. To test whether this was the case for bovine blastocysts, female IVF blastocysts ($n = 19$) were dissected physically into two parts, the 'IT', containing both ICM and TE cells (almost 1:1 ratio in cell number), and the TE-only part, and subjected to RNA-seq separately. We found that the mean expression levels of X-linked genes were similar in the IT and TE cells (1.000 ± 0.098 and 1.074 ± 0.137, respectively; **Figure 5A**). If the paternal X had been imprinted in the TE part, the expression level of X-linked genes would have been higher in the IT part than in the TE part. The similarity in X-linked gene expressions between the IT and TE cells argued against the imprinted inactivation of paternal X. The relative expressions of X-linked genes in the IT to those in the TE in respective blastocysts were 0.945 on average, ranging from 0.80 to 1.18 (**Figure 5B**). There was no difference in the expression level of *XIST* at $p < 0.01$ level between the IT and TE parts (**Figure 5C**), which represented further evidence against the imprinted X inactivation in TE cells. We compared the mean expression level of X-linked genes and A-genes in each part, and found that the mean X:A ratios were not different between IT and TE samples (0.967 ± 0.102 and 1.008 ± 0.089, respectively; $p = 0.227$; **Figure 5D**), and similar to the mean X:A ratio of whole female IVF blastocysts (1.01 ± 0.29) (**Figure 3C**). Thus, we failed to find evidence for imprinted inactivation of paternal X chromosome or a preferential inactivation of either of the parental X chromosomes in TE lineage cells; therefore, we interpreted the result as indicating that both maternal and parental X chromosomes are regulated similarly in ICM and TE lineage cells in bovine blastocysts.

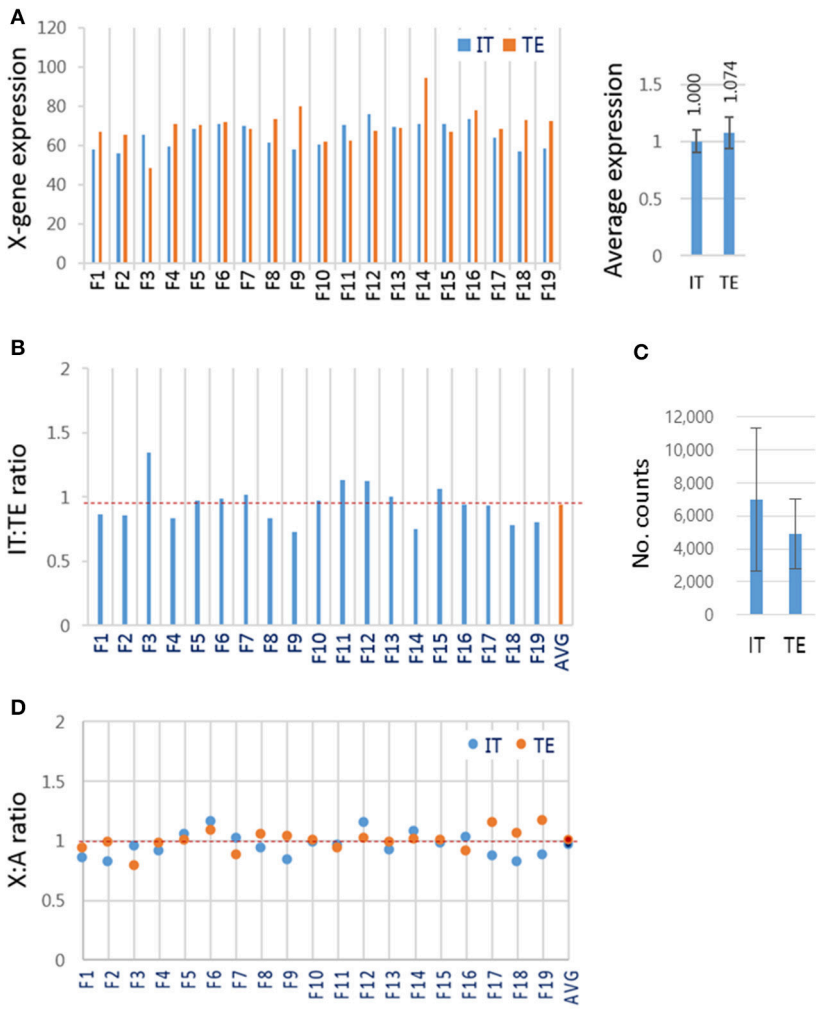

FIGURE 5 | X-chromosome gene expression in inner cell mass and trophectoderm lineage cells of female IVF blastocysts. (A) The mean expression levels of X-linked genes in different lineage cells of the blastocyst. Female IVF blastocyst was physically split using a syringe needle into the "IT" part containing both ICM and TE cells and the TE-only part and separately subjected to RNA-seq. Right panel, the mean expression levels of X-linked genes in the IT and TE cells. **(B)** The relative expression of X-linked genes in IT to that in TE part in each blastocyst. **(C)** The mean *XIST* expression levels in read counts. Error bars, standard deviations. **(D)** The mean X:A ratios in IT (blue) and TE (red) cells. AVG, average IT/TE ratio (see also dotted red line).

DISCUSSION

We found that the expression of X-linked genes in female IVF-BLs were almost twice that found in male IVF-BLs (**Figure 2C**). In addition to differences in the global expression levels of X-linked genes, the respective expression patterns were different in some clusters between female and male IVF-BLs, as evident from the heatmap (**Figure 4A**). We interpreted these findings as being caused by differences in X-chromosome dosage between male and female blastocysts, which implied that there is no mechanism for dosage compensation in bovine blastocysts. Our interpretation is in agreement with the observation that the lack of dosage compensation for the most highly expressed X-linked genes is tolerated not only in early mouse embryos (Namekawa et al., 2010), but also in embryonic stem cells (Elling et al., 2011; Leeb and Wutz, 2011). The resulting chromosome copy-number difference results in proteomic and metabolomic differences between the sexes (Gardner et al., 2010), which renders pre-implantation embryos of either sex more sensitive (or conversely, resistant) to essential signals for survival from the reproductive tract and also to numerous environmental factors, such as population density, famine, season, and stress, which are known to influence the sex ratio in mammals (Kruuk et al., 1999; Zorn et al., 2002; James, 2009). As shown in the heatmap of X-linked gene expression, SCNT-BLs displayed a contrasting sexual dimorphism, as did IVF-BLs, which demonstrated that the transcriptomic differences among X-linked genes is significantly more prominent between the sexes than between blastocyst groups of different origins (e.g., IVF vs. SCNT). Therefore, if the bovine blastocyst has an innate gender-specific response or behavior in the reproductive tract during the peri-implantation period, the response of SCNT-BLs may not differ from that found in gender-matched IVF-BLs.

In addition, we found that the imprinted X chromosome derived from donor cells was reactivated in female SCNT-BLs. An important observation was that, possibly due to insufficient XCR, the measured values of X-linked gene expression in SCNT-BLs consistently sat between the respective measures of donor cells and IVF-BLs: (1) the mean FPKMs of X-linked genes (1.0, 1.5, and 1.8 in female donor cells, female SCNT-BLs, and female IVF-BLs, respectively; **Figure 2C**); (2) the proportion of X-linked genes having an F:M ratio > 1 (51.2, 66.7, and 78.7%, respectively; **Figure 3B**); (3) the intermediate profile for X-linked gene expression levels across the chromosome observed using a sliding window analysis (**Figure 2D**); and (4) the mean FPKMs of X-linked genes relative to A-genes (0.64, 0.80, and 1.01, respectively; **Figure 3C**). We propose that this "in-between" ranking reflects the existence of chromosomal domains, or certain cell lineages, which are resistant to XCR in female SCNT-BLs. An alternative explanation, which is mutually non-exclusive to the theory of XCR-resistant domains, is that female SCNT-BLs might comprise a mosaic of cells that have different X-chromosome states; for example, one active and one inactive X chromosome (XaXi), such as that found in human pluripotent stem cell populations (Silva et al., 2008; Dvash et al., 2010; Anguera et al., 2012). Whatever the reason for the observed intermediate expression of X-linked genes in female SCNT-BLs, our findings indicated that reprogramming is incomplete at the mid-blastocyst stage, and might occur variably among blastocysts and even among cells in a blastocyst.

Owing to XCR in SCNT embryos, the imprinted X chromosome that is inherited from the female donor cell becomes the active X chromosome. This occurs in female SCNT-BLs, but not in male SCNT-BLs. XCR may be another process that facilitates reprogramming of the X chromosome, which might be used by female SCNT embryos because of the exceptional reconfiguration of the imprinted X chromosome. Conversely, XCR might be a burden to female SCNT embryos, which causes a serious delay in other concurrent and linked events of reprogramming. As shown by the X-linked gene expression profiles (**Figure 4A**), XCR might differentiate female SCNT-BLs from male SCNT-BLs, which would inevitably establish a sexual dimorphism in male and female SCNT-BLs, and may affect their cloning efficiency. However, because sham NT-BLs were comparable to their IVF counterparts, we concluded that manipulation and other nuclear transfer procedures do not interfere with the XCR process in female SCNT-BLs.

We found that upregulation of X-linked genes does not entail upregulation of A-genes in female blastocysts. If it had been true, the distribution of the F:M ratios of A-genes would have been skewed toward females, similar to that found for X-linked genes. However, we found that all three blastocyst groups, which derived differently, exhibited a well-balanced F:M ratio for A-gene expression (**Figure 3D**). We detected 2,020 aDEGs from the comparison of male and female IVF blastocysts. These aDEGs were well-balanced in number between the sexes, forming 7% (1030 male-high and 990 male-high aDEGs) of ∼14,300 transcripts expressed (FPKM > 0.1) in IVF blastocysts. This result differs from a previous result reporting an array-based analysis of global gene expression in bovine IVF blastocysts (Bermejo-Alvarez et al., 2010). In that study, out of ∼9300 transcripts expressed in bovine blastocysts, 12% (∼1100) were detected as female-high aDEGs and 17% (∼1600) as male-high aDEGs; this difference appeared large enough to shift the A-gene F:M ratio off-center. Moreover, when the lists of DEGs was compared with our DEGs, only 42 out of 99 annotated DEGs (∼42%) overlapped. The discrepancy could be explained by a report that the RNA-seq and microarray platforms can yield different DEG results (Zhang et al., 2015). In addition, there may be other explanations for the discrepancy; for example, different sample sizes, the need for cDNA amplification, sperm-sorting-based embryo sexing, and advanced data analytical tools. The limited availability of genomic materials for deep sequencing means that the study of the transcriptome of mammalian preimplantation-stage embryos remains under-investigated. Continued research effort will provide sufficient embryo transcriptome data for verification. In addition, the early embryo-specific Pip-seq method, by lowering significantly the current technical constraints that hamper transcriptomic analysis of early mammalian embryos, will likely have a role in these future studies.

AUTHOR CONTRIBUTIONS

YK led the project and supervised the study. BM and YK designed the experiments and interpreted the results. JP provided IVF and SCNT embryos. KJ pico-profiled blastocyst samples. BM and YK jointly performed bioinformatic analyses. BM and YK wrote the paper. All authors read and approved the final manuscript.

ACKNOWLEDGMENTS

This work was supported by grants from the National Research Foundation of Korea (015R1A2A2A01003117), the National Research Foundation-Science Research Center program (2011-0030049), the KIOM program (K16130), and the KRIBB program.

SUPPLEMENTARY MATERIAL

The Supplementary Material for this article can be found online at: http://journal.frontiersin.org/article/10.3389/fgene.2017.00042/full#supplementary-material

Supplementary Figure S1 | X- or Y-linked gene expression patterns.

Supplementary Figure S2 | X-chromosome wide gene expression pattern in donor cells.

Supplementary Table S1 | k-mean clustering of X-genes.

Supplementary Table S2 | xDEGs between male vs. female blastocysts.

Supplementary Table S3 | Sequencing depth and mapping rates.

REFERENCES

Anguera, M. C., Sadreyev, R., Zhang, Z., Szanto, A., Payer, B., Sheridan, S. D., et al. (2012). Molecular signatures of human induced pluripotent stem cells highlight sex differences and cancer genes. *Cell Stem Cell* 11, 75–90. doi: 10.1016/j.stem.2012.03.008

Bermejo-Alvarez, P., Rizos, D., Rath, D., Lonergan, P., and Gutierrez-Adan, A. (2010). Sex determines the expression level of one third of the actively expressed genes in bovine blastocysts. *Proc. Natl. Acad. Sci. U.S.A.* 107, 3394–3399. doi: 10.1073/pnas.0913843107

Cantone, I., Bagci, H., Dormann, D., Dharmalingam, G., Nesterova, T., Brockdorff, N., et al. (2016). Ordered chromatin changes and human X chromosome reactivation by cell fusion-mediated pluripotent reprogramming. *Nat. Commun.* 7:12354. doi: 10.1038/ncomms12354

Deng, X., Berletch, J. B., Nguyen, D. K., and Disteche, C. M. (2014). X chromosome regulation: diverse patterns in development, tissues and disease. *Nat. Rev. Genet.* 15, 367–378. doi: 10.1038/nrg3687

Dvash, T., Lavon, N., and Fan, G. (2010). Variations of X chromosome inactivation occur in early passages of female human embryonic stem cells. *PLoS ONE* 5:e11330. doi: 10.1371/journal.pone.0011330

Elling, U., Taubenschmid, J., Wirnsberger, G., O'malley, R., Demers, S. P., Vanhaelen, Q., et al. (2011). Forward and reverse genetics through derivation of haploid mouse embryonic stem cells. *Cell Stem Cell* 9, 563–574. doi: 10.1016/j.stem.2011.10.012

Gardner, D. K., Larman, M. G., and Thouas, G. A. (2010). Sex-related physiology of the preimplantation embryo. *Mol. Hum. Reprod.* 16, 539–547. doi: 10.1093/molehr/gaq042

Gutierrez-Adan, A., Oter, M., Martinez-Madrid, B., Pintado, B., and De La Fuente, J. (2000). Differential expression of two genes located on the X chromosome between male and female *in vitro*-produced bovine embryos at the blastocyst stage. *Mol. Reprod. Dev.* 55, 146–151. doi: 10.1002/(SICI)1098-2795(200002)55:2<146::AID-MRD3>3.0.CO;2-F

James, W. H. (2009). The variations of human sex ratio at birth during and after wars, and their potential explanations. *J. Theor. Biol.* 257, 116–123. doi: 10.1016/j.jtbi.2008.09.028

Johnston, C. M., Lovell, F. L., Leongamornlert, D. A., Stranger, B. E., Dermitzakis, E. T., and Ross, M. T. (2008). Large-scale population study of human cell lines indicates that dosage compensation is virtually complete. *PLoS Genet.* 4:e9. doi: 10.1371/journal.pgen.0040009

Kalantry, S., Purushothaman, S., Bowen, R. B., Starmer, J., and Magnuson, T. (2009). Evidence of Xist RNA-independent initiation of mouse imprinted X-chromosome inactivation. *Nature* 460, 647–651. doi: 10.1038/nature08161

Kim, D., Pertea, G., Trapnell, C., Pimentel, H., Kelley, R., and Salzberg, S. L. (2013). TopHat2: accurate alignment of transcriptomes in the presence of insertions, deletions and gene fusions. *Genome Biol.* 14:R36. doi: 10.1186/gb-2013-14-4-r36

Kruuk, L. E., Clutton-Brock, T. H., Albon, S. D., Pemberton, J. M., and Guinness, F. E. (1999). Population density affects sex ratio variation in red deer. *Nature* 399, 459–461. doi: 10.1038/20917

Kwon, S., Jeong, S., Jeong, Y. S., Park, J. S., Cui, X. S., Kim, N. H., et al. (2015a). Assessment of difference in gene expression profile between embryos of different derivations. *Cell. Reprogram.* 17, 49–58. doi: 10.1089/cell.2014.0057

Kwon, S., Jeong, S., Park, J. S., and Kang, Y. K. (2015b). Quantifying difference in gene expression profile between bovine blastocysts derived by *in vitro* fertilization and somatic cell nuclear transfer. *Gene Exp. Patterns* 19, 14–20. doi: 10.1016/j.gep.2015.05.005

Lee, J. T., and Bartolomei, M. S. (2013). X-inactivation, imprinting, and long noncoding RNAs in health and disease. *Cell* 152, 1308–1323. doi: 10.1016/j.cell.2013.02.016

Leeb, M., and Wutz, A. (2011). Derivation of haploid embryonic stem cells from mouse embryos. *Nature* 479, 131–134. doi: 10.1038/nature10448

Lyon, M. F. (1961). Gene action in the X-chromosome of the mouse (*Mus musculus* L.). *Nature* 190, 372–373. doi: 10.1038/190372a0

Mak, W., Nesterova, T. B., de Napoles, M., Appanah, R., Yamanaka, S., Otte, A. P., et al. (2004). Reactivation of the paternal X chromosome in early mouse embryos. *Science* 303, 666–669. doi: 10.1126/science.1092674

Min, B., Cho, S., Park, J. S., Jeon, K., and Kang, Y. K. (2016). The HIST1 locus escapes reprogramming in cloned bovine embryos. *G3 (Bethesda)* 6, 1365–1371. doi: 10.1534/g3.115.026666

Min, B., Cho, S., Park, J. S., Lee, Y. G., Kim, N., and Kang, Y. K. (2015). Transcriptomic features of bovine blastocysts derived by somatic cell nuclear transfer. *G3 (Bethesda).* 5, 2527–2538. doi: 10.1534/g3.115.020016

Monk, M., and Harper, M. I. (1979). Sequential X chromosome inactivation coupled with cellular differentiation in early mouse embryos. *Nature* 281, 311–313. doi: 10.1038/281311a0

Moreira de Mello, J. C., De Araujo, E. S., Stabellini, R., Fraga, A. M., De Souza, J. E., Sumita, D. R., et al. (2010). Random X inactivation and extensive mosaicism in human placenta revealed by analysis of allele-specific gene expression along the X chromosome. *PLoS ONE* 5:10947. doi: 10.1371/journal.pone.0010947

Morton, K. M., Herrmann, D., Sieg, B., Struckmann, C., Maxwell, W. M., Rath, D., et al. (2007). Altered mRNA expression patterns in bovine blastocysts after fertilisation *in vitro* using flow-cytometrically sex-sorted sperm. *Mol. Reprod. Dev.* 74, 931–940. doi: 10.1002/mrd.20573

Mueller, J. L., Mahadevaiah, S. K., Park, P. J., Warburton, P. E., Page, D. C., and Turner, J. M. (2008). The mouse X chromosome is enriched for multicopy testis genes showing postmeiotic expression. *Nat. Genet.* 40, 794–799. doi: 10.1038/ng.126

Namekawa, S. H., Payer, B., Huynh, K. D., Jaenisch, R., and Lee, J. T. (2010). Two-step imprinted X inactivation: repeat versus genic silencing in the mouse. *Mol. Cell. Biol.* 30, 3187–3205. doi: 10.1128/MCB.00227-10

Okamoto, I., and Heard, E. (2006). The dynamics of imprinted X inactivation during preimplantation development in mice. *Cytogenet. Genome Res.* 113, 318–324. doi: 10.1159/000090848

Okamoto, I., Otte, A. P., Allis, C. D., Reinberg, D., and Heard, E. (2004). Epigenetic dynamics of imprinted X inactivation during early mouse development. *Science* 303, 644–649. doi: 10.1126/science.1092727

Okamoto, I., Patrat, C., Thepot, D., Peynot, N., Fauque, P., Daniel, N., et al. (2011). Eutherian mammals use diverse strategies to initiate X-chromosome inactivation during development. *Nature* 472, 370–374. doi: 10.1038/nature09872

Park, J. S., Jeong, Y. S., Shin, S. T., Lee, K. K., and Kang, Y. K. (2007). Dynamic DNA methylation reprogramming: active demethylation and immediate remethylation in the male pronucleus of bovine zygotes. *Dev. Dyn* 236, 2523–2533. doi: 10.1002/dvdy.21278

Pasque, V., and Plath, K. (2015). X chromosome reactivation in reprogramming and in development. *Curr. Opin. Cell Biol.* 37, 75–83. doi: 10.1016/j.ceb.2015.10.006

Patrat, C., Okamoto, I., Diabangouaya, P., Vialon, V., Le Baccon, P., Chow, J., et al. (2009). Dynamic changes in paternal X-chromosome activity during imprinted X-chromosome inactivation in mice. *Proc. Natl. Acad. Sci. U.S.A.* 106, 5198–5203. doi: 10.1073/pnas.0810683106

Payer, B. (2016). Developmental regulation of X-chromosome inactivation. *Semin. Cell Dev. Biol.* 56, 88–99. doi: 10.1016/j.semcdb.2016.04.014

Peippo, J., Farazmand, A., Kurkilahti, M., Markkula, M., Basrur, P. K., and King, W. A. (2002). Sex-chromosome linked gene expression in *in-vitro* produced bovine embryos. *Mol. Hum. Reprod.* 8, 923–929. doi: 10.1093/molehr/8.10.923

Penaherrera, M. S., Jiang, R., Avila, L., Yuen, R. K., Brown, C. J., and Robinson, W. P. (2012). Patterns of placental development evaluated by X chromosome inactivation profiling provide a basis to evaluate the origin of epigenetic variation. *Hum. Reprod.* 27, 1745–1753. doi: 10.1093/humrep/des072

Penny, G. D., Kay, G. F., Sheardown, S. A., Rastan, S., and Brockdorff, N. (1996). Requirement for Xist in X chromosome inactivation. *Nature* 379, 131–137. doi: 10.1038/379131a0

Rattanasuk, S., Parnpai, R., and Ketudat-Cairns, M. (2011). Multiplex polymerase chain reaction used for bovine embryo sex determination. *J. Reprod. Dev.* 57, 539–542. doi: 10.1262/jrd.10-126M

Silva, S. S., Rowntree, R. K., Mekhoubad, S., and Lee, J. T. (2008). X-chromosome inactivation and epigenetic fluidity in human embryonic stem cells. *Proc. Natl. Acad. Sci. U.S.A.* 105, 4820–4825. doi: 10.1073/pnas.0712136105

Skuse, D. H. (2005). X-linked genes and mental functioning. *Hum. Mol. Genet.* 14 Spec No 1, R27–R32. doi: 10.1093/hmg/ddi112

Skuse, D. H., James, R. S., Bishop, D. V., Coppin, B., Dalton, P., Aamodt-Leeper, G., et al. (1997). Evidence from Turner's syndrome of an imprinted X-linked locus affecting cognitive function. *Nature* 387, 705–708. doi: 10.1038/42706

Tachibana, M., Ma, H., Sparman, M. L., Lee, H. S., Ramsey, C. M., Woodward, J. S., et al. (2012). X-chromosome inactivation in monkey embryos and pluripotent stem cells. *Dev. Biol.* 371, 146–155. doi: 10.1016/j.ydbio.2012.08.009

Trapnell, C., Roberts, A., Goff, L., Pertea, G., Kim, D., Kelley, D. R., et al. (2012). Differential gene and transcript expression analysis of RNA-seq experiments with TopHat and Cufflinks. *Nat. Protoc.* 7, 562–578. doi: 10.1038/nprot.2012.016

Vallot, C., Ouimette, J. F., and Rougeulle, C. (2016). Establishment of X chromosome inactivation and epigenomic features of the inactive X depend on cellular contexts. *Bioessays* 38, 869–880. doi: 10.1002/bies.201600121

Wang, E. T., Sandberg, R., Luo, S., Khrebtukova, I., Zhang, L., Mayr, C., et al. (2008). Alternative isoform regulation in human tissue transcriptomes. *Nature* 456, 470–476. doi: 10.1038/nature07509

Wang, P. J., McCarrey, J. R., Yang, F., and Page, D. C. (2001). An abundance of X-linked genes expressed in spermatogonia. *Nat. Genet.* 27, 422–426. doi: 10.1038/86927

Wrenzycki, C., Lucas-Hahn, A., Herrmann, D., Lemme, E., Korsawe, K., and Niemann, H. (2002). *In vitro* production and nuclear transfer affect dosage compensation of the X-linked gene transcripts G6PD, PGK, and Xist in preimplantation bovine embryos. *Biol. Reprod.* 66, 127–134. doi: 10.1095/biolreprod66.1.127

Xue, F., Tian, X. C., Du, F., Kubota, C., Taneja, M., Dinnyes, A., et al. (2002). Aberrant patterns of X chromosome inactivation in bovine clones. *Nat. Genet.* 31, 216–220. doi: 10.1038/ng900

Zhai, L., Mu, J., Zong, H., Depaoli-Roach, A. A., and Roach, P. J. (2000). Structure and chromosomal localization of the human glycogenin-2 gene GYG2. *Gene* 242, 229–235. doi: 10.1016/S0378-1119(99)00520-X

Zhang, W., Yu, Y., Hertwig, F., Thierry-Mieg, J., Zhang, W., Thierry-Mieg, D., et al. (2015). Comparison of RNA-seq and microarray-based models for clinical endpoint prediction. *Genome Biol.* 16:133. doi: 10.1186/s13059-015-0694-1

Zorn, B., Sucur, V., Stare, J., and Meden-Vrtovec, H. (2002). Decline in sex ratio at birth after 10-day war in Slovenia: brief communication. *Hum. Reprod.* 17, 3173–3177. doi: 10.1093/humrep/17.12.3173

Conflict of Interest Statement: The authors declare that the research was conducted in the absence of any commercial or financial relationships that could be construed as a potential conflict of interest.

The reviewer MC and handling Editor declared their shared affiliation, and the handling Editor states that the process nevertheless met the standards of a fair and objective review.

frontiers in Genetics

MINI REVIEW
published: 06 August 2018
doi: 10.3389/fgene.2018.00308

Nuclear Architecture in the Nervous System: Development, Function, and Neurodevelopmental Diseases

Kenji Ito[1,2] *and Takumi Takizawa*[1]*

[1] Department of Pediatrics, Graduate School of Medicine, Gunma University, Maebashi, Japan, [2] Division of Stem Cell Pathology, Center for Experimental Medicine and Systems Biology, Institute of Medical Science, University of Tokyo, Tokyo, Japan

Decades of study have shown that epigenetic regulation plays an important role in neural development and function. Several layers of epigenetic mechanisms control functions of the eukaryotic cell nucleus, a well-organized subcellular organelle with distinct compartments: chromatin, its related architectural proteins, and nuclear bodies. As these components function together in the epigenetic regulation of cellular development and functions, they are collectively termed nuclear architecture. In the nervous system, dynamic rearrangement of nuclear architecture correlates with alteration of transcription programs. During maturation and upon depolarization, neurons undergo a reorganization of nuclear architecture that alters gene expression programs. As such changes allow for specialized functions, including learning and memory, nuclear architecture is distinct among cell types. Studying nuclear architecture of neurons may uncover cell-division-independent mechanisms of global and local changes to nuclear architecture. We herein review recent research concerning nuclear architecture in the nervous system and will discuss its importance to the development, maturation, function, and diseases of the nervous system.

Keywords: chromatin, neuron, glia, differentiation, development, epigenetics, nuclear architecture, gene positioning

OPEN ACCESS

Edited by:
Rafael Franco,
University of Barcelona, Spain

Reviewed by:
Mojgan Rastegar,
University of Manitoba, Canada
Karen Meaburn,
National Institutes of Health (NIH), United States

***Correspondence:**
Takumi Takizawa
takizawt@gunma-u.ac.jp

Specialty section:
This article was submitted to Epigenomics and Epigenetics, a section of the journal Frontiers in Genetics

Received: *06 May 2018*
Accepted: *19 July 2018*
Published: *06 August 2018*

Citation:
Ito K and Takizawa T (2018) Nuclear Architecture in the Nervous System: Development, Function, and Neurodevelopmental Diseases. Front. Genet. 9:308. doi: 10.3389/fgene.2018.00308

INTRODUCTION

Eukaryotic nuclei stably retain large genomic DNA in a compact space without compromising its ability to read necessary information from genomic DNA to create diverse cell types in the right place at the right time. Uncovering how a cell selects and expresses appropriate genes to acquire its identity is central to understanding the mechanisms underlying the physiological functions of a cell.

Epigenetic alterations play pivotal roles in gene expression and cellar functions in the nervous system (Hirabayashi and Gotoh, 2010). Major epigenetic alterations, such as DNA methylation and histone posttranscriptional modifications, correlate with the structure of chromosomes and chromatin. The former is arranged within the interphase cell nucleus in a cell type and developmental stage-dependent manner (Misteli, 2007). Subdomains of chromosomes and genes in the nucleus also non-randomly change their positions during brain development (Takizawa and Meshorer, 2008). Akin to the genome, nuclear bodies, which occupy functionally/morphologically separate sub-nuclear regions such as the nucleoli, Cajal bodies (CBs), and promyelocytic leukemia

(PML) bodies, are also non-randomly arranged (Takizawa and Meshorer, 2008). The organization of these structures is associated with gene expression. The non-random assembly of genomes and nuclear bodies are collectively referred to as "nuclear architecture," and its involvement in gene expression has led to its recognition as an epigenetic agent.

Neurons, the principal cell type of the nervous system, are distinct in their ability to change their morphology, gene expression programs, and functions by adapting to their environment (Dotti et al., 1988; Arimura et al., 2004; Takano et al., 2015). This fundamental process is referred to as neuronal plasticity. It enables neurons to perform primary brain functions, such as learning and memory. Neurons acquire this property during maturation without cell division after having been committed to a cell type lineage. They intriguingly retain this ability for their exceptionally long lifespans. In the central nervous system (CNS), glial cells, such as astrocytes and oligodendrocytes, physically, metabolically, and functionally support neurons (Suzuki et al., 2011). Although neurons and glial cells both differentiate from common neural precursor cells (NPCs), their nuclear architecture has been shown to be distinct from one another (Takizawa and Meshorer, 2008). This observation implicates the importance of nuclear architecture in brain development and function.

We herein review a series of studies that demonstrate the functions and significance of nuclear architecture in the nervous system and discuss its relevance to brain function. The findings on post-mitotic neurons are especially intriguing, and therefore, understanding the underlying mechanisms of cell-division-independent rearrangement of nuclear architecture provides insight into the basic mechanisms of nuclear architecture.

NUCLEAR GEOMETRY

Along with the architecture inside the nucleus, the morphology of the organelle itself changes during neural differentiation and post-mitotic maturation. By analyzing three-dimensional reconstruction images of rat hippocampal neurons, Wittmann et al. (2009) found that a number of nuclei feature different degrees of infolding. Synaptic *N*-methyl-D-aspartate (NMDA) receptor activation dramatically increases the number of infolded nuclei. This observation is reversed when extrasynaptic NMDA receptors are activated by the bath-application of NMDA to the culture. Infolding increases the surface area of the nucleus, as well as the number of nuclear pore complexes. This further leads to an enhancement of nuclear calcium signaling especially in the smaller compartments of nuclei. Intriguingly, similar invaginations of the nuclear envelope (NE) have been observed in many types of mammalian cells (Fricker et al., 1997). An additional observation by Wittmann et al. (2009) supports the functional link between nuclear geometry and transcriptional regulation. Namely, synaptic-activity-induced phosphorylation of histone H3 on serine 10 is more robust in neurons with infolded nuclei. Invagination of the NE and subsequent rearrangement of the nuclear architecture may thus lead to changes in chromatin structure and activity-dependent gene expression. Although the precise mechanisms that regulate infolding are still unknown, the study suggests that changes in nuclear geometry and its regulation by extracellular inputs may play an important role in neuronal functions. These observations likely represent a "cytocrin system" in the nuclear architecture, of which an original concept has been proposed by Navarro et al. (2017) in the canonical epigenetics: extracellular factors could change nuclear geometry and cell functions (**Figure 1**).

NUCLEAR BODIES

The arrangement of nuclear bodies is related to the functions of post-mitotic neurons. Nucleoli are found adjacent to the nuclear periphery in immature Purkinje neurons but converge into one or two larger nucleoli while relocating toward the center of the nucleus during maturation (**Figure 2a**; Solovei et al., 2004). This rearrangement is likely associated with normal brain development and function, as it depends on methyl CpG binding

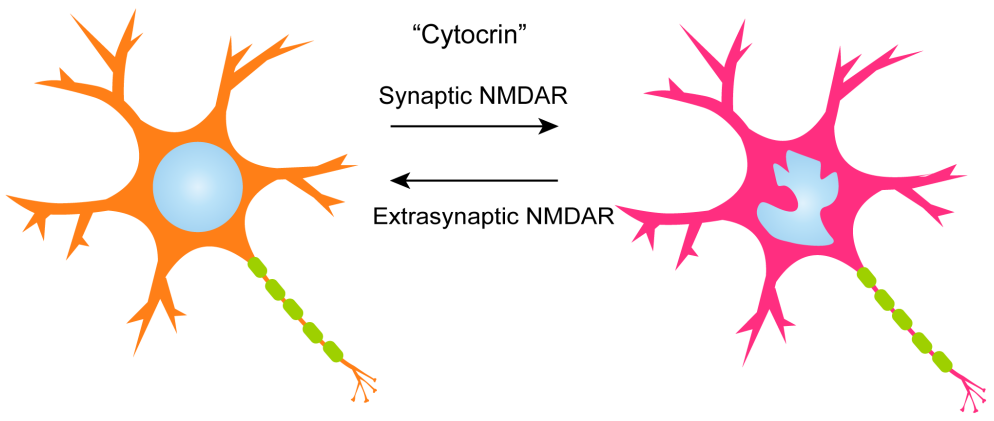

FIGURE 1 | A model of activity-dependent nuclear infolding in rat hippocampal neurons. During baseline synaptic activity, neuronal nuclei display only minor infoldings if any at all. Initiation of strong electrical activity through the synaptic NMDA receptor leads to nuclear infolding, which then enhances nuclear calcium signaling and changes in gene expression. This change is reversed by the activation of the extrasynaptic NMDAR signaling pathways.

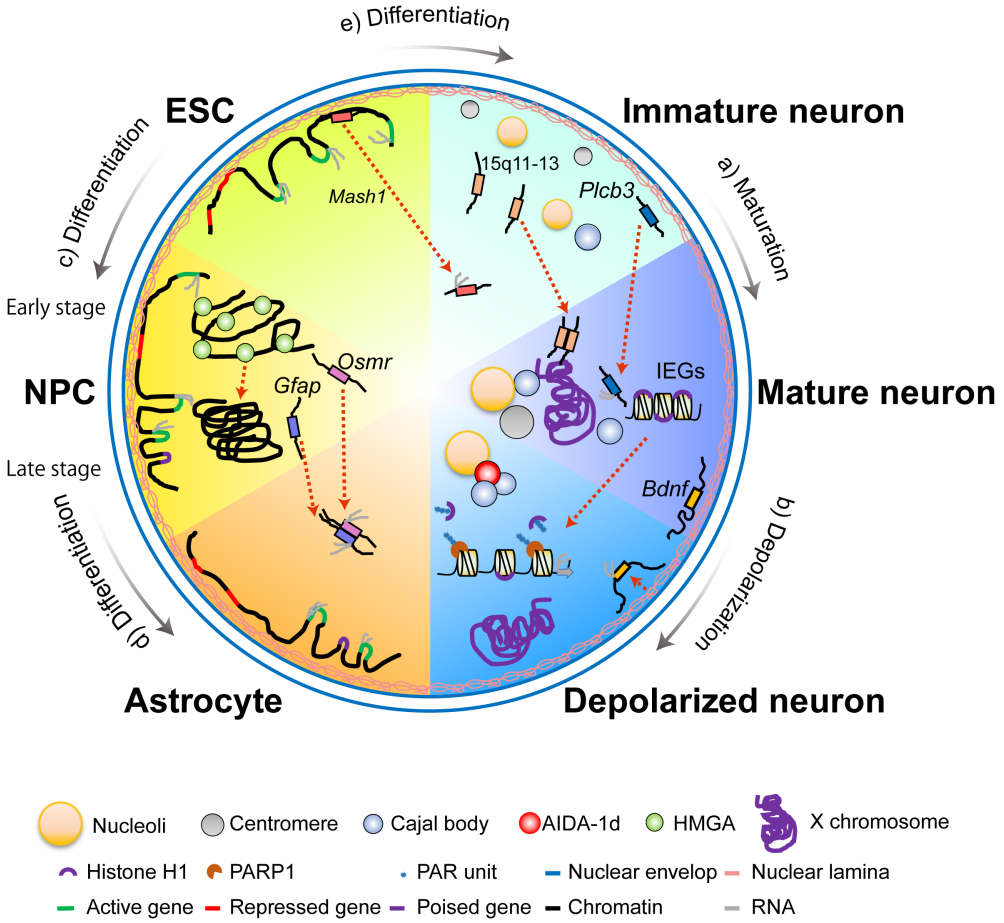

FIGURE 2 | Divided views of nuclear architecture of different types of cells in the nervous system. **(a)** During the maturation process of neurons, repositioning of nucleoli from the nuclear periphery to the nuclear interior occurs alongside the relocation of Cajal bodies (CBs) and centromeric domains. Homologous pairing of the 15q11–13 imprinted domains and repositioning of the *Plcb3* gene loci are also observed in neuronal maturation. **(b)** Upon neuronal depolarization, the X chromosome migrates from the nuclear interior to the nuclear periphery. On the other hand, *Bdnf* gene loci move slightly away from the nuclear periphery. This shift is concurrent with transcriptional upregulation. Nuclear depolarization also features PARP1-dependent eviction of the linker histone H1 from immediate early genes and AIDA-1d-mediated association between CBs and nucleoli enable rapid transcription and protein synthesis. **(c,d)** During subsequent differentiation of the mouse ESC via a lineage-committed neural precursor cell (NPC) into terminally differentiated astrocytes, genome-nuclear lamina (NL) interactions change dramatically. Illustrated are five genes representative of different genome-NL movements. The housekeeping genes constantly move away from the NL and are maintained in the active state (green→green→green). The cell-cycle-related genes move away from NL in ESC and NPC but relocate to the NL in the astrocytes, which induces transcriptional downregulation (green→green→red). An ESC-specific gene relocates from the nuclear interior in the ESC to the NL in the NPC and the astrocyte, which lead to transcriptional downregulation (green→red→red). The NPC- specific genes relocate from the NL in the ESC to the nuclear interior in the NPC and astrocytes, but the genes maintain a poised state in the astrocyte (red→green→purple). The astrocyte-specific genes relocate from the NL in the ESC to the nuclear interior in the NPC and the astrocyte, but the genes maintain a poised state in the NPC (red→purple→green). Over the course of the differentiation, NPCs undergo an early-stage (neurogenic) to late-stage (astrogenic) transition, and downregulation of HMGA is followed by global chromatin condensation. Gene clustering between *Gfap* and *Osmr* occur with accompanying transcriptional upregulation of both genes during differentiation of the NPC into the astrocyte. **(e)** Upon neural induction from the embryonic stem cell (ESC), *Mash1* gene loci relocate from the nuclear periphery toward the nuclear interior, concomitant with transcriptional upregulation.

protein 2 (MeCP2). Mutations of this protein cause a neurological disorder known as Rett syndrome (Singleton et al., 2011).

Cajal bodies, which are speculated to act as sites of assembly for small nuclear ribonucleoproteins, are often found adjacent to nucleoli in mature neurons (**Figure 2a**; Pena et al., 2001; Casafont et al., 2006). The number of CBs increases during neuronal differentiation (Janevski et al., 1997) and is closely related to transcriptional activity after differentiation (Santama et al., 1996; Pena et al., 2001). Investigations using primary rat hippocampal neurons have revealed that CBs mediate a direct link between synaptic activity and nuclear bodies (Jordan et al., 2007). Upon stimulation of NMDA receptors, a component of postsynaptic density, AIDA-1d translocates into the nucleus and binds to CBs (**Figure 2b**). This binding further modulates the number of nucleoli and global protein synthesis.

Although PML bodies have been implicated in a variety of cellular processes, ranging from transcription and cell-cycle progression to apoptosis and DNA repair, their precise role has yet to be defined. Investigations have, however, elucidated a putative role of PML bodies in regeneration and axonotomy;

although the number of PML bodies decreases during neural differentiation (Aoto et al., 2006), the quantity is reportedly increased in dorsal root ganglion neurons of patients with acute inflammatory demyelinating polyneuropathy (Villagrá et al., 2004).

Taken together, these data demonstrate a close relationship between the arrangement of nuclear bodies and neural differentiation/maturation, as well as the importance of the former to neuronal function. The underlying mechanisms that regulate the arrangement of nuclear bodies have not been fully elucidated as of yet. The studies from this point of view will provide a new venue for comprehension of neural differentiation, maturation, and neuronal activity.

CHROMOSOMES AND THEIR SPECIFIC REGIONS

In the interphase cell nucleus, chromosomes adopt a conserved, non-random arrangement in subnuclear domains called chromosome territories (CTs), which change according to cell differentiation and functions (Cremer and Cremer, 2010). Several studies on neurons during and after maturation demonstrate that positions of CTs and specific genome regions of chromosomes are not static in the interphase nucleus, as they can change via cell-division-independent mechanisms. A prominent example was identified by Barr and Bertram's (1949) seminal study. Upon electrical stimulation, the nucleolar satellite (i.e., the Barr body or the inactive X chromosome) in cat motor neurons moves from its usual position adjacent to the nucleolus toward the nuclear membrane (**Figure 2b**; Barr and Bertram, 1949). By examining epileptic human cortices, Borden and Manuelidis (1988) built upon the former observation by finding a dramatic repositioning of the centromeric heterochromatin region of the X chromosome in neurons within electrophysiologically defined seizure foci in both men and women. These studies suggest that specific CTs reposition in a manner that is dependent on neuronal activity and independent of cell division.

The repositioning of specific regions of a chromosome in post-mitotic neurons has also been reported. In mouse Purkinje neurons, the number of centromeric domains changes during maturation, along with their shift from the nuclear periphery to the nucleolus (**Figure 2a**; Martou and De Boni, 2000). This spatial redistribution may contribute to differentiation by placing specific genome sequences onto transcriptionally competent nuclear sites. In addition, the number of centromeric domains is reduced in tetanized rat hippocampal CA1 neurons relative to unpotentiated neurons (Billia et al., 1992). Given that a similar decrease was also observed in CA1 neurons exposed to NMDA, these data suggest that the repositioning of centromeric domains is involved in neuronal-activity-dependent large-scale transcription and protein synthesis.

Chromosome reorganization in post-mitotic neurons was further reported in a study on rod photoreceptor cells of different species. The vast majority of eukaryotic nuclei display a consistent nuclear architecture. Euchromatin predominantly occupies internal nuclear regions and heterochromatin is primarily found on the surface of the NE in regions devoid of nuclear pores and on the surface of the nucleolus. In nocturnal mammals, however, the positions of euchromatin and heterochromatin in the nuclei of rod photoreceptor cells are inverted to reduce light loss and collect it efficiently (Solovei et al., 2009). The low expression of both lamin A/C and lamin B receptor (LBR) underlies this inversion. Cells with conventional nuclear architecture express high levels of these proteins (Solovei et al., 2013). Similar to what is observed in rod photoreceptor cells, low expression of LBR in olfactory sensory neurons (OSNs) contributes to the aggregation of inactive olfactory receptor (OR) genes (Clowney et al., 2012). Further, the expression level of LBR has been observed to decrease during neuronal differentiation from NPCs (Bonev et al., 2017). The aforementioned findings may implicate the composition of the inner nuclear membrane (INM) in chromosome reorganization of post-mitotic neurons and the cell fate of NPCs, and the verification of this possibility may uncover new mechanisms of NPC differentiation.

CHROMATIN

Global structures of chromatin also change during neural differentiation and maturation. One of the structural features of global chromatin organization is the spacing between two adjacent nucleosomes, termed the nucleosome repeat length (NRL), which has been shown to change in rat cortical neurons during neuronal differentiation and maturation (Ermini and Kuenzle, 1978; Jaeger and Kuenzle, 1982). In addition to NRL, global chromatin packaging states are important for the differentiation competence of NPCs (Kishi et al., 2012). Over the course of differentiation, NPCs undergo an early-stage (neurogenic) to late-stage (astrogenic) transition. HMGA proteins, which are highly expressed in NPCs only during the former phase, are essential to the global opening state of chromatin and the neurogenic competency of NPCs (**Figures 2c,d**).

Global changes in chromatin organization are also important for transcriptional upregulation of activity-dependent immediate early genes (IEGs) in post-mitotic neurons. Chromatin accessibility is an indicator of global chromatin change. An investigation studied this property in adult mouse dentate granule neurons by subjecting them to synchronous neuronal activation using transposase-accessible chromatin *in vivo* via a sequencing assay (ATAC-seq). Changes elicited by the procedure were observed by comparing the neurons before and after the activation (Su et al., 2017). This study found that neuronal activity leads to genome-wide chromatin opening and observed that gained-open sites are enriched at active enhancer regions and binding sites for AP1-complex components, including *c-Fos*. Although this study suggests that *c-Fos* is implicated in initiating, but not maintaining, neuronal-activity-dependent chromatin opening, precise mechanisms underlying *c-Fos* activity remain elusive. A recent study, however, demonstrated that potassium chloride-induced depolarization of mouse cortical neurons causes a rapid release of linker histone H1 from chromatin

and an increase in IEG expression, including *c-Fos* (**Figure 2b**; Azad et al., 2018). Poly-ADP ribosylation and phosphorylation of H1 are essential to these two processes. An investigation has shown that administration of a PARP-1 inhibitor impedes long-term memory formation in Aplysia (Cohen-Armon et al., 2004). This observation is further supported by the finding that DNA from Alzheimer's disease (AD) patients is less sensitive to micrococcal nuclease - an enzyme that digests chromatin in the linker region between two adjacent nucleosomes - than that from patients with other neuronal disorders (Lewis et al., 1981; Lukiw and Crapper McLachlan, 1990). These studies therefore suggest the importance of *c-Fos* in the global control of chromatin organization, as well as the therapeutic potential of PARP-1 activity modulation in treating neurocognitive diseases via changing chromatin states.

In addition to linker histone H1, an additional global chromatin organizer CCCTC-binding factor (CTCF) features important roles in neuronal development (see review Davis and Elliott, 2018). In the adult mouse brain, a conditional knockout (CKO) of CTCF in excitatory forebrain neurons yields specific deficits in learning and memory, including spatial memory and fear memory (Sams et al., 2016). Genes involved in memory and learning functions, such as *Arc* and *brain-derived neurotrophic factor* (*Bdnf*), are downregulated in CTCF CKO hippocampi. A chromosome confirmation-capture-based (3C-based) analysis showed that this transcriptional abnormality is attributed to the loss of CTCF-dependent chromatin interaction within these genes loci. Further research has supported such findings: CTCF is mutated in a subset of individuals with intellectual disabilities (Gregor et al., 2013) and its binding partners such as cohesion (Wendt et al., 2008), CHD8 (Ishihara et al., 2006; O'Roak et al., 2012), and MeCP2 (Kernohan et al., 2014) have been implicated in neurodevelopmental disorders. These results suggest that targeting the abnormal functioning of CTCF and its binding partners may be an effective therapeutic strategy for treating neurodevelopmental disorders.

Among these CTCF-binding partners, MeCP2 has been shown to be involved in neuronal chromatin organization (see review Ausio et al., 2014). At first, MeCP2 was only recognized as a transcriptional repressor because it contains a methyl-CpG binding domain and a transcriptional repression domain. However, it has been found that MeCP2 is distributed widely across the genome of neurons (Skene et al., 2010), and its depletion leads to both an increase and a decrease in gene expression in the brain (Chahrour et al., 2008; Skene et al., 2010). In addition, MeCP2 binds to linker DNA and can displace linker histone H1 (Ghosh et al., 2010). These studies suggest that MeCP2 affects the structure of chromatin much like the linker histone H1. Despite their similarity, a recent study indicated that they work independently in chromatin binding (Ito-Ishida et al., 2018). Another global chromatin organizer, HMGA proteins, also competes with H1 to bind with chromatin (Kishi et al., 2012). Further studies on the functional relationship among these global chromatin organizer proteins in neurons will help to uncover the molecular basis of neurodevelopmental disorders.

SPECIFIC GENE LOCI

Along with global changes, local repositioning of specific gene loci correlates with the transcriptional activity in neural cells. Studies on this topic have operated from two distinct points of view, radial gene positioning and gene clustering.

Radial Gene Positioning

Akin to chromosomes and their specific regions, gene loci are non-randomly arranged within the mammalian nucleus. The radial repositioning of gene loci away from the nuclear periphery correlates with the transcriptional upregulation of genes during neural differentiation and development. The nuclear lamina, a protein meshwork located along the inner layer of the nuclear membrane, interacts with repressive chromatin regulators to tether heterochromatic sequences to the nuclear periphery. Indeed, an important proneural regulator gene, *Mash1*, is repositioned from the nuclear periphery toward the nuclear interior (**Figure 2e**). This migration is concurrent with the changes in chromatin structure and transcriptional upregulation upon neural induction from ES cells (Williams et al., 2006). Further support for the association between radial gene positioning and transcriptional upregulation has been observed in the maturation of mouse cerebellar Purkinje neurons. The repositioning of *Plcb3* from the nuclear periphery toward the nuclear interior is concomitant with transcriptional upregulation (**Figure 2a**; Martou et al., 2002). Although the relationship between the two processes is still under investigation, an increasing body of evidence suggests the interaction between the genome and the nuclear lamina is important for normal brain development and function. Intriguingly, lamina-associated heterochromatic domains became mobile during brain development. Peric-Hupkes et al. (2010) revealed this mechanism by performing DNA adenine methyltransferase identification (DamID) of Lamin B1 to map lamina-associated domains (LADs) during the subsequent differentiation of mouse embryonic stem cells via lineage-committed NPCs into terminally differentiated astrocytes (**Figures 2c,d**). Though LADs overlapped by 73–87% among the examined cell types, many gene loci that determine cellular identity relocate from the lamina. Several such genes that move away from the lamina are concurrently activated, while others become activated in the next phase of differentiation. Furthermore, most gene loci apparently relocate separately, not as clusters, and many gene loci migrate according to cell type, differentiation stage, and the expression levels of the genes. This mechanism may compose another layer of spatial-gene-positioning-related transcriptional regulation during neuronal differentiation. Studies using rat hippocampal dentate gyrus neurons have further found that intranuclear positions of *Bdnf* move away from the nuclear lamina upon neuronal activation following kainite-induced seizures (**Figure 2b**; Walczak et al., 2013). These results demonstrate that the genome-nuclear lamina interaction plays an important role in brain function.

Radial positioning of genes is also implicated in cell fate of NPCs. In *Drosophila* embryonic NPCs, Hunchback (Hb) is expressed in the early stage NPCs and is both necessary and sufficient to specify early-born neuronal identity. Interestingly,

gene loci of *Hb* move toward the nuclear periphery when competence to specify early-born fates is lost (Kohwi et al., 2013). As Hb expression can be induced when artificially placed in the nuclear interior, this repositioning seems to be required to efficiently and permanently silence Hb transcription. In mouse NPCs, an astrocyte-specific gene encoding *glial fibrillary acidic protein* (*Gfap*) is repositioned toward the nuclear center during astrocyte differentiation (Takizawa et al., 2008). Following its relocation to the nuclear interior, the active *Gfap* allele associates more frequently with nuclear speckles, a nuclear body enriched in pre-mRNA splicing factors. These results represent dynamic changes in the radial distribution of specific gene loci followed by concomitant alterations in transcriptional activity upon differentiation from NPCs.

Gene Clustering Between Gene Loci

An increasing amount of evidence supports the importance of gene clustering to biological processes, including transcriptional regulation and enhancement (Schoenfelder et al., 2010). By using a chromosome confirmation-capture-based (3C-based) technique and an expression array, 18 genes were identified to specifically associate with an astrocyte-specific gene, *Gfap*, in NPC-derived astrocytes (Ito et al., 2016). *Gfap* expression is induced by activation of transcription factor STAT3 (Takizawa et al., 2001). Given that several of the identified genes are also activated by the same transcription factor, their transcription may be co-regulated with *Gfap* on the same locale of the nucleus. *Osmr*, one of the 18 putative clustering genes, encodes the oncostatin M receptor (OSMR). Clustering of *Osmr* with *Gfap* enhances the transcription of both genes and requires the presence of both brahma-related gene 1 (BRG1), an ATP-dependent chromatin remodeling factor, and STAT3 (**Figure 2d**; Ito et al., 2018). Further, an investigation of mouse neural differentiation using ultrahigh resolution Hi-C, a 3C-based technique, revealed the involvement of cortical-neuron (CN)-specific transcription factors, such as Pax6, NeuroD2, and Tbr1, in CN-specific long-range chromatin interaction both *in vivo* and *in vitro* (Bonev et al., 2017). These studies demonstrate that transcription factors, which have been shown to be important for cell fate determination of NPCs, are involved in brain development via gene clustering.

Gene clustering between homologous gene loci has further been reported to contribute to gene regulation (Hogan et al., 2015). Homologous pairing of the 15q11–13 imprinted domains, which are deficient in maternal alleles in Angelman syndrome (AS), is observed in infantile and juvenile normal human brains (**Figure 2a**). However, it is not observed in brain samples derived from patients with AS, Rett syndrome, autism, or other conditions (Thatcher et al., 2005). The finding implicates gene clustering between homologous gene loci in pathophysiological states. The function and importance of long-range chromatin interactions, such as promoter-enhancer interaction within gene bodies or topologically associating domains in neural gene expression, is becoming increasingly well understood (see an excellent review Rajarajan et al., 2016). However, the mechanism and significance of gene clustering between gene loci in brain development and function are still unknown and require extensive investigation.

CONCLUSION AND FUTURE DIRECTION

Epigenetic changes are accompanied by the reconstruction of nuclear architecture. The proteins that participate in the construction of nuclear architecture, such as cohesin, NIPBL, MeCP2, CTCF, SATB2, and LMNB1, have been shown to be pivotal for a healthy nervous system. The dysfunction of these molecules reportedly causes neurodevelopmental disorders (see excellent review Rajarajan et al., 2016).

Neurons consist of many subtypes of cells, and this diversity underlies the intricate functions of the nervous system. Nuclear architecture is presumably distinct among such subtypes. To elucidate the differences in their nuclear architecture at a single-cell level and to characterize their components, such as genome-nuclear lamina interaction and chromatin conformation, novel methods have been developed (Kind et al., 2013; Nagano et al., 2013). In addition, *in vivo* studies are increasingly performed to characterize the natural states of nuclear architecture and avoid the limitations of *in vitro* approaches (Bonev et al., 2017). At the forefront of such *in vivo* investigations, the CRISPR/Cas9 system and its derivative technologies have been applied to studies of epigenetic states, such as DNA methylation and chromatin conformation (Guo et al., 2015; Liu et al., 2016; Morita et al., 2016). Although conducting single-cell-based analyses of nuclear architecture and gene expression *in vivo* poses difficulties, overcoming these experimental challenges will open a new avenue for uncovering the importance of nuclear architecture and its significance to brain function in diseased and healthy states.

AUTHOR CONTRIBUTIONS

All authors listed have made a substantial, direct and intellectual contribution to the work, and approved it for publication.

REFERENCES

Aoto, T., Saitoh, N., Ichimura, T., Niwa, H., and Nakao, M. (2006). Nuclear and chromatin reorganization in the MHC-Oct3/4 locus at developmental phases of embryonic stem cell differentiation. *Dev. Biol.* 298, 354–367. doi: 10.1016/j.ydbio.2006.04.450

Arimura, N., Menager, C., Fukata, Y., and Kaibuchi, K. (2004). Role of CRMP-2 in neuronal polarity. *J. Neurobiol.* 58, 34–47. doi: 10.1002/neu.10269

Ausio, J., Martinez de Paz, A., and Esteller, M. (2014). MeCP2: the long trip from a chromatin protein to neurological disorders. *Trends Mol. Med.* 20, 487–498. doi: 10.1016/j.molmed.2014.03.004

Azad, G. K., Ito, K., Sailaja, B. S., Biran, A., Nissim-Rafinia, M., Yamada, Y., et al. (2018). PARP1-dependent eviction of the linker histone H1 mediates immediate early gene expression during neuronal activation. *J. Cell Biol.* 217, 473–481. doi: 10.1083/jcb.201703141

Barr, M. L., and Bertram, E. G. (1949). A morphological distinction between neurones of the male and female, and the behaviour of the nucleolar satellite

during accelerated nucleoprotein synthesis. *Nature* 163:676. doi: 10.1038/163676a0

Billia, F., Baskys, A., Carlen, P. L., and De Boni, U. (1992). Rearrangement of centromeric satellite DNA in hippocampal neurons exhibiting long-term potentiation. *Brain Res. Mol. Brain Res.* 14, 101–108. doi: 10.1016/0169-328X(92)90016-5

Bonev, B., Mendelson, Cohen N, Szabo, Q., Fritsch, L., Papadopoulos, G. L., Lubling, Y., et al. (2017). Multiscale 3D genome rewiring during mouse neural development. *Cell* 171, 557.e24–572.e24. doi: 10.1016/j.cell.2017.09.043

Borden, J., and Manuelidis, L. (1988). Movement of the X chromosome in epilepsy. *Science* 242, 1687–1691. doi: 10.1126/science.3201257

Casafont, I., Navascues, J., Pena, E., Lafarga, M., and Berciano, M. T. (2006). Nuclear organization and dynamics of transcription sites in rat sensory ganglia neurons detected by incorporation of 5'-fluorouridine into nascent RNA. *Neuroscience* 140, 453–462. doi: 10.1016/j.neuroscience.2006.02.030

Chahrour, M., Jung, S. Y., Shaw, C., Zhou, X., Wong, S. T., Qin, J., et al. (2008). MeCP2, a key contributor to neurological disease, activates and represses transcription. *Science* 320, 1224–1229. doi: 10.1126/science.1153252

Clowney, E. J., LeGros, M. A., Mosley, C. P., Clowney, F. G., Markenskoff-Papadimitriou, E. C., Myllys, M., et al. (2012). Nuclear aggregation of olfactory receptor genes governs their monogenic expression. *Cell* 151, 724–737. doi: 10.1016/j.cell.2012.09.043

Cohen-Armon, M., Visochek, L., Katzoff, A., Levitan, D., Susswein, A. J., Klein, R., et al. (2004). Long-term memory requires polyADP-ribosylation. *Science* 304, 1820–1822. doi: 10.1126/science.1096775

Cremer, T., and Cremer, M. (2010). Chromosome territories. *Cold Spring Harb. Perspect. Biol.* 2:a003889. doi: 10.1101/cshperspect.a003889

Davis, L. I, and Elliott, O. E. (2018). The emerging roles for the chromatin structure regulators CTCF and cohesin in neurodevelopment and behavior. *Cell. Mol. Life Sci.* 75, 1205–1214. doi: 10.1007/s00018-017-2706-7

Dotti, C. G., Sullivan, C. A., and Banker, G. A. (1988). The establishment of polarity by hippocampal neurons in culture. *J. Neurosci.* 8, 1454–1468. doi: 10.1523/JNEUROSCI.08-04-01454.1988

Ermini, M., and Kuenzle, C. C. (1978). The chromatin repeat length of cortical neurons shortens during early posnatal development. *FEBS Lett.* 90, 167–172. doi: 10.1016/0014-5793(78)80322-6

Fricker, M., Hollinshead, M., White, N., and Vaux, D. (1997). Interphase nuclei of many mammalian cell types contain deep, dynamic, tubular membrane-bound invaginations of the nuclear envelope. *J. Cell Biol.* 136, 531–544. doi: 10.1083/jcb.136.3.531

Ghosh, R. P., Horowitz-Scherer, R. A., Nikitina, T., Shlyakhtenko, L. S., and Woodcock, C. L. (2010). MeCP2 binds cooperatively to its substrate and competes with histone H1 for chromatin binding sites. *Mol. Cell. Biol.* 30, 4656–4670. doi: 10.1128/MCB.00379-10

Gregor, A., Oti, M., Kouwenhoven, E. N., Hoyer, J., Sticht, H., Ekici, A. B., et al. (2013). De novo mutations in the genome organizer CTCF cause intellectual disability. *Am. J. Hum. Genet.* 93, 124–131. doi: 10.1016/j.ajhg.2013.05.007

Guo, Y., Xu, Q., Canzio, D., Shou, J., Li, J., Gorkin, D. U., et al. (2015). CRISPR Inversion of CTCF Sites Alters Genome Topology and Enhancer/Promoter Function. *Cell* 162, 900–910. doi: 10.1016/j.cell.2015.07.038

Hirabayashi, Y., and Gotoh, Y. (2010). Epigenetic control of neural precursor cell fate during development. *Nat. Rev. Neurosci.* 11, 377–388. doi: 10.1038/nrn2810

Hogan, M. S., Parfitt, D. E., Zepeda-Mendoza, C. J., Shen, M. M., and Spector, D. L. (2015). Transient pairing of homologous Oct4 alleles accompanies the onset of embryonic stem cell differentiation. *Cell Stem Cell* 16, 275–288. doi: 10.1016/j.stem.2015.02.001

Ishihara, K., Oshimura, M., and Nakao, M. (2006). CTCF-dependent chromatin insulator is linked to epigenetic remodeling. *Mol. Cell* 23, 733–742. doi: 10.1016/j.molcel.2006.08.008

Ito, K., Noguchi, A., Uosaki, Y., Taga, T., Arakawa, H., and Takizawa, T. (2018). Gfap and Osmr regulation by BRG1 and STAT3 via interchromosomal gene clustering in astrocytes. *Mol. Biol. Cell* 29, 209–219. doi: 10.1091/mbc.E17-05-0271

Ito, K., Sanosaka, T., Igarashi, K., Ideta-Otsuka, M., Aizawa, A., Uosaki, Y., et al. (2016). Identification of genes associated with the astrocyte-specific gene Gfap during astrocyte differentiation. *Sci. Rep.* 6:23903. doi: 10.1038/srep23903

Ito-Ishida, A., Yamalanchili, H. K., Shao, Y., Baker, S. A., Heckman, L. D., Lavery, L. A., et al. (2018). Genome-wide distribution of linker histone H1.0 is independent of MeCP2. *Nat. Neurosci.* 21, 794–798. doi: 10.1038/s41593-018-0155-8

Jaeger, A. W., and Kuenzle, C. C. (1982). The chromatin repeat length of brain cortex and cerebellar neurons changes concomitant with terminal differentiation. *EMBO J.* 1, 811–816.

Janevski, J., Park, P. C., and De Boni, U. (1997). Changes in morphology and spatial position of coiled bodies during NGF-induced neuronal differentiation of PC12 cells. *J. Histochem. Cytochem.* 45, 1523–1531. doi: 10.1177/002215549704501109

Jordan, B. A., Fernholz, B. D., Khatri, L., and Ziff, E. B. (2007). Activity-dependent AIDA-1 nuclear signaling regulates nucleolar numbers and protein synthesis in neurons. *Nat. Neurosci.* 10, 427–435. doi: 10.1038/nn1867

Kernohan, K. D., Vernimmen, D., Gloor, G. B., and Berube, N. G. (2014). Analysis of neonatal brain lacking ATRX or MeCP2 reveals changes in nucleosome density, CTCF binding and chromatin looping. *Nucleic Acids Res.* 42, 8356–8368. doi: 10.1093/nar/gku564

Kind, J., Pagie, L., Ortabozkoyun, H., Boyle, S., de, Vries SS, Janssen, H., et al. (2013). Single-cell dynamics of genome-nuclear lamina interactions. *Cell* 153, 178–192. doi: 10.1016/j.cell.2013.02.028

Kishi, Y., Fujii, Y., Hirabayashi, Y., and Gotoh, Y. (2012). HMGA regulates the global chromatin state and neurogenic potential in neocortical precursor cells. *Nat. Neurosci.* 15, 1127–1133. doi: 10.1038/nn.3165

Kohwi, M., Lupton, J. R., Lai, S. L., Miller, M. R., and Doe, C. Q. (2013). Developmentally regulated subnuclear genome reorganization restricts neural progenitor competence in *Drosophila*. *Cell* 152, 97–108. doi: 10.1016/j.cell.2012.11.049

Lewis, P. N., Lukiw, W. J., De Boni, U., and McLachlan, D. R. (1981). Changes in chromatin structure associated with Alzheimer's disease. *J. Neurochem.* 37, 1193–1202. doi: 10.1111/j.1471-4159.1981.tb04670.x

Liu, X. S., Wu, H., Ji, X., Stelzer, Y., Wu, X., Czauderna, S., et al. (2016). Editing DNA methylation in the mammalian genome. *Cell* 167, 233.e17–247.e17. doi: 10.1016/j.cell.2016.08.056

Lukiw, W. J., and Crapper McLachlan, D. R. (1990). Chromatin structure and gene expression in Alzheimer's disease. *Brain Res. Mol. Brain Res.* 7, 227–233. doi: 10.1016/0169-328X(90)90032-9

Martou, G., and De Boni, U. (2000). Nuclear topology of murine, cerebellar Purkinje neurons: changes as a function of development. *Exp. Cell Res.* 256, 131–139. doi: 10.1006/excr.1999.4793

Martou, G., Park, P. C., and De Boni, U. (2002). Intranuclear relocation of the Plc beta3 sequence in cerebellar purkinje neurons: temporal association with de novo expression during development. *Chromosoma* 110, 542–549. doi: 10.1007/s00412-001-0179-8

Misteli, T. (2007). Beyond the sequence: cellular organization of genome function. *Cell* 128, 787–800. doi: 10.1016/j.cell.2007.01.028

Morita, S., Noguchi, H., Horii, T., Nakabayashi, K., Kimura, M., Okamura, K., et al. (2016). Targeted DNA demethylation in vivo using dCas9-peptide repeat and scFv-TET1 catalytic domain fusions. *Nat. Biotechnol.* 34, 1060–1065. doi: 10.1038/nbt.3658

Nagano, T., Lubling, Y., Stevens, T. J., Schoenfelder, S., Yaffe, E., Dean, W., et al. (2013). Single-cell Hi-C reveals cell-to-cell variability in chromosome structure. *Nature* 502, 59–64. doi: 10.1038/nature12593

Navarro, G., Franco, N., Martinez-Pinilla, E., and Franco, R. (2017). The epigenetic cytocrin pathway to the nucleus. epigenetic factors, epigenetic mediators, and epigenetic traits. a biochemist perspective. *Front. Genet.* 8:179. doi: 10.3389/fgene.2017.00179

O'Roak, B. J., Vives, L., Fu, W., Egertson, J. D., Stanaway, I. B., Phelps, I. G., et al. (2012). Multiplex targeted sequencing identifies recurrently mutated genes in autism spectrum disorders. *Science* 338, 1619–1622. doi: 10.1126/science.1227764

Pena, E., Berciano, M. T., Fernandez, R., Ojeda, J. L., and Lafarga, M. (2001). Neuronal body size correlates with the number of nucleoli and Cajal bodies, and with the organization of the splicing machinery in rat trigeminal ganglion neurons. *J. Comp. Neurol.* 430, 250–263. doi: 10.1002/1096-9861(20010205)430:2<250::AID-CNE1029>3.0.CO;2-L

Peric-Hupkes, D., Meuleman, W., Pagie, L., Bruggeman, S. W., Solovei, I., Brugman, W., et al. (2010). Molecular maps of the reorganization of genome-nuclear lamina interactions during differentiation. *Mol. Cell* 38, 603–613. doi: 10.1016/j.molcel.2010.03.016

Rajarajan, P., Gil, S. E., Brennand, K. J., and Akbarian, S. (2016). Spatial genome organization and cognition. *Nat. Rev. Neurosci.* 17, 681–691. doi: 10.1038/nrn.2016.124

Sams, D. S., Nardone, S., Getselter, D., Raz, D., Tal, M., Rayi, P. R., et al. (2016). Neuronal CTCF is necessary for basal and experience-dependent gene regulation, memory formation, and genomic structure of BDNF and arc. *Cell Rep.* 17, 2418–2430. doi: 10.1016/j.celrep.2016.11.004

Santama, N., Dotti, C. G., and Lamond, A. I. (1996). Neuronal differentiation in the rat hippocampus involves a stage-specific reorganization of subnuclear structure both in vivo and in vitro. *Eur. J. Neurosci.* 8, 892–905. doi: 10.1111/j.1460-9568.1996.tb01576.x

Schoenfelder, S., Sexton, T., Chakalova, L., Cope, N. F., Horton, A., Andrews, S., et al. (2010). Preferential associations between co-regulated genes reveal a transcriptional interactome in erythroid cells. *Nat. Genet.* 42, 53–61. doi: 10.1038/ng.496

Singleton, M. K., Gonzales, M. L., Leung, K. N., Yasui, D. H., Schroeder, D. I., Dunaway, K., et al. (2011). MeCP2 is required for global heterochromatic and nucleolar changes during activity-dependent neuronal maturation. *Neurobiol. Dis.* 43, 190–200. doi: 10.1016/j.nbd.2011.03.011

Skene, P. J., Illingworth, R. S., Webb, S., Kerr, A. R., James, K. D., Turner, D. J., et al. (2010). Neuronal MeCP2 is expressed at near histone-octamer levels and globally alters the chromatin state. *Mol. Cell* 37, 457–468. doi: 10.1016/j.molcel.2010.01.030

Solovei, I., Kreysing, M., Lanctôt, C., Kösem, S., Peichl, L., Cremer, T., et al. (2009). Nuclear architecture of rod photoreceptor cells adapts to vision in mammalian evolution. *Cell* 137, 356–368. doi: 10.1016/j.cell.2009.01.052

Solovei, I., Schermelleh, L., Düring, K., Engelhardt, A., Stein, S., Cremer, C., et al. (2004). Differences in centromere positioning of cycling and postmitotic human cell types. *Chromosoma* 112, 410–423. doi: 10.1007/s00412-004-0287-3

Solovei, I., Wang, A. S., Thanisch, K., Schmidt, C. S., Krebs, S., Zwerger, M., et al. (2013). LBR and lamin A/C sequentially tether peripheral heterochromatin and inversely regulate differentiation. *Cell* 152, 584–598. doi: 10.1016/j.cell.2013.01.009

Su, Y., Shin, J., Zhong, C., Wang, S., Roychowdhury, P., Lim, J., et al. (2017). Neuronal activity modifies the chromatin accessibility landscape in the adult brain. *Nat. Neurosci.* 20, 476–483. doi: 10.1038/nn.4494

Suzuki, A., Stern, S. A., Bozdagi, O., Huntley, G. W., Walker, R. H., Magistretti, P. J., et al. (2011). Astrocyte-neuron lactate transport is required for long-term memory formation. *Cell* 144, 810–823. doi: 10.1016/j.cell.2011.02.018

Takano, T., Xu, C., Funahashi, Y., Namba, T., and Kaibuchi, K. (2015). Neuronal polarization. *Development* 142, 2088–2093. doi: 10.1242/dev.114454

Takizawa, T., Gudla, P. R., Guo, L., Lockett, S., and Misteli, T. (2008). Allele-specific nuclear positioning of the monoallelically expressed astrocyte marker GFAP. *Genes Dev.* 22, 489–498. doi: 10.1101/gad.1634608

Takizawa, T., and Meshorer, E. (2008). Chromatin and nuclear architecture in the nervous system. *Trends Neurosci.* 31, 343–352. doi: 10.1016/j.tins.2008.03.005

Takizawa, T., Nakashima, K., Namihira, M., Ochiai, W., Uemura, A., Yanagisawa, M., et al. (2001). DNA methylation is a critical cell-intrinsic determinant of astrocyte differentiation in the fetal brain. *Dev. Cell* 1, 749–758. doi: 10.1016/S1534-5807(01)00101-0

Thatcher, K. N., Peddada, S., Yasui, D. H., and Lasalle, J. M. (2005). Homologous pairing of 15q11-13 imprinted domains in brain is developmentally regulated but deficient in Rett and autism samples. *Hum. Mol. Genet.* 14, 785–797. doi: 10.1093/hmg/ddi073

Villagrá, N. T., Berciano, J., Altable, M., Navascués, J., Casafont, I., Lafarga, M., et al. (2004). PML bodies in reactive sensory ganglion neurons of the guillain-Barre syndrome. *Neurobiol. Dis.* 16, 158–168. doi: 10.1016/j.nbd.2004.02.005

Walczak, A., Szczepankiewicz, A. A., Ruszczycki, B., Magalska, A., Zamlynska, K., Dzwonek, J., et al. (2013). Novel higher-order epigenetic regulation of the Bdnf gene upon seizures. *J. Neurosci.* 33, 2507–2511. doi: 10.1523/JNEUROSCI.1085-12.2013

Wendt, K. S., Yoshida, K., Itoh, T., Bando, M., Koch, B., Schirghuber, E., et al. (2008). Cohesin mediates transcriptional insulation by CCCTC-binding factor. *Nature* 451, 796–801. doi: 10.1038/nature06634

Williams, R. R., Azuara, V., Perry, P., Sauer, S., Dvorkina, M., Jørgensen, H., et al. (2006). Neural induction promotes large-scale chromatin reorganisation of the Mash1 locus. *J. Cell Sci.* 119, 132–140. doi: 10.1242/jcs.02727

Wittmann, M., Queisser, G., Eder, A., Wiegert, J. S., Bengtson, C. P., Hellwig, A., et al. (2009). Synaptic activity induces dramatic changes in the geometry of the cell nucleus: interplay between nuclear structure, histone H3 phosphorylation, and nuclear calcium signaling. *J. Neurosci.* 29, 14687–14700. doi: 10.1523/JNEUROSCI.1160-09.2009

Conflict of Interest Statement: The authors declare that the research was conducted in the absence of any commercial or financial relationships that could be construed as a potential conflict of interest.

frontiers in Genetics

MINI REVIEW
published: 12 October 2017
doi: 10.3389/fgene.2017.00144

Epigenetics in the Eye: An Overview of the Most Relevant Ocular Diseases

*Hanan A. Alkozi[1], Rafael Franco[2,3] and Jesús J. Pintor[1]**

[1] Department of Biochemistry and Molecular Biology IV, Faculty of Optics and Optometry, University Complutense of Madrid, Madrid, Spain, [2] Department of Biochemistry and Molecular Biomedicine of the University of Barcelona, Institut de Biomedicina de la Universitat de Barcelona (IBUB), Barcelona, Spain, [3] Cell and Molecular Neuropharmacology, Centro de Investigación Biomédica en Red Enfermedades Neurodegenerativas (CIBERNED), Instituto de Salud Carlos III, Madrid, Spain

Sight for mammals is one of the most appreciated senses. In humans there are several factors that contribute to the increment in all kind of eye diseases. This mini-review will focus on some diseases whose prevalence is steadily increasing year after year for non-genetic reasons, namely cataracts, dry eye, and glaucoma. Aging, diet, inflammation, drugs, oxidative stress, seasonal and circadian style-of-live changes are impacting on disease prevalence by epigenetics factors, defined as stable heritable traits that are not explained by changes in DNA sequence. The mini-review will concisely show the data showing epigenetics marks in these diseases and on how knowledge on the epigenetic alterations may guide therapeutic approaches to have a healthy eye.

Keywords: cataracts, glaucoma, dry eye, keratoconus, eye diseases

OPEN ACCESS

Edited by:
Alfred Sze-Lok Cheng, The Chinese University of Hong Kong, Hong Kong

Reviewed by:
Michael W. Y. Chan, National Chung Cheng University, Taiwan
Jafar Sharif, RIKEN Center for Integrative Medical Sciences (IMS), Japan

****Correspondence:***
Jesús J. Pintor
jpintor@ucm.es

Specialty section:
This article was submitted to Epigenomics and Epigenetics, a section of the journal Frontiers in Genetics

Received: *22 July 2017*
Accepted: *22 September 2017*
Published: *12 October 2017*

Citation:
Alkozi HA, Franco R and Pintor JJ (2017) Epigenetics in the Eye: An Overview of the Most Relevant Ocular Diseases. Front. Genet. 8:144. doi: 10.3389/fgene.2017.00144

INTRODUCTION

The eye in mammals is an extraordinarily specialized sensory organ. From the outward–inward direction, the eye receives light that passing through the cornea reaches the pupil; light is finally focused by the crystalline lens. When light reaches the neurosensory retina, a series of phototransduction cascades unfold to convert the photonic energy into a neural signal going from the photoreceptors to the ganglion cells, where the information travels through the optic nerve into the brain. In the central nervous system the information is processed and consciously appreciated as vision (Forrester et al., 2015).

Ocular diseases and consequently, visual impairment, can occur when any cellular component of the eye becomes dysfunctional. Many ophthalmic pathologies are known to have both heritable and environmental etiopathological factors (Sanfilippo et al., 2010) (**Figure 1**). Hence, discovering the molecular mechanisms of such diseases have positive impacts in the search for therapeutic approaches (Lipinski et al., 2013; Campbell et al., 2016; Garoon and Stout, 2016). Well-powered genome-wide association and linkage studies have helped in detecting some of the causes of ocular diseases. Taking into account the human lifespan, a high percentage (circa 90%) of the genes of the human genome are expressed in eye structures (Sheffield and Stone, 2011). However, the precise reason behind developmental genetic features and regulation of gene expression by environmental factors remains poorly understood.

Gene–environment interaction dynamics are currently known to be potentially mediated by epigenetic marks established during development and/or acquired by food habits and environmental factors (Leenen et al., 2016; Hewitt et al., 2017). Limited but increasing evidence suggest an epigenetic basis in several ocular diseases (Wei et al., 2012; Busanello et al., 2017).

Epigenetics can be defined as the mitotically and mitotically heritable potential for gene expression that does not involve variation in the DNA sequence (Ushijima et al., 2003; Fedoriw et al., 2012; Waddington, 2012). Epigenetics variations have an important role in regulating key biological processes, such as cell differentiation, genomic imprinting, and X-chromosome inactivation (Fedoriw et al., 2012; Li et al., 2012; Wutz, 2013). Epigenetic traits are also directly or indirectly related to a wide range of diseases, from allergies to cancer (Rakyan et al., 2011).

The main mechanisms underlying epigenetics effects include DNA methylation, post-translational histone modification, chromatin remodeling, and RNA-associated gene regulation by non-coding RNAs (Ecker et al., 2017). Wide range of studies are focused on discovering possible epigenetic regulations in several pathologies. Although the field is in its beginnings, DNA methylation is by far the most widely studied epigenetic process, and many studies have begun to explore the link between DNA methylation patterns and a wide range of diseases (Hewitt et al., 2017).

DNA methyltransferase (DNMT) activity is increased in numerous diseases, and inhibitors of these enzymes are extensively studied as a pharmacological approach focusing on epigenetics-based anti-cancer therapy (Lyko and Brown, 2005). A proof of the potential of enzyme inhibitors involved in placing epigenetic marks in the DNA is the approval by the US Food and Drug Administration of a DNMT inhibitor, 5-azacytidine, as anti-tumor agent (see Kaminskas et al., 2005; Sampol et al., 2017, and references therein).

DNA methyltransferases are a family of enzymes that methylate DNA at the carbon-5 position of cytosine residues. Methylated DNA can then interact with methyl-binding proteins that function as adaptors between patches of methylated DNA and chromatin-modifying enzymes (e.g., histone deacetylases and histone methyltransferases). Histone-modifying enzymes then covalently modify histones to induce the formation of chromatin structures that repress gene transcription. There are two types of DNMTs inhibitors, namely, nucleoside and non-nucleoside inhibitors (Lyko and Brown, 2005). Acetylation or deacetylation of histone N-terminal ends is able to produce changes in the interaction between histones and DNA in chromatin, this chromatin remodeling being identified as a key step to regulate gene expression. Histone acetyltransferases and deacetylases are, respectively, the enzymes committed to the addition and removal of acetyl groups from lysine residues within histone N-terminal ends; they play an essential role in developmental processes, whereas they appear as dysregulated in a variety of diseases (Nusinzon and Horvath, 2005; Verdone et al., 2005). Generally, hyperacetylation is associated to transcriptional activation, while hypoacetylation is linked to silencing (Saha and Pahan, 2006).

During the last decade, technological advances applied to functional genomics have illustrated a new scenario in the field of RNA biology. To date, approximately 35% (about 57,000; GENCODE version 17) (Consortium, 2012) of the human sequences identified by the ENCODE project, include open reading frames but most of the remaining ones are known as "non-coding" RNAs. Non-coding RNAs are classified in different groups in accordance to their length, function, localization, orientation, or other criteria. Overall, their relevance is increasingly acknowledged by researchers because they may regulate gene expression thus arising as epigenetic players. Countless microRNAs have been discovered and described in the past few years (Morozova et al., 2012; Romano et al., 2017) and they are attributed far more physiological roles than expected when first discovered. There are still questions to sort out before apprehending the real relevance of non-coding RNAs. As an example some of those RNAs which are not translated into any protein may arrange into silencing (RISC) complexes that block the expression of given genes (Esquela-Kerscher and Slack, 2006). Other identified small RNA species are known as: PIWI-interacting RNAs (Li and Liu, 2011) circular RNAs (Tay et al., 2014), or telomeric RNAs (Schoeftner and Blasco, 2010). Longer RNAs include the so-called long non-coding RNAs, which are longer than 200 nucleotides and represent more than 20% of the human genome. It is yet unclear their relevance and function although evidence points to a substantial role in cell growth and apoptosis (Hung et al., 2011; Zhang and Peng, 2015), and in cell pluripotency and differentiation (Klattenhoff et al., 2013). Moreover, it is suggested that these long nucleic acids may act in cooperation with chromatin modifiers, thus becoming players in epigenetics-related regulation of gene expression (De Lucia and Dean, 2011; Kitagawa et al., 2012; Marchese and Huarte, 2014).

Several factors that result in changes at the epigenetic level also impact on the health of the eye. Such factors include aging, diet, inflammation, drugs, oxidative stress, and seasonal and diurnal changes (Handy et al., 2011; Mazzio and Soliman, 2012). In the present article we revise the epigenetic determinants of the most prevalent ocular diseases: cataracts, glaucoma, and dry eye.

CATARACTS

Cataracts are the result of opacity (clouding) in the crystalline lens, blocking the transmission of light that reaches the retina. According to the World Health Organization (WHO) it is the number one leading cause of reversible vision loss; although it is reversible by means of appropriate interventions, WHO estimates that, worldwide, cataracts are the cause of approximately 50% of the cases of blindness (Mahdi et al., 2014; Patil et al., 2014). Due to the increase of life expectancy that leads to progressive expansion of the elderly population, the National Eye Institute, estimates the number of people in the U.S. with cataract will double by the 2050, from the current 24.4 million to about 50 million cases. Cataracts may start as early as in 40 years old individuals and the risk, which increases with age, is estimated in 70% in 80-year-old caucasians and in 53 and 61% in afroamericans and hispanic americans, respectively. It is known that the eye has many protective mechanisms but they succumb upon sustained challenging by environmental stressors like electrophilic reactive species, drugs, inflammation, radiation, sunlight, and diabetes (**Figure 1**). Currently, there is not any pharmacological therapy for treatment or prevention for of cataracts; fortunately clear vision can be restored by surgical intervention and replacement of the cloudy lens by a synthetic transparent one. However, it is

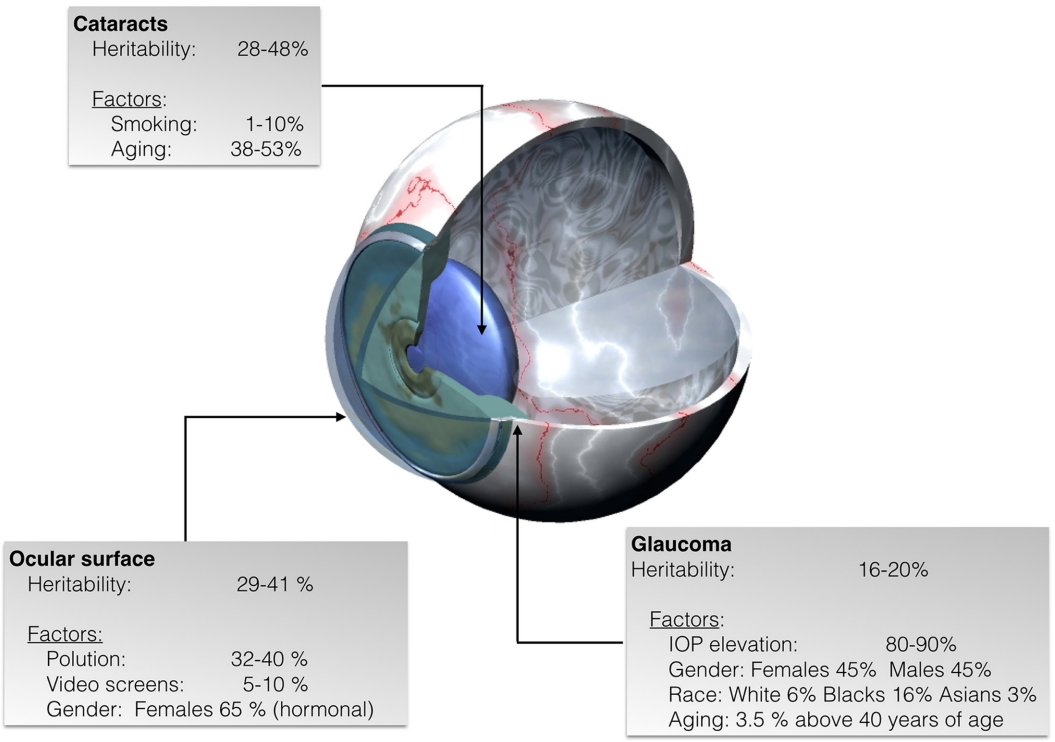

FIGURE 1 | Representative scheme of eye diseases showing the estimated percentage of heritability as well as the percentage of non-inheritable factors some of which lead to specific epigenetic patterns in cataracts, glaucoma, and ocular surface diseases.

important to highlight complications associated to surgery and to the emotional concerns and costs derived from surgery and its potential complications.

Klotho gene family seems to be involved in the susceptibility and development of cataracts. Interestingly, differential epigenetics patterns in the DNA around these genes are found in the senile cataract (Jin et al., 2015). Klotho is a quite recently discovered gene family showing close correlation between expression and age. Klotho gene family consists of three members, α-Klotho, β-Klotho, and γ-Klotho, that encode type I transmembrane glycoproteins with extracellular β-glycosidase-like domains. Expression of these proteins appears as a factor related to the progression of age-related and chronic diseases in mammals. These proteins seemingly regulate the metabolism of several vitamins and minerals such as vitamin D and calcium and it is suggested that they have a role in immunological functions and in protecting the cardiovascular system (Arking et al., 2003; Kurosu et al., 2005; Alesutan et al., 2013) (**Figure 1**).

In studies performed on cataract models, an age-dependent increased methylation of Klotho's gene promoters has been detected (Zhang et al., 2017). On the other hand, it is well-known that lens crystallin proteins play a crucial role in maintaining lens transparency (Andley, 2009; Christopher et al., 2014). As a major structural protein component, α-crystallin represents 35% of all crystallins in the lens (Thampi et al., 2002) and it serves as molecular chaperone to prevent aggregation of other crystallins (Horwitz, 2003). Recent studies showed a decreased level of α-crystallin in age-related nuclear cataract. The reduction of α-crystallin expression is linked with the hypermethylation of the CpG island in the CRYAA gene promoter (**Table 1**). Moreover, the treatment with DNA-methylation inhibitors results in restoring CRYAA gene expression (Zhou et al., 2012a,b). Such evidence sustains an epigenetic-based repression of CRYAA in age-related nuclear cataracts. A reasonable therapeutic approach, which is already suggested to treat cancer, would be the use of inhibitors of the methyltransferase since in this way it would be possible to treat this cause of cataracts.

Another epigenetic-based silencing has been reported for a nuclear factor, namely the erythroid 2-related factor 2 (Nrf2). This protein is a transcriptional activator that may protect the lens by binding to antioxidant response elements, which are *Cis*-acting enhancer sequences (*cis*-acting) in regulatory locus of genes related to detoxification. Although this suppression has been linked to aging and cataract formation, Nrf2 action negatively correlates with a protein called Keap1, whose expression increases with age. In fact, it seems that when Keap1 increases, it stimulates the proteasome-mediated degradation of Nrf2 that in turn would suppress Nrf2− dependent antioxidant protection of the lens (McMahon et al., 2003). Results of the analysis performed using age-related cataract crystalline lenses showed a significant demethylation in Keap1 and a decline in Nrf2, these results being similar to the ones found in lenses from a group of patients between 65 and 80 years of age (Gao et al., 2015).

GLAUCOMA

Glaucoma refers to a wide spectrum of ocular conditions with multifactorial etiology distinguished by progressive irreversible optic neuropathy and peripheral visual field loss (Casson et al., 2012). Glaucoma is the second leading cause of vision loss, and it has been estimated that about 61 million people worldwide suffer from this disease; the number of afflicted individuals may increase to about 80 million by year 2020 (Quigley and Broman, 2006). Risk factors that contribute to glaucoma development are numerous and include increased intraocular pressure (IOP), age, and genetic mutations (Topouzis et al., 2009, 2011) (**Figure 1**). Strong evidence shows that predisposing single nucleotide polymorphisms (SNPs) and environmental effects are also key factors in the development of glaucoma (Chen et al., 2012; Guo et al., 2012).

Glaucoma courses with epigenetic alteration in several ocular structures. For instance, histone 2 and 3 deacetylase (HDAC 2 and 3) expression are significantly upregulated after acute optic nerve injury; however, histone H4 acetylase is downregulated. These data indicate that epigenetic patterns do vary upon optic nerve damage (Schmitt et al., 2014). Moreover, inhibition of retinal HDAC activity in the retina was successfully able to both, preserve the expression of a representative retinal ganglion cell-specific gene and attenuate cell loss in response to optic nerve damage (Pelzel et al., 2010). In addition, a positive effect was observed after using valporic acid (VPA) as a neuroprotective agent for injured retinae, this agent is suggested to directly inhibit HDAC activity and cause histone hyperacetylation (Phiel et al., 2001; Biermann et al., 2010). These reports revealed that abnormal histone acetylation/deacetyalation might be related to retinal ganglion cell damage in glaucoma.

A different aspect of the pathophysiology of glaucoma is the accumulation of extracellular matrix (ECM) in the trabecular meshwork, the conventional pathway of aqueous humor drainage. When the trabecular meshwork is blocked by an abnormal structure in the ECM, aqueous humor does not find a way out and it accumulates within the eye, so IOP increases. Apart from subsequent fibrosis, another relevant finding is the hypoxic environment of the trabecular meshwork of glaucomatous eyes; hypoxia leads to substantial increase in DNA methylation in locuses related to the regulation of the expression of the pro-fibrotic (TGF)β1 factor and the Ras protein activator like 1 (RASAL1) (McDonnell et al., 2016) (**Figure 1**).

Convergent evidence suggests an association between glaucoma and some genetic variants in the CDKN2B-CDKN2A gene cluster at 9p21 chromosome (Wiggs et al., 2012). CDKN2B-AS, also known as ANRIL (Antisense Non-coding RNA in the INK4 Locus), is a long non-coding RNA transcribed in the antisense direction of CDKN2B-CDKN2A (Pasquale et al., 2013). This chromosome locus is a hotspot for numerous disease related polymorphisms; in fact, ANRIL has been recently associated *inter alia* to several cancers, diabetes, and glaucoma (**Table 1**) (Congrains et al., 2013). Although the mechanism behind the association between glaucoma and ANRIL is poorly understood, it seems to be more epigenetic than genetic. Various hypothesis have been proposed to explain the link such as that occurrence of polymorphisms at this locus changes the expression of target genes responsible of cell cycle regulation, subsequently inducing retinal ganglion cell apoptosis (Burdon et al., 2011). Another study suggests that the ANRIL region is involved in regulating the vulnerability of the optic nerve subsequent to the progression of the disease (Pasquale et al., 2013).

TABLE 1 | Ocular disorders and the corresponding altered epigenetic factors.

Disease	Epigenetic factors	Reference
Cataract	(1) Hypermethylation of Klotho's gene promotor (2) Hypermethylation of the CpG island in CRYAA gene promotor (3) Demethylation of Keap1	Zhou et al., 2012a,b; Gao et al., 2015; Zhang et al., 2017
Glaucoma	(1) Upregulation of histone 2 and 3 deacetylase (HDAC 2 and 3) (2) Downregulation of histone H4 acetylase (3) Increase in DNA methylation	Schmitt et al., 2014; McDonnell et al., 2016
Ocular surface disorders	(1) Altered histone methylation pattern (2) Involvement of long non-coding RNAs in keratoconus	Ito, 2007; Szczesniak et al., 2017

OCULAR SURFACE DISORDERS

The surface of the eye is constantly facing external environmental stress; it contains the cornea, which is highly responsible of the refractive effect of the eye. It is highly innervated, avascular and transparent and it obtains nutrients from the aqueous humor and the tear film (Brubaker et al., 1975; Forrester et al., 2015). The ocular surface is prone to harmful events starting by tear-film disruption that may end up in a dry eye, which is a prevalent disease. Several studies have suggested the involvement of epigenetics in the pathophysiology of disorders affecting the ocular surface.

Dry eye is one of the under-diagnosed ocular surface diseases. It has become the most common ocular surface alteration worldwide and it is defined by the International Dry Eye Workshop (DEWS) as "a multifactorial disease of the tears and ocular surface that results in symptoms of discomfort, visual disturbance, and tear film instability with potential damage to the ocular surface. It is accompanied by increased osmolarity of the tear film and inflammation of the ocular surface" (International Dry Eye Workshop (DEWS) Definition and Classification, 2007).

Previous studies attributed dry eye to inflammation and the release of pro-inflammatory cytokines such as the promotion of the activity of nuclear factor kappa-light-chain-enhancer of activated B cells (NF-κB), but also dry eye may have an altered histone methylation pattern (Ito, 2007). Apart from inflammatory components, dry ocular surface is overexposed to infective agents, to environmental allergens and pollutants (**Figure 1**). Another quite common corneal disease is keratoconus, which often comes accompanied with

dry eye. Keratoconus is a degenerative disorder characterized by thinning of the corneal stromal layer leading to a cornea with conical shape and consequently resulting in loss of visual capability. A very recent database has been created in order to characterize keratoconus transcriptome and to identify long non-coding RNAs which might be involved in keratoconus etiology. These results have shown that some of those non-coding RNAs could affect the expression of at least 996 genes in keratoconus patients (**Table 1**) (compared to healthy subjects). The differentially regulated genes include very relevant cellular metabolism and fate regulators such as TGF-β and SMAD9, SMAD6, TGFB3, and TGFBR1 members of Hippo/Wnt pathways (Szczesniak et al., 2017). All those have been previously associated with keeping ocular health (Morgan et al., 2013). Based on these epigenetics-based data, novel therapies are being approached and investigation on novel epigenetics mechanisms are undertaken to have a better understanding of the etiology of ocular surface disorders.

In summary, epigenetics play an important role in the physiology of numerous ocular diseases. Understanding such changes could open a novel window for therapeutical approaches in addition to current therapies. Moreover, further investigation could be helpful for early detection of pathologies with irreversible effect of vision loss such as glaucoma as well as disorders of the retina where solutions are often aiming to treat the symptoms rather than the disease itself.

AUTHOR CONTRIBUTIONS

HA: bibliographical search and writing; RF: organization and writing; JP: organization, writing, and figure design.

ACKNOWLEDGMENTS

This work was supported by grants from Ministerio de Economía y Competitividad (SAF2013-44416-R) and (SAF2016-77084R), and Ministerio de Sanidad RETICS (RD12/0034/0003) and (RD16/0008/0017). HA is a fellowship holder of Saudi Arabia government.

REFERENCES

Alesutan, I., Feger, M., Pakladok, T., Mia, S., Ahmed, M. S., Voelkl, J., et al. (2013). 25-Hydroxyvitamin D3 1-alpha-hydroxylase-dependent stimulation of renal klotho expression by spironolactone. *Kidney Blood Press. Res.* 37, 475–487. doi: 10.1159/000355728

Andley, U. P. (2009). Effects of alpha-crystallin on lens cell function and cataract pathology. *Curr. Mol. Med.* 9, 887–892. doi: 10.2174/156652409789105598

Arking, D. E., Becker, D. M., Yanek, L. R., Fallin, D., Judge, D. P., Moy, T. F., et al. (2003). KLOTHO allele status and the risk of early-onset occult coronary artery disease. *Am. J. Hum. Genet.* 72, 1154–1161. doi: 10.1086/375035

Biermann, J., Grieshaber, P., Goebel, U., Martin, G., Thanos, S., Di Giovanni, S., et al. (2010). Valproic acid-mediated neuroprotection and regeneration in injured retinal ganglion cells. *Invest. Ophthalmol. Vis. Sci.* 51, 526–534. doi: 10.1167/iovs.09-3903

Brubaker, R. F., Ezekiel, S., Chin, L., Young, L., Johnson, S. A., and Beeler, G. W. (1975). The stress-strain behavior of the corneoscleral envelope of the eye. I. Development of a system for making in vivo measurements using optical interferometry. *Exp. Eye Res.* 21, 37–46. doi: 10.1016/0014-4835(75)90055-X

Burdon, K. P., Macgregor, S., Hewitt, A. W., Sharma, S., Chidlow, G., Mills, R. A., et al. (2011). Genome-wide association study identifies susceptibility loci for open angle glaucoma at TMCO1 and CDKN2B-AS1. *Nat. Genet.* 43, 574–578. doi: 10.1038/ng.824

Busanello, A., Santucci, D., Bonini, S., and Micera, A. (2017). Environmental impact on ocular surface disorders: possible epigenetic mechanism modulation and potential biomarkers: a review. *Ocul. Surf.* doi: 10.1016/j.jtos.2017.05.012 [Epub ahead of print].

Campbell, J. P., McFarland, T. J., and Stout, J. T. (2016). Ocular gene therapy. *Dev. Ophthalmol.* 55, 317–321. doi: 10.1159/000434698

Casson, R. J., Chidlow, G., Wood, J. P., Crowston, J. G., and Goldberg, I. (2012). Definition of glaucoma: clinical and experimental concepts. *Clin. Exp. Ophthalmol.* 40, 341–349. doi: 10.1111/j.1442-9071.2012.02773.x

Chen, L. J., Tam, P. O., Leung, D. Y., Fan, A. H., Zhang, M., Tham, C. C., et al. (2012). SNP rs1533428 at 2p16.3 as a marker for late-onset primary open-angle glaucoma. *Mol. Vis.* 18, 1629–1639.

Christopher, K. L., Pedler, M. G., Shieh, B., Ammar, D. A., Petrash, J. M., and Mueller, N. H. (2014). Alpha-crystallin-mediated protection of lens cells against heat and oxidative stress-induced cell death. *Biochim. Biophys. Acta* 1843, 309–315. doi: 10.1016/j.bbamcr.2013.11.010

Congrains, A., Kamide, K., Ohishi, M., and Rakugi, H. (2013). ANRIL: molecular mechanisms and implications in human health. *Int. J. Mol. Sci.* 14, 1278–1292. doi: 10.3390/ijms14011278

Consortium, E. P. (2012). An integrated encyclopedia of DNA elements in the human genome. *Nature* 489, 57–74. doi: 10.1038/nature11247

De Lucia, F., and Dean, C. (2011). Long non-coding RNAs and chromatin regulation. *Curr. Opin. Plant Biol.* 14, 168–173. doi: 10.1016/j.pbi.2010.11.006

Ecker, S., Chen, L., Pancaldi, V., Bagger, F. O., Fernandez, J. M., Carrillo, et al. (2017). Genome-wide analysis of differential transcriptional and epigenetic variability across human immune cell types. *Genome Biol.* 18:18. doi: 10.1186/s13059-017-1156-8

Esquela-Kerscher, A., and Slack, F. J. (2006). Oncomirs - microRNAs with a role in cancer. *Nat. Rev. Cancer* 6, 259–269. doi: 10.1038/nrc1840

Fedoriw, A., Mugford, J., and Magnuson, T. (2012). Genomic imprinting and epigenetic control of development. *Cold Spring Harb. Perspect. Biol.* 4:a008136. doi: 10.1101/cshperspect.a008136

Forrester, J. V., Dick, A. D., McMenamin, P. G., Roberts, F., and Eric Pearlman. (2015). *The Eye E-Book: Basic Sciences in Practice*. Amsterdam: Elsevier Health Sciences, 1–102.

Gao, Y., Yan, Y., and Huang, T. (2015). Human agerelated cataracts: epigenetic suppression of the nuclear factor erythroid 2related factor 2mediated antioxidant system. *Mol. Med. Rep.* 11, 1442–1447. doi: 10.3892/mmr.2014.2849

Garoon, R. B., and Stout, J. T. (2016). Update on ocular gene therapy and advances in treatment of inherited retinal diseases and exudative macular degeneration. *Curr. Opin. Ophthalmol.* 27, 268–273. doi: 10.1097/ICU.0000000000000256

Guo, Y., Zhang, H., Chen, X., Yang, X., Cheng, W., and Zhao, K. (2012). Association of TP53 polymorphisms with primary open-angle glaucoma: a meta-analysis. *Invest. Ophthalmol. Vis. Sci.* 53, 3756–3763. doi: 10.1167/iovs.12-9818

Handy, D. E., Castro, R., and Loscalzo, J. (2011). Epigenetic modifications: basic mechanisms and role in cardiovascular disease. *Circulation* 123, 2145–2156. doi: 10.1161/CIRCULATIONAHA.110.956839

Hewitt, A. W., Januar, V., Sexton-Oates, A., Joo, J. E., Franchina, M., Wang, J. J., et al. (2017). DNA methylation landscape of ocular tissue relative to matched peripheral blood. *Sci. Rep.* 7:46330. doi: 10.1038/srep46330

Horwitz, J. (2003). Alpha-crystallin. *Exp. Eye Res.* 76, 145–153. doi: 10.1016/S0014-4835(02)00278-6

Hung, T., Wang, Y., Lin, M. F., Koegel, A. K., Kotake, Y., Grant, G. D., et al. (2011). Extensive and coordinated transcription of noncoding RNAs within cell-cycle promoters. *Nat. Genet.* 43, 621–629. doi: 10.1038/ng.848

International Dry Eye Workshop (DEWS) Definition and Classification (2007). The definition and classification of dry eye disease: report of the Definition and

Classification Subcommittee of the International Dry Eye WorkShop (2007). *Ocul. Surf.* 5, 75–92.

Ito, K. (2007). Impact of post-translational modifications of proteins on the inflammatory process. *Biochem. Soc. Trans.* 35(Pt 2), 281–283. doi: 10.1042/BST0350281

Jin, S. L., Zhang, Y., Chen, Z. H., Qian, D. W., Qine, Y. J., Yongjie, Q., et al. (2015). Epigenetic changes of the Klotho gene in age-related cataracts. *Eur. Rev. Med. Pharmacol. Sci.* 19, 2544–2553.

Kaminskas, E., Farrell, A. T., Wang, Y. C., Sridhara, R., and Pazdur, R. (2005). FDA drug approval summary: azacitidine (5-azacytidine, Vidaza) for injectable suspension. *Oncologist* 10, 176–182. doi: 10.1634/theoncologist.10-3-176

Kitagawa, M., Kotake, Y., and Ohhata, T. (2012). Long non-coding RNAs involved in cancer development and cell fate determination. *Curr. Drug Targets* 13, 1616–1621. doi: 10.2174/138945012803530026

Klattenhoff, C. A., Scheuermann, J. C., Surface, L. E., Bradley, R. K., Fields, P. A., Steinhauser, M. L., et al. (2013). Braveheart, a long noncoding RNA required for cardiovascular lineage commitment. *Cell* 152, 570–583. doi: 10.1016/j.cell.2013.01.003

Kurosu, H., Yamamoto, M., Clark, J. D., Pastor, J. V., Nandi, A., Gurnani, P., et al. (2005). Suppression of aging in mice by the hormone Klotho. *Science* 309, 1829–1833. doi: 10.1126/science.1112766

Leenen, F. A., Muller, C. P., and Turner, J. D. (2016). DNA methylation: conducting the orchestra from exposure to phenotype? *Clin. Epigenet.* 8, 92. doi: 10.1186/s13148-016-0256-8

Li, L., and Liu, Y. (2011). Diverse small non-coding RNAs in RNA interference pathways. *Methods Mol. Biol.* 764, 169–182. doi: 10.1007/978-1-61779-188-8_11

Li, Y., Tan, T., Zong, L., He, D., Tao, W., and Liang, Q. (2012). Study of methylation of histone H3 lysine 9 and H3 lysine 27 during X chromosome inactivation in three types of cells. *Chromosome Res.* 20, 769–778. doi: 10.1007/s10577-012-9311-2

Lipinski, D. M., Thake, M., and MacLaren, R. E. (2013). Clinical applications of retinal gene therapy. *Prog. Retin. Eye Res.* 32, 22–47. doi: 10.1016/j.preteyeres.2012.09.001

Lyko, F., and Brown, R. (2005). DNA methyltransferase inhibitors and the development of epigenetic cancer therapies. *J. Natl. Cancer Inst.* 97, 1498–1506. doi: 10.1093/jnci/dji311

Mahdi, A. M., Rabiu, M., Gilbert, C., Sivasubramaniam, S., Murthy, G. V., Ezelum, C., et al. (2014). Prevalence and risk factors for lens opacities in Nigeria: results of the national blindness and low vision survey. *Invest. Ophthalmol. Vis. Sci.* 55, 2642–2651. doi: 10.1167/iovs.12-10303

Marchese, F. P., and Huarte, M. (2014). Long non-coding RNAs and chromatin modifiers: their place in the epigenetic code. *Epigenetics* 9, 21–26. doi: 10.4161/epi.27472

Mazzio, E. A., and Soliman, K. F. (2012). Basic concepts of epigenetics: impact of environmental signals on gene expression. *Epigenetics* 7, 119–130. doi: 10.4161/epi.7.2.18764

McDonnell, F., Irnaten, M., Clark, A. F., O'Brien, C. J., and Wallace, D. M. (2016). Hypoxia-induced changes in DNA methylation alter RASAL1 and TGFbeta1 expression in human trabecular meshwork cells. *PLOS ONE* 11:e0153354. doi: 10.1371/journal.pone.0153354

McMahon, M., Itoh, K., Yamamoto, M., and Hayes, J. D. (2003). Keap1-dependent proteasomal degradation of transcription factor Nrf2 contributes to the negative regulation of antioxidant response element-driven gene expression. *J. Biol. Chem.* 278, 21592–21600. doi: 10.1074/jbc.M300931200

Morgan, J. T., Murphy, C. J., and Russell, P. (2013). What do mechanotransduction, Hippo, Wnt, and TGFbeta have in common? YAP and TAZ as key orchestrating molecules in ocular health and disease. *Exp. Eye Res.* 115, 1–12. doi: 10.1016/j.exer.2013.06.012

Morozova, N., Zinovyev, A., Nonne, N., Pritchard, L. L., Gorban, A. N., and Harel-Bellan, A. (2012). Kinetic signatures of microRNA modes of action. *RNA* 18, 1635–1655. doi: 10.1261/rna.032284.112

Nusinzon, I., and Horvath, C. M. (2005). Histone deacetylases as transcriptional activators? Role reversal in inducible gene regulation. *Sci. STKE* 2005:re11. doi: 10.1126/stke.2962005re11

Pasquale, L. R., Loomis, S. J., Kang, J. H., Yaspan, B. L., Abdrabou, W., Budenz, D. L., et al. (2013). CDKN2B-AS1 genotype-glaucoma feature correlations in primary open-angle glaucoma patients from the United States. *Am. J. Ophthalmol.* 155, 342.e5–353.e5. doi: 10.1016/j.ajo.2012.07.023

Patil, S., Gogate, P., Vora, S., Ainapure, S., Hingane, R. N., Kulkarni, A. N., et al. (2014). Prevalence, causes of blindness, visual impairment and cataract surgical services in Sindhudurg district on the western coastal strip of India. *Indian J. Ophthalmol.* 62, 240–245. doi: 10.4103/0301-4738.128633

Pelzel, H. R., Schlamp, C. L., and Nickells, R. W. (2010). Histone H4 deacetylation plays a critical role in early gene silencing during neuronal apoptosis. *BMC Neurosci.* 11:62. doi: 10.1186/1471-2202-11-62

Phiel, C. J., Zhang, F., Huang, E. Y., Guenther, M. G., Lazar, M. A., and Klein, P. S. (2001). Histone deacetylase is a direct target of valproic acid, a potent anticonvulsant, mood stabilizer, and teratogen. *J. Biol. Chem.* 276, 36734–36741. doi: 10.1074/jbc.M101287200

Quigley, H. A., and Broman, A. T. (2006). The number of people with glaucoma worldwide in 2010 and 2020. *Br. J. Ophthalmol.* 90, 262–267. doi: 10.1136/bjo.2005.081224

Rakyan, V. K., Down, T. A., Balding, D. J., and Beck, S. (2011). Epigenome-wide association studies for common human diseases. *Nat. Rev. Genet.* 12, 529–541. doi: 10.1038/nrg3000

Romano, G. L., Platania, C. B. M., Drago, F., Salomone, S., Ragusa, M., Barbagallo, C., et al. (2017). Retinal and circulating miRNAs in age-related macular degeneration: an in vivo animal and human study. *Front. Pharmacol.* 8:168. doi: 10.3389/fphar.2017.00168

Saha, R. N., and Pahan, K. (2006). HATs and HDACs in neurodegeneration: a tale of disconcerted acetylation homeostasis. *Cell Death Differ.* 13, 539–550. doi: 10.1038/sj.cdd.4401769

Sampol, A., Delgado, E., and Lopez, B. (2017). Feasibility and cost-effectiveness of at home azacitidine administration. *Med. Clin.* 149, 224–225. doi: 10.1016/j.medcli.2017.04.019

Sanfilippo, P. G., Hewitt, A. W., Hammond, C. J., and Mackey, D. A. (2010). The heritability of ocular traits. *Surv. Ophthalmol.* 55, 561–583. doi: 10.1016/j.survophthal.2010.07.003

Schmitt, H. M., Pelzel, H. R., Schlamp, C. L., and Nickells, R. W. (2014). Histone deacetylase 3 (HDAC3) plays an important role in retinal ganglion cell death after acute optic nerve injury. *Mol. Neurodegener.* 9:39. doi: 10.1186/1750-1326-9-39

Schoeftner, S., and Blasco, M. A. (2010). Chromatin regulation and non-coding RNAs at mammalian telomeres. *Semin. Cell Dev. Biol.* 21, 186–193. doi: 10.1016/j.semcdb.2009.09.015

Sheffield, V. C., and Stone, E. M. (2011). Genomics and the eye. *N. Engl. J. Med.* 364, 1932–1942. doi: 10.1056/NEJMra1012354

Szczesniak, M. W., Kabza, M., Karolak, J. A., Rydzanicz, M., Nowak, D. M., Ginter-Matuszewska, B., et al. (2017). KTCNlncDB-a first platform to investigate lncRNAs expressed in human keratoconus and non-keratoconus corneas. *Database* 2017:baw168. doi: 10.1093/database/baw168

Tay, Y., Rinn, J., and Pandolfi, P. P. (2014). The multilayered complexity of ceRNA crosstalk and competition. *Nature* 505, 344–352. doi: 10.1038/nature12986

Thampi, P., Zarina, S., and Abraham, E. C. (2002). alpha-Crystallin chaperone function in diabetic rat and human lenses. *Mol. Cell. Biochem.* 229, 113–118. doi: 10.1023/A:1017980713089

Topouzis, F., Harris, A., Wilson, M. R., Koskosas, A., Founti, P., Yu, F., et al. (2009). Increased likelihood of glaucoma at the same screening intraocular pressure in subjects with pseudoexfoliation: the Thessaloniki Eye Study. *Am. J. Ophthalmol.* 148, 606.e1–613.e1. doi: 10.1016/j.ajo.2009.03.024

Topouzis, F., Wilson, M. R., Harris, A., Founti, P., Yu, F., Anastasopoulos, E., et al. (2011). Risk factors for primary open-angle glaucoma and pseudoexfoliative glaucoma in the Thessaloniki eye study. *Am. J. Ophthalmol.* 152, 219.e1–228.e1. doi: 10.1016/j.ajo.2011.01.032

Ushijima, T., Watanabe, N., Okochi, E., Kaneda, A., Sugimura, T., and Miyamoto, K. (2003). Fidelity of the methylation pattern and its variation in the genome. *Genome Res.* 13, 868–874. doi: 10.1101/gr.969603

Verdone, L., Caserta, M., and Di Mauro, E. (2005). Role of histone acetylation in the control of gene expression. *Biochem. Cell Biol.* 83, 344–353. doi: 10.1139/o05-041

Waddington, C. H. (2012). The epigenotype. 1942. *Int. J. Epidemiol.* 41, 10–13. doi: 10.1093/ije/dyr184

Wei, L., Liu, B., Tuo, J., Shen, D., Chen, P., Li, Z., et al. (2012). Hypomethylation of the IL17RC promoter associates with age-related macular degeneration. *Cell Rep.* 2, 1151–1158. doi: 10.1016/j.celrep.2012.10.013

Wiggs, J. L., Yaspan, B. L., Hauser, M. A., Kang, J. H., Allingham, R. R., Olson, L. M., et al. (2012). Common variants at 9p21 and 8q22 are associated with increased susceptibility to optic nerve degeneration in glaucoma. *PLOS Genet.* 8:e1002654. doi: 10.1371/journal.pgen.1002654

Wutz, A. (2013). Epigenetic regulation of stem cells: the role of chromatin in cell differentiation. *Adv. Exp. Med. Biol.* 786, 307–328. doi: 10.1007/978-94-007-6621-1_17

Zhang, C., and Peng, G. (2015). Non-coding RNAs: an emerging player in DNA damage response. *Mutat. Res. Rev. Mutat. Res.* 763, 202–211. doi: 10.1016/j.mrrev.2014.11.003

Zhang, Y., Wang, L., Wu, Z., Yu, X., Du, X., and Li, X. (2017). The expressions of klotho family genes in human ocular tissues and in anterior lens capsules of age-related cataract. *Curr. Eye Res.* 42, 871–875. doi: 10.1080/02713683.2016.1259421

Zhou, P., Luo, Y., Liu, X., Fan, L., and Lu, Y. (2012a). Down-regulation and CpG island hypermethylation of CRYAA in age-related nuclear cataract. *FASEB J.* 26, 4897–4902. doi: 10.1096/fj.12-213702

Zhou, P., Ye, H. F., Jiang, Y. X., Yang, J., Zhu, X. J., Sun, X. H., et al. (2012b). alphaA crystallin may protect against geographic atrophy-meta-analysis of cataract vs. cataract surgery for geographic atrophy and experimental studies. *PLOS ONE* 7:e43173. doi: 10.1371/journal.pone.0043173

Conflict of Interest Statement: The authors declare that the research was conducted in the absence of any commercial or financial relationships that could be construed as a potential conflict of interest.

Advantages of publishing in Frontiers

OPEN ACCESS
Articles are free to read for greatest visibility and readership

FAST PUBLICATION
Around 90 days from submission to decision

HIGH QUALITY PEER-REVIEW
Rigorous, collaborative, and constructive peer-review

TRANSPARENT PEER-REVIEW
Editors and reviewers acknowledged by name on published articles

Frontiers
Avenue du Tribunal-Fédéral 34
1005 Lausanne | Switzerland

Visit us: www.frontiersin.org
Contact us: info@frontiersin.org | +41 21 510 17 00

REPRODUCIBILITY OF RESEARCH
Support open data and methods to enhance research reproducibility

DIGITAL PUBLISHING
Articles designed for optimal readership across devices

FOLLOW US
@frontiersin

IMPACT METRICS
Advanced article metrics track visibility across digital media

EXTENSIVE PROMOTION
Marketing and promotion of impactful research

LOOP RESEARCH NETWORK
Our network increases your article's readership